Oncology and Translational Medicine

Volume 9 • Number 3 • June 2023

Oncology and Translational Medicine Volume 9 • Number 3 • June 2023 pp 99-146

邮发代号：38-121
ISSN 2095-9621

GENERAL INFORMATION
≫otm.tjh.com.cn

ISSN 2095-9621
CN 42-1865/R

Oncology and Translational Medicine

肿瘤学与转化医学（英文）

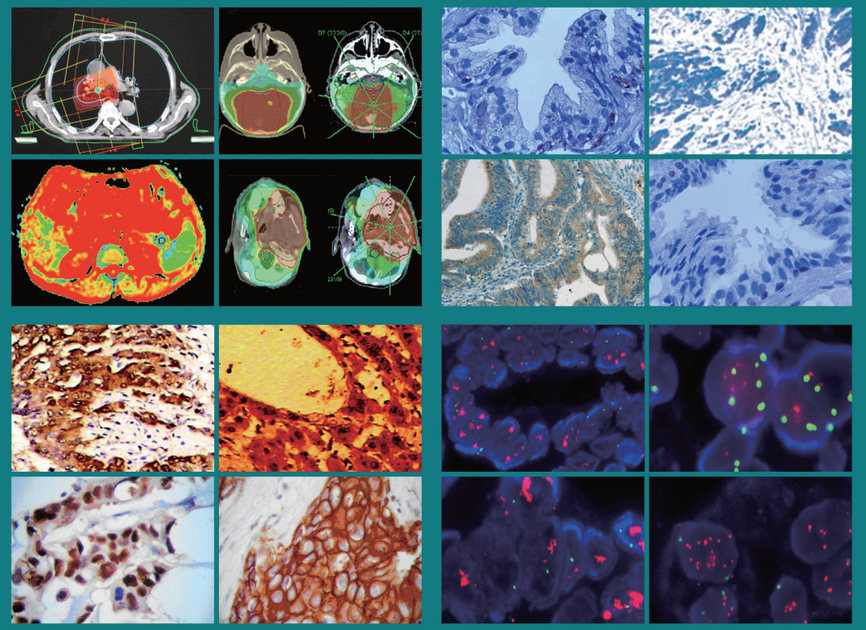

Volume 9
Number 3
June 2023

OTM

Oncology and Translational Medicine
June 2023 Volume 9 Number 3

Contents

中国抗癌协会系列期刊
JOURNAL OF THE CHINA ANTICANCER ASSOCIATION

Oncology and Translational Medicine

Oncology and Translational Medicine

Editors

Oncology and Translational Medicine
DOI 10.1007/s10330-022-0599-9

June 2023, Vol. 9, No. 3, P99–P114

REVIEW ARTICLE

EZH2 is a biomarker associated with lung cancer diagnosis and immune infiltrates without prognostic specificity: a study based on the cancer genome atlas data*

Xiaokun Wang[1], Min Qi[2], Xu Zhu[3], Zhengtong Zhao[3], Yufeng Cao[4], Daijun Xing[4], Fuman Wang[3], Gaoyang Lin[3] (✉)

[1] Cardiac Center (Department of Vascular Surgery), The Affiliated Qingdao Hiser Hospital of Qingdao University (Qingdao Hospital of Traditional Chinese Medicine), Qingdao 266033, China
[2] Department of Clinical Laboratory, The Affiliated Qingdao Hiser Hospital of Qingdao University (Qingdao Hospital of Traditional Chinese Medicine), Qingdao 266033, China
[3] Department of Cardiothoracic Surgery, The Affiliated Qingdao Hiser Hospital of Qingdao University (Qingdao Hospital of Traditional Chinese Medicine), Qingdao 266033, China
[4] Department 3 of the Cancer Center, The Affiliated Qingdao Hiser Hospital of Qingdao University (Qingdao Hospital of Traditional Chinese Medicine), Qingdao 266033, China

Abstract

Enhancer of zeste homolog 2 (EZH2) is the catalytic subunit of polycomb repressive complex 2 (PRC2). Dysregulation of EZH2 causes alteration of gene expression and functions, thereby promoting cancer development. Recent studies suggest that EZH2 has a potential prognostic role in patients with non-small cell lung cancer (NSCLC). However, the prognostic value of EZH2 expression levels in NSCLC is controversial. In this study, we evaluated the prognostic value in lung cancer (LC-LUAD/LUSC) based on data from The Cancer Genome Atlas (TCGA) database. Kruskal-Wallis test, Wilcoxon signed-rank test, and logistic regression were used to evaluate the relationship between EZH2 expression and clinicopathological features. Cox regression and the Kaplan-Meier method were adopted to evaluate prognosis-related factors. Gene set enrichment analysis (GSEA) was performed to identify the key pathways related to EZH2. The correlations between EZH2 and cancer immune infiltrates were investigated by single-sample Gene Set Enrichment Analysis (ssGSEA). EZH2 was found to be up regulated with amplification in tumor tissues in multiple LC cohorts. High EZH2 expression was associated with poorer overall survival (OS). GSEA suggested that EZH2 regulates innate immune system, ECM affiliated, matrisome, surfactant metabolism. Notably, ssGSEA indicated that EZH2 expression was positively correlated with infiltrating levels of Th2 cells and significantly negatively correlated with mast cell infiltration level. These results suggest that EZH2 is associated with LC immune infiltration and significantly over-expressed in lung cancer, and its diagnostic value is better than prognosis, which lays a foundation for further study of the immunomodulatory role of EZH2 in LC.

Received: 10 Octorber 2022
Revised: 1 November 2022
Accepted: 1 December 2022

Key words: Enhancer of zeste homolog 2; lung cancer; diagnosis; prognosis; immune infiltrating

Lung cancer is the second commonly diagnosed cancer (11.4% of total cases), closely to female breast cancer (11.7%). But, Lung cancer is the leading cause of cancer death (18.0% of the total cancer deaths) [1]. Non-small-cell lung cancer (NSCLC), which is the dominant form of lung cancer, is an early asymptomatic disease that constitutes a major global health problem. Non–small-cell lung cancer (NSCLC), including lung adenocarcinoma

✉ Correspondence to: Gaoyang Lin. Email: lingaoyanglynn@126.com
* Supported by a grant from the Qingdao 2020 Medical Scientific Research Guidance Plan (No. 2020-WJZD036).

(LUAD), squamous cell carcinoma (LUSC), and large-cell carcinoma accounts for approximately 85% of all lung cancer cases [2]. Despite the development progressive of the clinical diagnosis and therapeutic strategies in lung cancer research, yet the overall five year survival rate is still less than 21% [3]. The lack of biomarkers to facilitate the diagnosis of early-stage disease and cancer metastasis remains one of critical challenges in NSCLC therapy [4]. Therefore, a profound understanding of the molecular mechanisms contributing to the development and progression of NSCLC is essential for developing specific diagnostic methods, as well as for designing individualized and effective physiological strategies.

With the development of molecular biology, researchers have found that in addition to changes in specific gene loci and activation of abnormal signaling pathways, there are also changes in some special epigenetic traits [5]. Abnormal epigenetic regulation of transcription plays an important role in carcinogenesis and cancer development [6]. A lot of evidence shows that epigenetic regulation plays an important role in the occurrence and development of tumors. Epigenetic modification can regulate chromatin status and gene expression through pathways such as DNA methylation and demethylation, histone modification, and chromatin remodeling without changing the DNA sequence [7, 8]. Human EZH2 gene is located on the long arm of chromosome 7 at 7q35. It contains 20 exons and encodes a protein composed of 746 amino acids [9]. Sequence analysis revealed that EZH family proteins contain four homologous domains [10]. Enhancer of zeste homolog 2 (EZH2) is a member of the family of polycomb group genes (PcGs), which is a group of important epigenetic regulators that repress transcription [6]. EZH2 is an enzymatic catalytic subunit of PRC2 that can alter gene expression by trimethylation of Lys-27 in histone 3 (H3K27me3) [11]. When the PRC2 complex is formed and recruited to the promoter region of the target genes, the SET domain of EZH2 catalyzes H3K27me3, leading to silencing its target genes involved in cell proliferation, cell differentiation, and cancer development [12]. Besides H3K27me3, PRC2 also methylates non-histone protein substrates, including the transcription factor GATA4 [13]. In addition, EZH2 methylates non-histone targets or directly interacts with other proteins to activate downstream genes in a PRC2-independent manner [14, 15]. Via the above 3 ways, EZH2 works as a master regulator of cell cycle progression [16], autophagy, and apoptosis [17], promotes DNA damage repair and inhibits cellular senescence [18] and plays an important role in cell lineage determination and relative signaling pathways [19]. Numerous studies have revealed that dysregulation of EZH2 is correlated with poor prognosis in solid tumor patients, in terms of higher tumor grade, distant metastases, and shorter disease-free survival [20], including breast cancer [21], liver cancer [22], lung cancer [23], ect.

EZH2 gene is highly expressed in NSCLC, and its expression level is closely related to the prognosis of patients. At the same time, studies have also confirmed that the application of EZH2 inhibitor can effectively reduce the invasion and migration ability of NSCLC and induce tumor cell apoptosis [24, 25]. However, based on their results, the prognostic value of EZH2 expression levels in LC is controversial. Therefore, we conducted a systematic bioinformatics analysis of EZH2 expression, diagnostic value, immune cell infiltration and prognosis in non-small cell lung cancer based on TCGA database. EZH2 is expected to be a new therapeutic target with a good application prospect and clinical diagnostic value in LC.

Materials and methods

Data collection and analysis

EZH2 expression profiles and TCGA and Genotype-Tissue Expression (GTEx) clinical pan-cancer data were downloaded from the University of California, Santa Cruz (UCSC) Xena database (https://xenabrowser.net/datapages/), including data on the 31 types tumor. To evaluate EZH2 expression, tumor tissues were obtained from TCGA, and normal tissues were obtained from TCGA and the GTEx database.

Data acquisition and preprocessing

The RNA-seq data of 1037 LC and 108 normal tissues and patient clinical information were downloaded from the Lung cancer (LUAD/ LUSC) Project of The Cancer Genome Atlas (TCGA) (https://portal.gdc.cancer.gov/) [26] until 30 August 2022 . Then, RNA-seq data in FPKM format were transferred to TPM (transcripts per million reads) format, retained, and further analyzed.

Differentially expressed gene analysis

We used the unpaired Student's t-test within the DESeq2 R package (3.6.3) [27] to compare the expression data (HTseq-Counts) between high- and low-expression groups according to the median EZH2 expression level. The thresholds for the DEGs were |log2-fold change (FC)| > 1.5 and adjusted $P < 0.05$.

Enrichment analysis

Metascape (3.0) (http://metascape.org), a user-friendly, well maintained, free, gene list online analysis tool for gene analysis and annotation [28], was adopted to perform Gene Ontology (GO) analysis. Cluster Profiler package in R (3.6.3) [29] was used to perform Gene Set Enrichment Analysis (GSEA) and detect the correlation between EZH2 and the pathway. As a computational method,

GSEA determines whether a priori defined set of genes have statistical significance and concordant differences in two biological states. The samples were divided into high- and low-expression groups according to the median expression level of EZH2. DEseq was used to compare the different expressions between different groups. Gene set permutations were performed with 1,000 times random combinations for each analysis. In the whole process, the expression level of EZH2 was regarded as a phenotype. Additionally, the adjusted P and normalized enrichment score (NES) were utilized to sort the enriched pathways in each phenotype [30]. c2.cp.v7.0.symbols.gmt [Curated] in MSigDB collections was selected as a reference gene set. Gene sets with a false discovery rate (FDR) < 0.25 and adjusted $P < 0.05$ were considered significantly enriched.

Immune infiltration analysis by single-sample gene set enrichment analysis

ssGSEA classifies marker gene sets in a single sample with common biologic functions, chromosomal localization, and physiological regulation. In this study, the ssGSEA method was realized by the GSVA package [31] in R to analyze the immune infiltration for 24 types of immune cells and correlation between EZH2 and every immunocyte in LC samples according to the published literature [32]. The relative enrichment score of signature genes was quantified from the gene expression profile for each tumor sample. Spearman's correlation was adopted to analyze the correlation between EZH2 and 24 types of immune cells, and the Wilcoxon rank-sum test was adopted to analyze the infiltration of immune cells between the high-expression groups of EZH2.

Protein-protein interaction network

The Search Tool for the Retrieval of Interacting Genes (STRING) database (http://string-db.org) [33] was applied to predict the PPI network. The combined score threshold of interaction was 0.4. Furthermore, visualize the PPI network by using Cytoscape (version 3.7.2).

Statistical analysis

The statistical data acquired from TCGA were merged and processed by R 3.6.3. The Wilcoxon rank-sum test and Wilcoxon signed-rank test were used for comparing the expression levels of EZH2 between LC and the control group. Kruskal–Wallis test, Wilcoxon rank-sum test, Wilcoxon signed-rank test, and Spearman's correlation were used to analyze the relation between EZH2 expression and grade of clinicopathological factors. Normal and adjusted Pearson's κ^2 test, Fisher's exact test, and univariate logistic regression were used to analyze whether the grade of clinicopathological factors affects EZH2 expression. Spearman's correlation and the Wilcoxon rank-sum test were adopted to analyze the infiltration of immunocytes between the high- and low expression groups of EZH2. Comparison of multiple groups was performed using a nonparametric Kruskal–Wallis test followed by a post hoc Dunn's test with Bonferroni correction for pairwise comparisons. Univariate Cox regression analysis and multivariate Cox regression analysis were used to evaluate the influence of EZH2 expression and other clinicopathological factors (age and gender) on survival. The significant variables in the univariate analysis ($P < 0.1$) were included into the multivariate analysis [34, 35]. The Kaplan–Meier curve was drawn to evaluate the prognostic value of EZH2. Hazard risk (HR) of individual factors was estimated by measuring the HR with a 95% confidence interval (CI).

Receiver operating characteristic (ROC) analysis was performed by the pROC package [36]. The calculated area under the curve (AUC) value ranges, which were from 0.5 to 1.0, indicated the discrimination ability of 50%–100%. We constructed a nomogram by the rms R package based on the results of the multivariate analysis. The predicted survival probability for 1, 3, and 5 years is visualized in the nomogram, which includes a calibration plot as well as significant clinical characteristics. All statistical tests were considered significant when two-tailed $P \leq 0.05$.

Results

Pan-cancer and lung cancer (TCGA-LUAD/LUSC) EZH2 expression analysis

We first evaluated EZH2 expression in TCGA and GTEx pan-cancer database, and found higher EZH2 expression in 29 tumors compared with the corresponding normal tissues, including: ACC, BLCA, BRCA, CESC, CHOL, COAD, DLBC, ESCA, GBM, HNSC, KICH, KIRP, LAML, LGG, LIHC, LUAD, LUSC, OV, PAAD, PRAD, READ, SKCM, STAD, TGCT, THYM, UCEC, and UCS. But, only 2 tumors were found that EZH2 expression was lower than that in the corresponding normal tissues, including: KRIC, THCA (Fig. 1a). Particularly, The Mann-Whitney U test results showed that the unpaired Tumor of lung cancer was higher than the Normal, and the median difference between the two groups was 1.868 (1.73-2.008), which was statistically significant ($P < 0.001$) (Fig. 1b). High EZH2 expression was observed in LUAD, LUSC in the TCGA cohort compared with the adjacent tissues. In LUAD, the median difference was 0.733 (0.616-0.848), which was statistically significant ($P < 0.001$) (Fig. 1c) and Weltch t' test showed that Tumor was higher than Normal average in LUSC, and the difference was 1.562 (1.454-1.669) ($t = 28.593$, $P < 0.001$) (Fig. 1d). Above all, suggesting that EZH2 may play a role in the pathogenesis and diagnosis of LC (LUAD/LUSC).

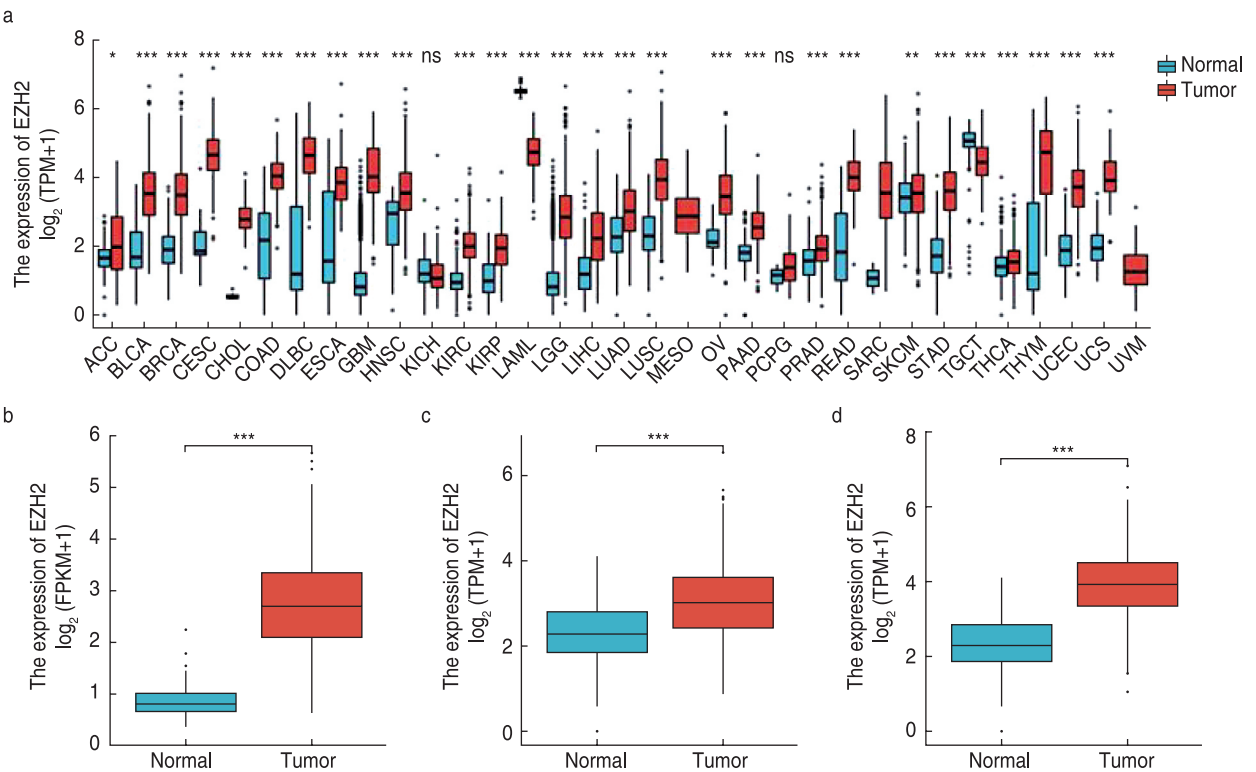

Fig. 1 Pan-cancer EZH2 expression analysis. (a) EZH2 expression in tumor and normal tissues in pan-cancer data of The Cancer Genome Atlas (TCGA) and GTEx; (b) EZH2 expression in tumor and normal tissues in LC from TCGA; (c) EZH2 expression in non-paired tumor and normal tissues in LUAD from TCGA; (d) EZH2 expression in non-paired tumor and normal tissues in LUSC from TCGA. Data were shown as mean ± SD. Identification of significance: ns, $P \geq 0.05$; * $P < 0.05$; ** $P < 0.01$; *** $P < 0.001$

Clinical characteristics

The clinical data of 1037 Lung cancer patients included patient T stage, N stage, M stage, pathologic stage, gender, age, smoker, primary therapy outcome, anatomic neoplasm subdivision2, age median (IQR), residual tumor (Table 1). A total of 620 males and 417 females with a mean age of 67 years were analyzed in the present study, including 918 smoking patients and 93 non-smoking patients. The chi squared test showed that EZH2 was significantly correlated with T stage (P = 0.047), Gender (P = 0.01), Age (P = 0.019), Smoker (P < 0.01), and Anatomic neoplasm subdivision2 (P = 0.036). Fisher's exact test showed that EZH2 was not significantly correlated with Residual tumor (P = 0.111), N stage (P = 0.343). Wilcoxon rank sum test showed that EZH2 was significantly correlated with Age median (IQR) (P =0.011). EZH2 expression was not significantly correlated with other clinicopathological features, for instance: M stage (P = 0.334), Pathologic stage (P = 0.164), Primary therapy outcome (P = 0.399).

Identification of differentially expressed genes in lung cancer

Based on the cutoff criteria (|logFC| > 1.5 and adjusted P < 0.05), we identified a total of 1760 DEGs (1399 up-regulated and 361 down-regulated) after using the DESeq2 package in R [37] to analyze the HTSeq-count data from TCGA. DEG expressions were illustrated by a volcano plot (Fig. 2a). DEGs included 987 differentially expressed mRNAs (46 unprocessed pseudogenes, 2 unitary pseudogenes, 48 transcribed unprocessed pseudogenes, 41 TECs, 591 protein coding genes, 259 processed pseudogenes) which contained 42 up regulated unprocessed pseudogenes, 2 up regulated unitary pseudogenes, 24 up regulated transcribed unprocessed pseudogenes, 34 up regulated TECs, 340 up regulated protein coding genes, 274 up regulated processed pseudogenes and 4 unprocessed pseudogenes down regulated, 24 transcribed unprocessed pseudogenes down regulated, 7 TECs down regulated, 251 protein coding genes down regulated, 12 processed pseudogenes down regulated. DEGs included 773 differentially expressed RNAs (61 snRNA, 43 snoRNA, 4 Rrna pseudogene, 85 misc-RNA, 21 miRNA, 559 lncRNA) which contained 43 snoRNA upregulated, 4 rRNA pseudogene up regulated, 85 misc-RNA up regulated and 21 miRNAs (18 up regulated and 3 down regulated), 61 snRNA (60 up regulated and 1 down regulated), 559 lncRNAs (473 up regulated and 86 down regulated) (Fig. 2b). The heat map showed the correlation between high expression of

Table 1 Demographic and clinicopathological parameters of patients with Lung cancer in TCGA–LC (LUAD/LUSC)

Characteristics	Low expression of EZH2		High expression of EZH2		*P*
	n	%	*n*	%	
Total (*n*)	518		519		
T stage					0.47
T1	161	15.6	128	12.4	
T2	272	26.3	311	30.1	
T3	59	5.7	61	5.9	
T4	25	2.4	17	1.6	
M stage					0.343
N0	334	32.9	334	32.9	
N4	104	10.2	122	12	
N1	62	6.1	52	5.1	
N3	2	0.2	5	0.5	
M stage					0.334
M0	379	47.1	394	48.9	
M1	19	2.4	13	1.6	
Pathologic stage					0.164
I	279	27.2	260	25.4	
II	128	12.5	157	15.3	
III	83	8.1	85	8.3	
IV	20	2	13	1.3	
Gender					0.001
Female	234	22.6	183	17.6	
Male	284	27.4	336	32.4	
Age					0.019
≤ 65	202	20	244	24.2	
> 65	298	29.5	265	26.3	
Smoker					< 0.01
No	63	6.2	30	3	
Yes	439	43.4	479	47.4	
Primary therapy outcome					0.399
PD	59	7.3	43	5.3	
SD	29	3.6	25	3.1	
PR	5	0.6	6	0.7	
CR	315	39	325	40.3	
Anatomic neoplasm subdivision					0.036
Central lung	89	20.7	120	28	
Peripheral lung	117	27.3	103	24	
Age (years), median (IQR)	68 (60–74)		66 (60–73)		0.111
Residual tumor					0.111
R0	361	45.9	393	49.9	
R1	17	2.2	8	1	
R2	5	0.6	3	0.4	

TOP10 differentially expressed genes, low expression of TOP10 differentially expressed genes, high expression of TOP10 differentially expressed lncRNAs, and low expression of TOP10 differentially expressed lncRNAs and EZH2 gene co-expression (Fig. 2c, 2d).

Functional enrichment analysis of differentially expressed genes

We used Metascape to perform GO enrichment analyses of the functions of EZH2-associated DEGs in LC. The GO results displayed that EZH2-associated DEGs had significant regulation on metabolic process, cellular process, response to stimulus, biological regulation, localization, biological process involved in interaction between organisms, multicellular organismal process, negative regulation of biological process, immune system process, signaling, regulation of biological process, reproductive process, locomotion, and positive regulation of biological process (Fig. 3a). A network of EZH2 and its potential co-expression genes in EZH2-related DEGs are shown in Fig. 3b.

As many pathways contribute to tumor formation,

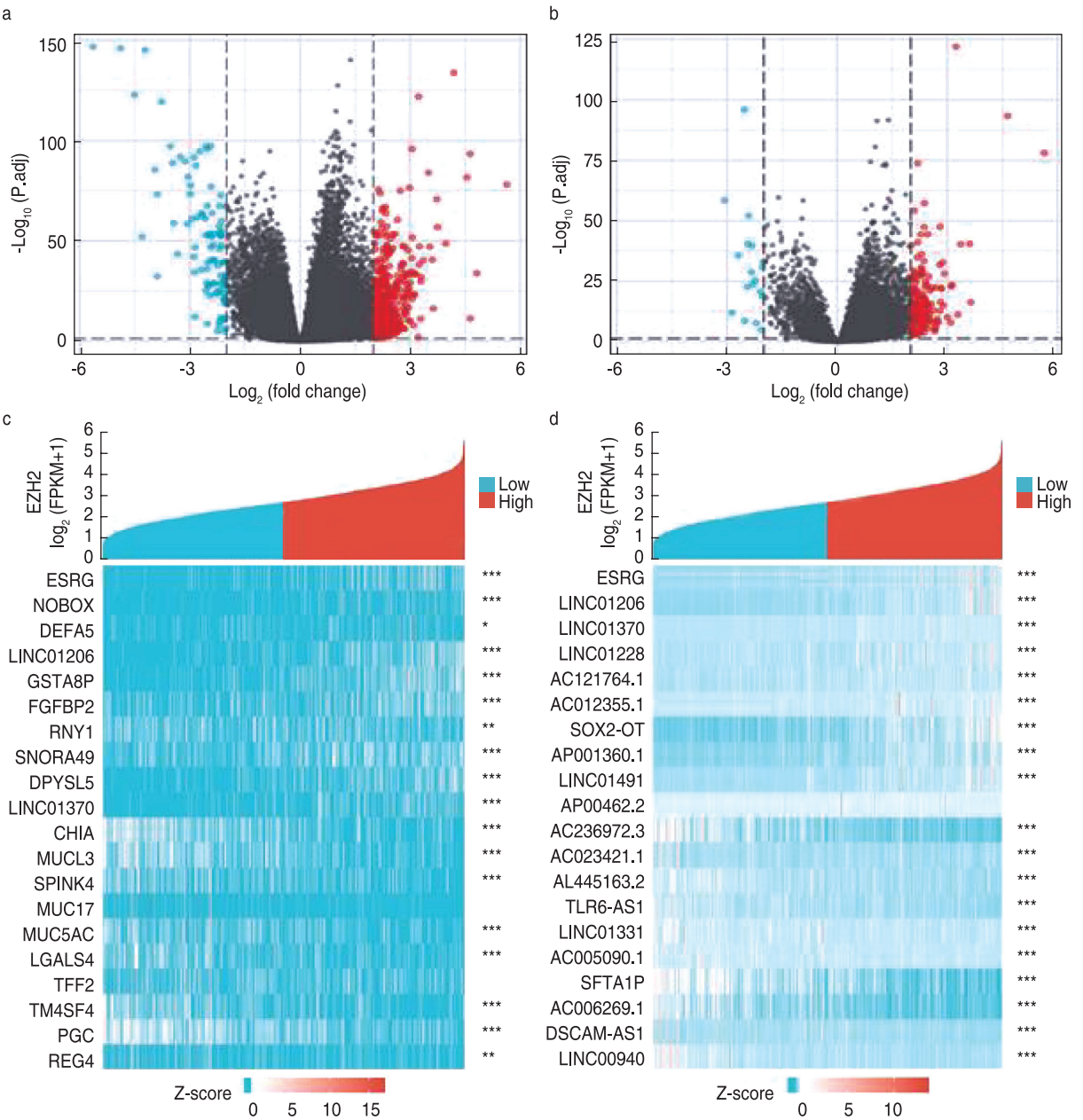

Fig. 2 Results of differentially expressed gene (DEG) analysis. (a) Volcano plot of DGEs; (b) Volcanco plot of differentially expressed lncRNAs; (c) Heat map analysis of co-expression of TOP10 high and low DEGs and EZH2 gene; (d) Heat map analysis of co-expression of TOP10 high and low lncRNAs and EZH2 gene

high EZH2 expression associated with poor survival may be related to active signaling pathways in LC. We performed GSEA of differences between low- and high–EZH2 expression data sets to identify the key signaling pathways associated with EZH2. A total of 11 pathways showed significant differences (False discovery rate (FDR. q value) < 0.25, p. adjusted < 0.05) in the enrichment of the MSigDB collection (c2.cp.v7.2.symbols.gmt). The most significantly enriched signaling pathways based on their NES. In particular, EZH2 was related to innate immune system, ECM affiliated, matrisome, surfactant metabolism, neutrophil degranulation, diseases of metabolism, metabolism of lipids, SLC mediated trans membrane transport, post translational protein modification, disease (Fig. 3c–3f).

The correlation between EZH2 expression and immune infiltration

We employed Spearman's correlation to show the association between the expression level (TPM) of EZH2

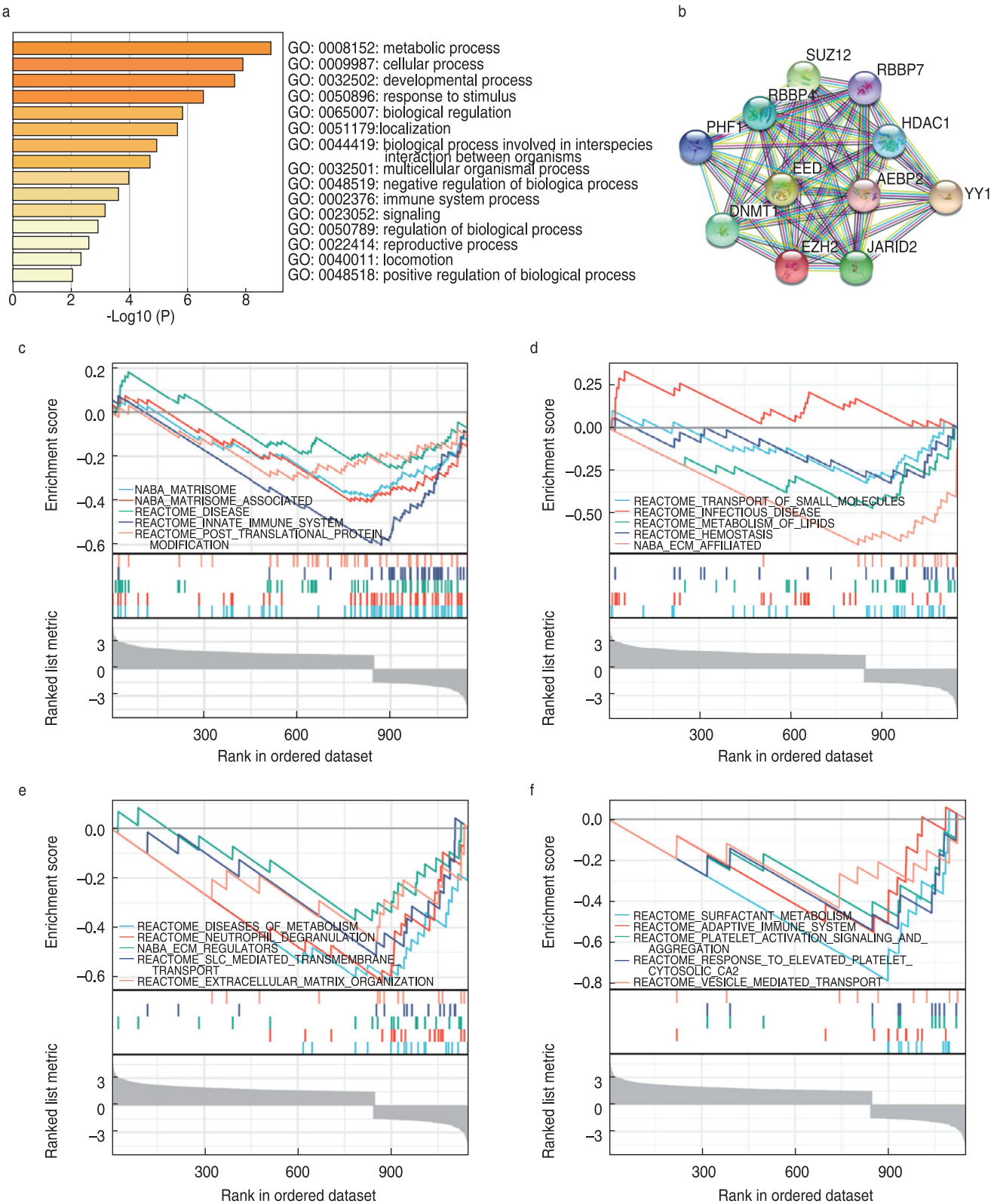

Fig. 3 Enrichment analysis of EZH2 in LC. (a) Top 15 biological process enrichment related to EZH2-related genes with enrichment heat-map; (b) Network of EZH2 and its potential co-expression genes in DNTTIP1-related DEGs; (c -f) Results of enrichment analysis from GSEA

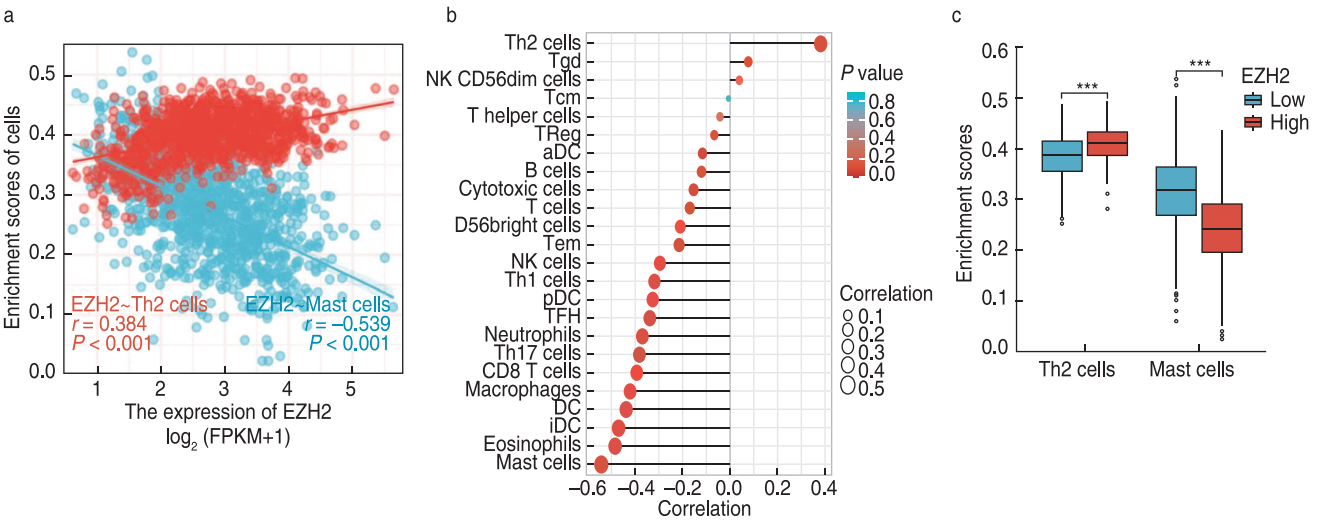

Fig. 4 Results of analysis between EZH2 expression and immune infiltration. (a) Th2 cells were significantly positively correlated with EZH2 expression and mast cells were significantly negatively correlated with EZH2 expression; (b) Correlation between the relative abundances of 24 immune cells and EZH2 expression level; The color of dots shows the absolute value of Spearman R; (c) Th2 cells and mast cells infiltration level in different EZH2 expression groups

and immune cell infiltration level quantified by ssGSEA in the LC (LUAD/ LUSC) tumor microenvironment. Th2 cells were significantly positively correlated with EZH2 expression (Spearman R = 0.384, $P < 0.001$) and Mast cells were significantly negatively correlated with EZH2 expression (Spearman R = -0.539, $P < 0.001$) (Fig. 4a). Other immune cell subsets, including Eosinophils, iDC, DC, Macrophages, CD8 T cells, Th17 cells, Neutrophils, TFH, pDC, NK cells, Th1 cells, were also correlated with EZH2 expression (Fig. 4b). The Th2 cell infiltration level in the EZH2 high expression group was significantly different from that of the low expression group ($P < 0.001$), and the Mast cell infiltration level in the EZH2 low expression group was significantly different from that of the high expression group ($P < 0.001$) (Fig. 4c).

Associations between EZH2 expression and clinico-pathologic variables

The Kruskal-Wallis test revealed that the between-group differences in Race, T stage, N stage, Pathologic stage, Residual tumor, Primary therapy outcome of LC (Fig. 5g-l), and Wilcoxon rank-sum test revealed that expression of EZH2 was significantly correlated with Age ($P < 0.001$), Gender ($P < 0.001$), Smoker ($P < 0.01$), Number pack years smoked ($P < 0.001$), Anatomic neoplasm subdivision ($P < 0.001$) and Anatomic neoplasm subdivision ($P < 0.01$) (Fig. 5a-f). Bonferroni correction was applied to the p value of Dunn's test to correct for multiple comparisons within the Race, T stage, N stage, Pathologic stage, Residual tumor, Primary therapy outcome of LC (Fig. 5). Logistic regression analysis showed that EZH2 was significantly correlated with T stage ($P = 0.022$), residual tumor ($P = 0.039$), age ($P = 0.016$), smoker ($P < 0.001$), and gender ($P = 0.001$) (Table 2).

EZH2 is highly expressed in paired LC samples compared with normal tissues from TCGA (Fig. 6a). The area under the curve (AUC) of EZH2 was 0.987, which indicated that EZH2 might be a potential diagnostic molecule in lung cancer patients (Fig. 6b).

In the Cox regression model, variables with $P < 0.1$ in univariate Cox regression were included in multivariate Cox regression. The variables that met this threshold were Age ($P = 0.022$), pathologic stage ($P < 0.001$), T stage ($P < 0.001$), M stage ($P < 0.001$), residual tumor ($P < 0.001$) (Table 3). Furthermore, multivariate Cox regression showed that residual tumor ($P = 0.006$) was independent prognostic factors for overall survival ($P < 0.05$).

The Kaplan-Meier survival curve drawn by the survminer package in R was used to evaluate the prognostic value of EZH2 in overall survival of LC. The prognostic values of EZH2 in relation to the overall survival under different subgroups of LC in TCGA are shown in Fig. 7a. The Kaplan-Meier survival curve of the EZH2 in overall survival in different subgroups of LC in TCGA-LC (LUAD/ LUSC). Gene expression values were divided into high- and low-expression groups according to the median value. The expression of EZH2 had significant effect in N1 & N2 & N3 subgroups of N stage, and stage II & stage III & stage IV subgroups of pathologic stage. High expression of EZH2 was associated with poor overall survival in LC N stage (N1 & N2 & N3) (HR = 0.70 (0.52-0.95), $P = 0.023$) and Pathologic stage (II & III & IV) (HR = 0.74 (0.57-0.96), $P = 0.024$) (Fig. 7b). EZH2 expression has no prognostic value in LC overall

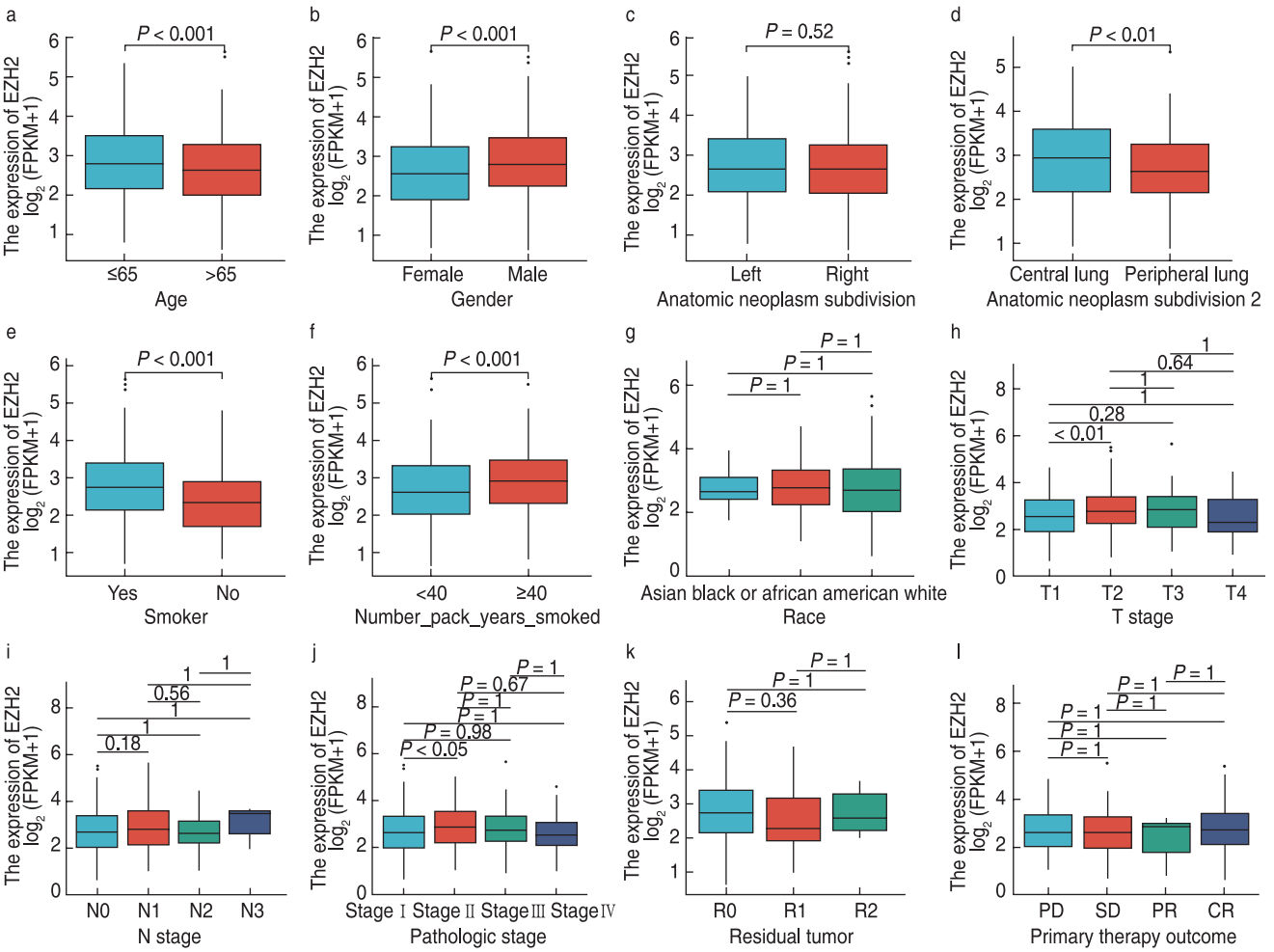

Fig. 5 Association between the EZH2 expression and different clinicopathological characteristics. (a) Association between the EZH2 expression and Age of LC; (b) Gender; (c) Anatomic neoplasm subdivision; (d) Anatomic neoplasm subdivision 2; (e) Smoker; (f) Number-pack-years-smoked; (g) Race; (h) T stage of LC; (i) N stage of L; (j) pathologic stage of LC; (k) Residual tumor; (l) Primary therapy outcome

Table 2 EZH2 expression associated with clinicopathological characteristics (logistic regression)

Characteristics	Total (*n*)	Odds Ratio (OR)	*P* value
T stage (T2&T3&T4 *vs.* T1)	1,034	1.374 (1.047–1.808)	0.022
N stage (N1&N2&N3 *vs.* N0)	1,015	1.065 (0.822–1.382)	0.632
M stage (M1 *vs.* M0)	805	0.658 (0.313–1.340)	0.254
Pathologic stage (Stage IV & Stage III *vs.* Stage I & Stage II)	1,025	0.929 (0.682–1.264)	0.638
Residual tumor (R1&R2 *vs.* R0)	787	0.459 (0.212–0.941)	0.039
Age (>65 *vs.* ≤65 years)	1,009	0.736 (0.573–0.944)	0.016
Smoker (Yes *vs.* No)	1,011	2.291 (1.468–3.650)	< 0.001
Gender (Male *vs.* Female)	1,037	1.513 (1.179–1.943)	0.001

survival (OS) (HR = 0.92 (0.76-1.12), $P = 0.427$), disease specific survival (DSS) (HR = 0.88 (0.66-1.16). $P = 0.348$), progress free interval (PFI) (HR = 0.84 (0.68-1.04), $P = 0.106$) (Fig. 7c). The lower part of these figures is shown in the risk table which records the number of people still under follow-up at each time point. The prognosis data are derived from an article published in Cell [38].

Discussion

The polycomb group (PcG) proteins were first identified in Drosophila as regulatory factors that

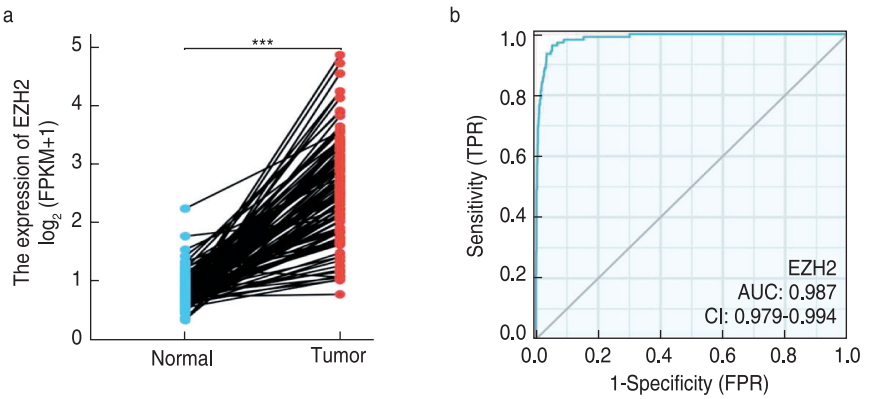

Fig. 6 Prognostic value of EZH2 in LC (LUAD/ LUSC). (a) EZH2 was also highly expressed in paired LC samples compared with paired normal tissues from TCGA; (b) ROC curve indicates that EZH2 is a potential diagnostic marker in LC patients

Table 3 Univariate and multivariate analyses of clinicopathological parameters in patients with lung cancer in TCGA-LC (LUAD/ LUSC)

Characteristics	Total (*n*)	Univariate analysis		Multivariate analysis	
		Hazard ratio (95% CI)	*P* value	Hazard ratio (95% CI)	*P* value
Age (years)					
> 65	561	Reference			
≤ 65	445	0.791 (0.646-0.967)	0.022	0.794 (0.603-1.045)	0.099
Gender					
Female	410	Reference			
Male	612	1.164 (0.949-1.428)	0.145		
Pathologic stage					
I	533	Reference			
III, IV, II	477	1.913 (1.566-2.337)	< 0.001	1.488 (0.995-2.225)	0.053
T	1019				
T1	289	Reference			
T2&T3&T4	730	1.574 (1.239-1.999)	< 0.001	1.229 (0.876-1.722)	0.233
N stage					
N0	660	Reference			
N1	222	1.541 (1.225-1.938)	< 0.001	0.930 (0.619-1.397)	0.726
M stage					
M0	760	Reference			
M1	32	2.269 (1.439-3.577)	< 0.001	1.533 (0.841-2.796)	0.163
Residual tumor					
R1&R2	32	Reference			
R0	742	0.339 (0.212-0.541)	< 0.001	0.429 (0.233-0.788)	0.006
Smoker					
No	90	Reference			
Yes	906	0.883 (0.617-1.263)	0.496		
EZH2					
Low	509	Reference			
High	513	0.902 (0.741-1.097)	0.301		

transcriptionally silence the expression of the bithorax homeobox (Hox) gene cluster [39]. It has been reported that PcG proteins interact with each other and generate two major complexes, polycomb repressive complexes 1 and 2 (PRC1 and PRC2) [40]. PRC2 is a highly conserved complex in many species of plants and animals. It is mainly composed of four subunits: EZH2, EED, SUZ12, and RbAp46/48 (Fig. 8a) [41]. Enhancer of zeste homolog 2 (EZH2), the core catalytic subunit of the PRC2 complex, and its SET domain at the C- terminus provides the histone methyltransferase activity (Fig. 8b), plays a critical role in regulating a wide range of biological processes, including tumor development and malignancy, stem cell renewal and development, immune response, and cell senescence [42]. Aberrant epigenetic regulation plays a critical role in tumorigenesis by altering genome-wide gene expression.

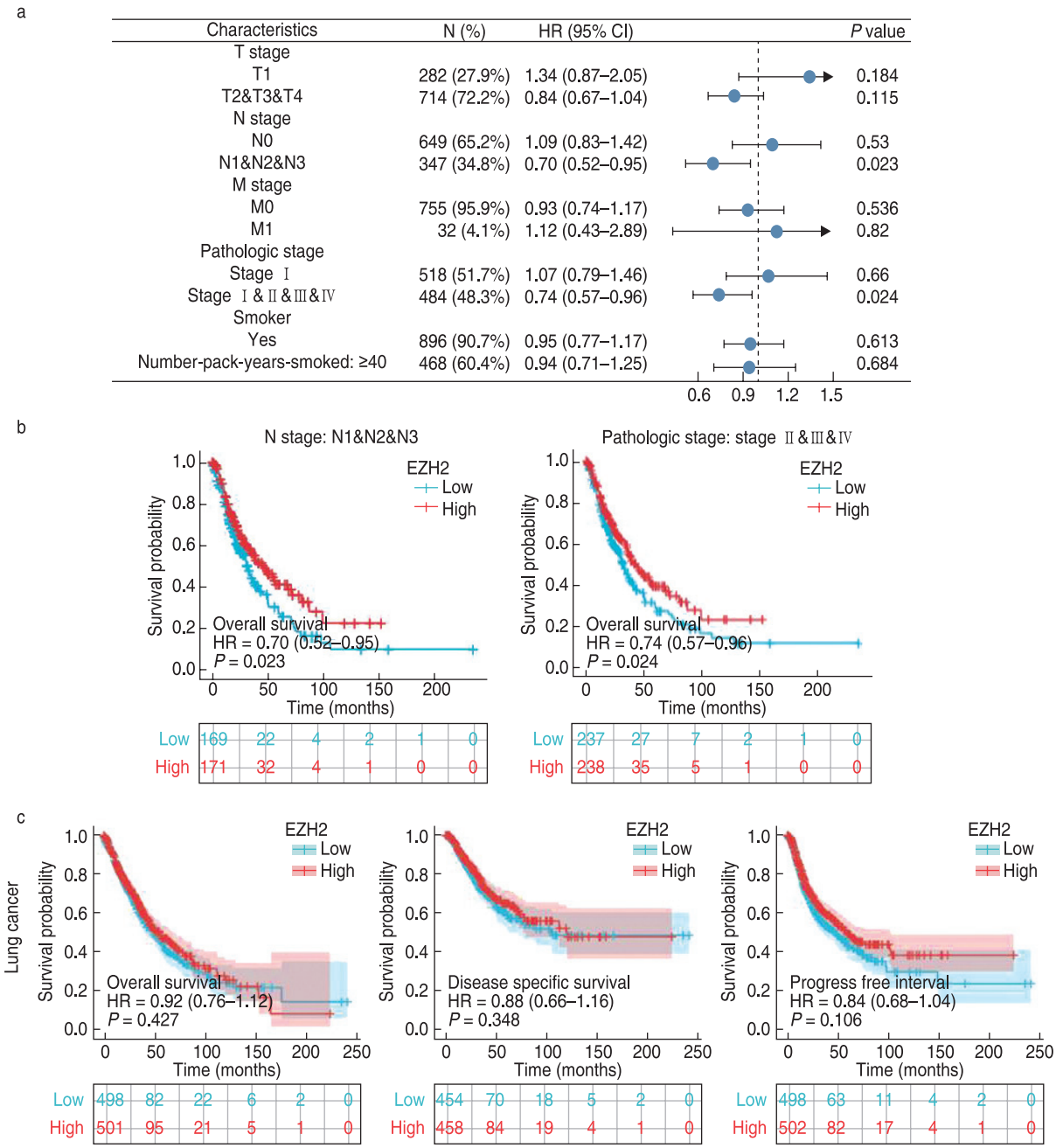

Fig. 7 Prognostic value of EZH2 in different analyses. (a) Forest plot of prognostic value of EZH2 in overall survival of LC; (b) The Kaplan–Meier survival curve of the EZH2 in overall survival in different subgroups of LC in TCGA–LC (LUAD/ LUSC). High expression of EZH2 was associated with poor overall survival in LC N stage (N1 & N2 & N3) and Pathologic stage (II & III & IV) subgroups; (c) EZH2 expression has no prognostic value in LC (LUAD/ LUSC) Overall Survival (OS), Disease Specific Survival (DSS), and Progress Free Interval (PFI)

In this study, we comprehensively investigated the expression, immune infiltration, diagnosis and prognostic value of epigenetic regulatory genes such as EZH2 in LC (LUAD/ LUSC) tissues using public databases.

In this study, bio-informatics analysis of sequencing data from TCGA was performed to gain a deeper understanding of the potential function of EZH2 in LC and guide future research in LC. Elevated EZH2 expression in LC was associated with advanced clinicopathological features (Age, Gender, Anatomic neoplasm subdivision2, Smoker, Number_pack_years_smoked, T1 vs T2 stage, pathological stage I vs II), poor prognosis, and survival time. Furthermore, in univariate and multivariate Cox regression analyses, we found that after removing

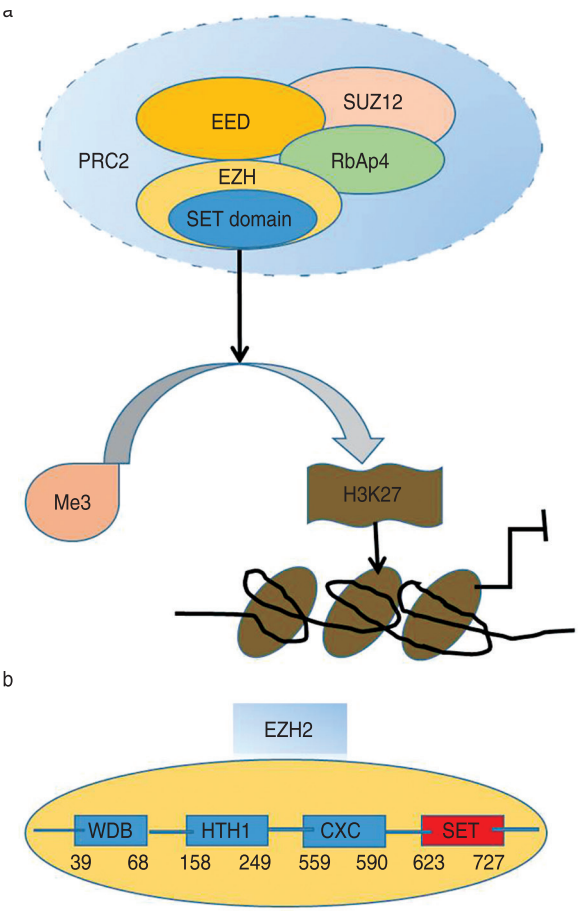

Fig. 8 The polycomb repressive complex 2 (PRC2) complex composition, regulation function, and schematic diagram of the enhancer of zeste homolog 2 (EZH2) domains. (a) The PRC2 complex contains four core subunits which include EZH2, EED, SUZ12, and RbAp46/48. PRC2 induces target genes' transcriptional repression through EZH2- mediated H3K27 trimethylation. (b) EZH2 has four domains: WD- binding domain; PRC2 HTH 1 domain, CXC domain, and SET domain

confounding factors, EZH2 was not an independent prognostic factor, which is not showed a higher prognostic value than many other clinical variables. Our results suggested that EZH2 is a potential prognostic and diagnostic marker deserving further clinical validation.

The PPI network indicates that EZH2 can interact with several histone deacetylase members such as HDAC1, EED, RBBP4, SUZ12, RBBP7, AEBP2, etc. HDAC1 are key enzymes that maintain the acetylation balance of nucleosomes in basic units of chromosomes. Their catalytic histone deacetylation is closely related to the inhibition of gene transcription [43]. The Polycomb Repressive Complexes (PRCs) are large protein multimers that modify lysine residues on histones. The two primary PRCs noted in mammals are PRC1, formed by several distinct proteins but most notably RING1A/B and BMI1, and PRC2. The core subunits of PRC2 are enhancer of zeste homolog 1/2 (EZH1/EZH2), embryonic ectoderm development (EED), and suppressor of zeste 12 (SUZ12) [44]. Within the PRC2 complex, EZH2 (and to a lesser extent, EZH1) is the catalytic subunit responsible for methyltransferase activity. Both EZH proteins were observed to be phosphorylated, although EZH1 phosphorylation was shown to lead to degradation, while EZH2 phosphorylation led to reduced function [45, 46].

GSEA showed that innate immune system, ECM affiliated, Matrisome, Surfactant metabolism activation in LC were enriched in the EZH2 high-expression phenotype. These findings indicated that EZH2 might participate in the regulation of metastasis and immune response in the tumorigenesis of LC. ssGSEA and Spearman's correlation were adopted to uncover connections between EZH2 expression and immune infiltration levels in LC. Our results demonstrated that EZH2 expression was significantly positively correlated with Th2 cells. Our results suggest a possible mechanism where EZH2 regulates the balance of Th1/Th2 in LC. The Th2 cells produce IL-4 and IL-10 and inhibit the host immune system, hence having a role in promoting tumor growth [47, 48]. This indicates that over-expression of EZH2 promotes Th2 cell immune response and infiltration in tumor progression. Th1/Th2 balance can be regulated to inhibit tumor progression. A global Th1/Th2-like cytokine shift (a decrease in Th1 and an increase in Th2 cytokines) can be induced to promote HCC metastasis [49]. On the other hand, there was significantly an inverse correlation between Mast cells and EZH2. Furthermore, there was a strong-to-moderate correlation between DC, macrophages, Th17 cells, *et al.* and EZH2 expression. The NSCLC cells could release CCL5 and recruit MCs to the tumor micro-environment. Moreover, the MCs-derived factors were responsible for tumor growth. When NSCLC cells were activated, MCs produced various factors that induced EMT and migration [50]. Interestingly, EZH2 gene has a significant negative correlation with MC. High expression of EZH2 in NSCLC has a lower MC infiltration, which may be an important mechanism for the better prognosis of cancer patients. Due to the role of DCs in initiating anti-tumor immunity, there is a negative selective pressure hampering the accumulation of DCs by tumor secreted mediators that inhibit dendropoiesis, promote DC apoptosis [51], and accelerate DC turnover. The suppression of DCs is normally found in tumors and may facilitate LC progression. Th17 immune cells were associated with both good and bad prognoses [52]. Th17 cells can also drive anti-tumor immune responses by recruiting immune cells into tumors, activating effector CD8+ T cells, or even directly by converting toward Th1 phenotype and producing IFN-γ [53]. The down regulation of Th17 caused by EZH2 over-expression may affect h1/h2 balance, leading to a bad prognosis. All findings according to ssGSEA support that EZH2 has a role in

regulating and recruiting immune infiltrating cells in LC. However, more trials are needed to accurately understand the relationship between EZH2 and Th1/Th2 balance in vivo.

The high expression of EZH2 is closely related to a poor prognosis in many tumors, but its value in the prognosis of NSCLC is still controversial [54, 55]. To our best knowledge, previous meta analyses did not specifically explain the prognostic relationship between EZH2 and lung cancer [56], or no bioinformatics evidence was used to support it [57]. Therefore, we searched TCGA database and Kaplan-Meier plotter database for large-scale global lung cancer database mining to find EZH2 potential correlation with LC. In our study, EZH2 expression was significantly higher in LC tissues compared to the normal lung tissues. Our study demonstrates that higher EZH2 expression correlates with poorer OS, DSS and PFI in LC patients. In addition, the Kaplan-Meier survival curves with high HR for poor OS, DSS and PFI when EZH2 was highly expressed in LC, however, there was no statistically significant difference in the low expression of EZH2 group, suggesting that EZH2 has certain prognostic guiding value but does not have specificity as a prognostic biomarker in LC. Moreover, Kaplan-Meier survival analysis was performed in LC patients according to their EZH2 expression levels, stratified by clinicopathological characteristics. A high level of EZH2 expression was associated with poor prognosis of LC patients with N stage (N1 & N2 & N3) and Pathologic stage (II & III & IV), thus indicating that the high association between EZH2 expression level and survival may be influenced by the degree of invasion and metastasis.

As single-stranded RNA molecules with a length of 200 to 100,000nt, long-chain noncoding RNAs have multiple interactions with EZH2. Single genetic variance analysis showed that the total number of lncRNA ID is 14077, among them, meet | log2 (FC) | > 1.5 & p.adj < 0.05 threshold of lncRNA has 559, under the threshold, the High expression in the High group (logFC is) as the number of 473,The number of Low expression (logFC negative) in Low group was 86;The heat map correlation analysis of EZH2 co-expression showed that AP000462.2 had no significant correlation (Spearman P = 0.289). Long intergenic non-coding RNA 00467 promotes lung adenocarcinoma proliferation, migration and invasion by binding with EZH2 and repressing HTRA3 expression [58]. LncRNA MSTO2P promotes proliferation and autophagy of lung cancer cells by up-regulating EZH2 expression [59]. lncRNA PVT1 Promotes Metastasis of Non-Small Cell Lung Cancer Through EZH2-Mediated Activation of Hippo/ NOTCH1 Signaling Pathways [60]. lncRNA ZEB2-AS1 Aggravates Progression of Non-Small Cell Lung Carcinoma via Suppressing PTEN Level [61]. This shows that, through the up-regulation of the EZH2 expression, long noncoding RNA silences tumor suppressor genes and promotes lung cancer invasion and migration, which are associated with poor prognosis. This is consistent with our findings. However, the high expression of EZH2 is not only related to the regulation of long noncoding.

Although our investigation of the relationship between EZH2 and LC furthered our understanding of the vital role of EZH2 in LC, some limitations remained. First, cell experiments and clinical samples should be used to verify the correlation between EZH2 mRNA and protein expression. In the present study, we only used mRNA levels to predict protein expression [62]. Second, clinical factors such as the details of patient treatment should be sufficiently considered to clarify the specific role of EZH2 in the development of LC. Third, while multicenter research based on public databases intends to overcome the shortage of single-center studies, retrospective studies have two major shortages. One is missing variables. In our study, to clarify the specific role of EZH2 in the development of LC comprehensively, more clinical factors should be taken into consideration such as the detail of treatments for every single patient involved. However, the information of treatments was often inconsistent or even lacking in public databases; the other is sample size imbalance. We have a smaller number of healthy samples in our control group than that of LC patients in our study; the sample size imbalance may lead to statistical bias. Therefore, future prospective studies are needed to reduce analysis bias. Finally, we cannot illustrate the expression of LC from the protein level and also can not evaluate the direct mechanisms of EZH2 involved in LC progression. Consequently, further studies are needed to clarify the direct mechanisms of EZH2 in LC.

EZH2 is not only related to LC, but it is also closely related to the occurrence and development of other tumors. In diffuse large B cell lymphoma, it is found that inhibition of EZH2 activity may provide a promising treatment for EZH2 mutant lymphoma [63]. However, Another study found that diffuse large B cell lymphomas based on EZH2 mutations and BCL2 translocation genetic subtypes have higher survival rates than other subtypes [64]. This also suggests to some extent that EZH2 not only promotes tumor progression but may play a benefical role in certain tumors or certain tumor subtypes. Depending on the cellular environment and the activated oncogenic pathways, the changes in epigenetic modifications caused by EZH2 defects may lead to tumor progression through various mechanisms.

In summary, Unlike genetic mutations, epigenetic aberrations are reversible so targeting the relevant epigenetic factors by small molecules is potentially an efficient approach to “fix” dysregulated gene/ chromosome-regulatory systems caused by epigenetic changes in cancer. Additional experiments are needed to

evaluate the relationship between EZH2 expression and clinical features, LC stage, and prognosis using additional clinical data, which might facilitate the identification of new markers for evaluating tumor stage, aiding drug development, and improving treatment efficiency.

Acknowledgments

We thank the author team for their solidarity and cooperation in the completion of this study and each author for their efforts and help in this research paper.

Funding

We are grateful of funding a grant from the Qingdao 2020 Medical Scientific Research Guidance Plan (No. 2020-WJZD036).

Conflicts of interest

The authors indicated no potential conflicts of interest.

Author contributions

Conceptualization, writing-original draft, and supervision: Xiaokun Wang, Min Qi and Gaoyang Lin; methodology and formal analysis: Xu Zhu, Zhengtong Zhao, Gaoyang Lin, Yufeng Cao, and Y-FT; resources: Fuman Wang and Daijun Xing; validation and visualization: Xiaokun Wang, Min Qi, Xu Zhu, Zhengtong Zhao, Yufeng Cao, and Gaoyang Lin; writing-review and editing: Xiaokun Wang and Gaoyang Lin; funding acquisition: Gaoyang Lin and Yufeng Cao. All authors contributed to the article and approved the submitted version.

Data availability statement

The datasets presented in this study can be found in online repositories. The names of the repository/repositories and accession number(s) can be found in the article.

References

1. Sung H, Ferlay J, Siegel RL, et al. Global Cancer Statistics 2020: GLOBOCAN Estimates of Incidence and Mortality Worldwide for 36 Cancers in 185 Countries. CA Cancer J Clin. 2021;71(3):209-249.
2. Torre LA, Bray F, Siegel RL, et al. Global cancer statistics, 2012. CA Cancer J Clin. 2015;65(2):87-108.
3. Lu T, Yang X, Huang Y, et al. Trends in the incidence, treatment, and survival of patients with lung cancer in the last four decades. Cancer Manag Res. 2019;11:943-953.
4. Verdecchia A, Francisci S, Brenner H, et al; EUROCARE-4 Working Group. Recent cancer survival in Europe: a 2000-02 period analysis of EUROCARE-4 data. Lancet Oncol. 2007 Sep;8(9):784-796.
5. Gong H, Yuan Y, Li Y, et al. Role of EZH2 Inhibitor Combined with Gefitinib in EGFR-TKIs Resistant Lung Cancer Cells. Zhongguo Fei Ai Za Zhi. 2019;22(5):255-263. Chinese.
6. Duan R, Du W, Guo W. EZH2: a novel target for cancer treatment. J Hematol Oncol. 2020;13(1):104.
7. Greer EL, Shi Y. Histone methylation: a dynamic mark in health, disease and inheritance. Nat Rev Genet. 2012;13(5):343-357.
8. Margueron R, Reinberg D. The Polycomb complex PRC2 and its mark in life. Nature. 2011;469(7330):343-349.
9. Cardoso C, Mignon C, Hetet G, et al. The human EZH2 gene: genomic organisation and revised mapping in 7q35 within the critical region for malignant myeloid disorders. Eur J Hum Genet. 2000;8(3):174-180.
10. Margueron R, Li G, Sarma K, et al. Ezh1 and Ezh2 maintain repressive chromatin through different mechanisms. Mol Cell. 2008;32(4):503-518.
11. Christofides A, Karantanos T, Bardhan K, et al. Epigenetic regulation of cancer biology and anti-tumor immunity by EZH2. Oncotarget. 2016;7(51):85624-85640.
12. He A, Shen X, Ma Q, et al. PRC2 directly methylates GATA4 and represses its transcriptional activity. Genes Dev. 2012;26(1):37-42.
13. Kim E, Kim M, Woo DH, et al. Phosphorylation of EZH2 activates STAT3 signaling via STAT3 methylation and promotes tumorigenicity of glioblastoma stem-like cells. Cancer Cell. 2013;23(6):839-852.
14. Xu K, Wu ZJ, Groner AC, et al. EZH2 oncogenic activity in castration-resistant prostate cancer cells is Polycomb-independent. Science. 2012;338(6113):1465-1469.
15. Kim J, Lee Y, Lu X, et al. Polycomb- and methylation-independent roles of EZH2 as a transcription activator. Cell Rep. 2018;25(10):2808-2820.e4.
16. Nutt SL, Keenan C, Chopin M, et al. EZH2 function in immune cell development. Biol Chem. 2020;401(8):933-943.
17. Yao Y, Hu H, Yang Y, et al. Downregulation of enhancer of Zeste Homolog 2 (EZH2) is essential for the induction of autophagy and apoptosis in colorectal cancer cells. Genes (Basel). 2016;7(10):83.
18. Ito T, Teo YV, Evans SA, et al. Regulation of cellular senescence by polycomb chromatin modifiers through distinct DNA damage- and histone methylation-dependent pathways. Cell Rep. 2018;22(13):3480-3492.
19. Batool A, Jin C, Liu YX. Role of EZH2 in cell lineage determination and relative signaling pathways. Front Biosci (Landmark Ed). 2019;24(5):947-960.
20. April-Monn SL, Andreasi V, Schiavo Lena M, et al. EZH2 Inhibition as New Epigenetic Treatment Option for Pancreatic Neuroendocrine Neoplasms (PanNENs). Cancers (Basel). 2021;13(19):5014.
21. Anwar T, Gonzalez ME, Kleer CG. Noncanonical functions of the polycomb group protein EZH2 in breast cancer. Am J Pathol. 2021;191(5):774-783.
22. Chen S, Wang G, Tao K, et al. Long noncoding RNA metastasis-associated lung adenocarcinoma transcript 1 cooperates with enhancer of zeste homolog 2 to promote hepatocellular carcinoma development by modulating the microRNA-22/Snail family transcriptional repressor 1 axis. Cancer Sci. 2020;111(5):1582-1595.
23. Tellez CS, Picchi MA, Juri D, et al. Chromatin remodeling by the histone methyltransferase EZH2 drives lung pre-malignancy and is a target for cancer prevention. Clin Epigenetics. 2021;13(1):44.
24. Ma J, Zhang J, Weng YC, et al. EZH2-Mediated microRNA-139-5p Regulates Epithelial-Mesenchymal Transition and Lymph Node Metastasis of Pancreatic Cancer. Mol Cells. 2018;41(9):868-880.
25. Xu C, Hou Z, Zhan P, et al. EZH2 regulates cancer cell migration through repressing TIMP-3 in non-small cell lung cancer. Med Oncol. 2013;30(4):713.
26. Blum A, Wang P, Zenklusen JC. SnapShot: TCGA-analyzed tumors. Cell. 2018;173(2):530.
27. Love MI, Huber W, Anders S. Moderated estimation of fold change and dispersion for RNA-seq data with DESeq2. Genome Biol.

2014;15(12):550.
28. Zhou Y, Zhou B, Pache L, et al. Metascape provides a biologist-oriented resource for the analysis of systems-level datasets. Nat Commun. 2019;10(1):1523.
29. Yu G, Wang LG, Han Y, et al. ClusterProfiler: an R package for comparing biological themes among gene clusters. OMICS. 2012; 16(5):284-287.
30. Subramanian A, Tamayo P, Mootha VK, et al. Gene set enrichment analysis: a knowledge-based approach for interpreting genome-wide expression profiles. Proc Natl Acad Sci U S A. 2005; 102(43):15545-15550.
31. Hänzelmann S, Castelo R, Guinney J. GSVA: gene set variation analysis for microarray and RNA-seq data. BMC Bioinformatics. 2013;14:7.
32. Bindea G, Mlecnik B, Tosolini M, et al. Spatiotemporal dynamics of intratumoral immune cells reveal the immune landscape in human cancer. Immunity. 2013;39(4):782-795.
33. Szklarczyk D, Gable AL, Lyon D, et al. STRING v11: protein-protein association networks with increased coverage, supporting functional discovery in genome-wide experimental datasets. Nucleic Acids Res. 2019;47(D1):D607-D613.
34. Boeck S, Wittwer C, Heinemann V, et al. Cytokeratin 19-fragments (CYFRA 21-1) as a novel serum biomarker for response and survival in patients with advanced pancreatic cancer. Br J Cancer. 2013;108(8):1684-1694.
35. Fischer-Rasokat U, Renker M, Liebetrau C, et al. Long-term survival in patients with or without implantable cardioverter defibrillator after transcatheter aortic valve implantation. J Clin Med. 2021;10(13):2929.
36. Robin X, Turck N, Hainard A, et al. pROC: an open-source package for R and S+ to analyze and compare ROC curves. BMC Bioinformatics. 2011;12:77.
37. Love MI, Huber W, Anders S. Moderated estimation of fold change and dispersion for RNA-seq data with DESeq2. Genome Biol. 2014; 15(12):550.
38. Liu J, Lichtenberg T, Hoadley KA, et al; Cancer genome atlas research network; Hu H. An integrated TCGA pan-cancer clinical data resource to drive high-quality survival outcome analytics. Cell. 2018;173(2):400-416.e11.
39. Morey L, Helin K. Polycomb group protein-mediated repression of transcription. Trends Biochem Sci. 2010;35(6):323-332.
40. Sauvageau M, Sauvageau G. Polycomb group proteins: multi-faceted regulators of somatic stem cells and cancer. Cell Stem Cell. 2010;7(3):299-313.
41. O'Meara MM, Simon JA. Inner workings and regulatory inputs that control Polycomb repressive complex 2. Chromosoma. 2012;121(3):221-234.
42. Han Li C, Chen Y. Targeting EZH2 for cancer therapy: progress and perspective. Curr Protein Pept Sci. 2015;16(6):559-570.
43. Sanaei M, Kavoosi F. Effect of DNA methyltransferase in comparison to and in combination with histone deacetylase inhibitors on hepatocellular carcinoma HepG2 cell line. Asian Pac J Cancer Prev. 2019;20(4):1119-1125.
44. Gaballa JM, Braga Neto MB, Ramos GP, et al. The role of histone methyltransferases and long non-coding RNAs in the regulation of T cell fate decisions. Front Immunol. 2018;9:2955.
45. Cha TL, Zhou BP, Xia W, et al. Akt-mediated phosphorylation of EZH2 suppresses methylation of lysine 27 in histone H3. Science. 2005;310(5746):306-310.
46. Liu P, Shuaib M, Zhang H, et al. Ubiquitin ligases HUWE1 and NEDD4 cooperatively control signal-dependent PRC2-Ezh1α/β-mediated adaptive stress response pathway in skeletal muscle cells. Epigenetics Chromatin. 2019;12(1):78.
47. Ko KS, Lee M, Koh JJ, et al. Combined administration of plasmids encoding IL-4 and IL-10 prevents the development of autoimmune diabetes in nonobese diabetic mice. Mol Ther. 2001;4(4):313-316.
48. Zhao P, Bu X, Wei X, et al. Dendritic cell immunotherapy combined with cytokine-induced killer cells promotes skewing toward Th2 cytokine profile in patients with metastatic non-small cell lung cancer. Int Immunopharmacol. 2015;25(2):450-456.
49. Budhu A, Forgues M, Ye QH, et al. Prediction of venous metastases, recurrence, and prognosis in hepatocellular carcinoma based on a unique immune response signature of the liver microenvironment. Cancer Cell. 2006;10(2):99-111.
50. Qu J, Cheng T, Liu L, et al. Mast cells induce epithelial-to-mesenchymal transition and migration in non-small cell lung cancer through IL-8/Wnt/β-catenin pathway. J Cancer. 2019;10(22):5567.
51. Pirtskhalaishvili G, Shurin GV, Esche C, et al. Cytokine-mediated protection of human dendritic cells from prostate cancer-induced apoptosis is regulated by the Bcl-2 family of proteins. Br J Cancer. 2000;83(4):506-513.
52. Guéry L, Hugues S. Th17 cell plasticity and functions in cancer immunity. Biomed Res Int. 2015;2015:314620.
53. Nistala K, Adams S, Cambrook H, et al. Th17 plasticity in human autoimmune arthritis is driven by the inflammatory environment. Proc Natl Acad Sci U S A. 2010;107(33):14751-14756.
54. Wu S, Wu D, Pan Y, et al. Correlation between EZH2 and CEP55 and lung adenocarcinoma prognosis. Pathol Res Pract. 2019;215(2):292-301.
55. Wang X, Brea LT, Yu J. Immune modulatory functions of EZH2 in the tumor microenvironment: implications in cancer immunotherapy. Am J Clin Exp Urol. 2019;7(2):85-91.
56. Jiang T, Wang Y, Zhou F, et al. Prognostic value of high EZH2 expression in patients with different types of cancer: a systematic review with meta-analysis. Oncotarget. 2016;7(4):4584-4597.
57. Wang X, Zhao H, Lv L, et al. Prognostic significance of EZH2 expression in non-small cell lung cancer: A meta-analysis. Sci Rep. 2016;6:19239.
58. Wang X, Liu H, Shen K, et al. Long intergenic non-coding RNA 00467 promotes lung adenocarcinoma proliferation, migration and invasion by binding with EZH2 and repressing HTRA3 expression. Mol Med Rep. 2019;20(1):640-654.
59. Wang LJ, Sun GZ, Chen YF. LncRNA MSTO2P promotes proliferation and autophagy of lung cancer cells by up-regulating EZH2 expression. Eur Rev Med Pharmacol Sci. 2019;23(8):3375-3382.
60. Zeng SHG, Xie JH, Zeng QY, et al. lncRNA PVT1 Promotes Metastasis of Non-Small Cell Lung Cancer Through EZH2-Mediated Activation of Hippo/NOTCH1 Signaling Pathways. Cell J. 2021;23(1):21-31.
61. Chen X, Wang K. lncRNA ZEB2-AS1 aggravates progression of non-small cell lung carcinoma via suppressing PTEN level. Med Sci Monit. 2019;25:8363-8370.
62. Fortelny N, Butler GS, Overall CM, et al. Protease-Inhibitor Interaction Predictions: Lessons on the Complexity of Protein-Protein Interactions. Mol Cell Proteomics. 2017;16(6):1038-1051.
63. McCabe MT, Ott HM, Ganji G, et al. EZH2 inhibition as a therapeutic strategy for lymphoma with EZH2-activating mutations. Nature. 2012;492(7427):108-112.
64. Schmitz R, Wright GW, Huang DW, et al. Genetics and pathogenesis of diffuse large B-cell lymphoma. N Engl J Med. 2018;378(15):1396-1407.

DOI 10.1007/s10330-022-0599-9
Cite this article as: Wang XK, Qi M, Zhu X, et al. EZH2 is a biomarker associated with lung cancer diagnosis and immune infiltrates without prognostic specificity: a study based on the cancer genome atlas data. Oncol Transl Med. 2023;9(3):99–114.

Oncology and Translational Medicine
DOI 10.1007/s10330-022-0620-0
June 2023, Vol. 9, No. 3, P115–P120

ORIGINAL ARTICLE

AGAP2-AS1 affects TNM staging and prognosis of lung cancer patients by acting on SLC7A11 mRNA stability and ferroptosis*

Lin Huang[1], Bin Li[2], Zuowei Hu[1] (✉)

[1] Department of Oncology, Wuhan No.1 Hospital, Wuhan 430022, China
[2] Department of Thyroid and Breast, Wuhan No.1 Hospital, Wuhan 430022, China

Abstract

Objective The initiation and progression of lung carcinomas are critically regulated by long non-coding RNAs (lncRNAs). However, the role of lncRNAs in the pathways causing lung cancer remains unknown.

Methods Cell morphology was regularly observed using an inverted phase-contrast microscope. Cell viability was assessed using CCK-8 according to the manufacturer's instructions. Total RNA was retrotranscribed from each specimen using the RNAiso Plus Kit. The RT-PCR data were calculated using the Ct approach for comparison. Flow cytometric analyses were prepared by Click-iT™ Plus TUNEL Assay for In Situ apoptosis detection, with Alexa Fluor™ 594 dye, as instructed. RNA immunoprecipitation assays were used to determine RNA concentration.

Results Activated natural killer cells repeat and PH domain-containing protein 2 antisense RNA 1 (AGAP2-AS1) levels in cancerous tissues were significantly correlated with cancerous tumor node metastasis (TNM) stage, with cancerous AGAP2-AS1 levels being higher in cancerous tissues than healthy tissues. Patients withelevated AGAP2-AS1 levels had considerably worse outcomes than those with reduced AGAP2-AS1 levels,regardless of the progression-free or overall survival. Functionally, AGAP2-AS1 downregulation represseslung cancer cell growth. AGAP2-AS1 elimination induces erastin-mediated ferroptosis in lung cancer cells.However, the ferritin inhibitor FERSINT-1 negated this result, whereas ERASTIN induced lung cancer cellmortality. After AGAP2-AS1 silencing, erastin-treated lung cancer cells showed a remarkable decrease inGSH levels. These results indicated that AGAP2-AS1 enhanced the stabilization of SLC7A11 mRNA via Recombinant Insulin Like Growth Factor Binding Protein 2(IGF BP2). Patients with elevated AGAP2-AS1 had considerably worse outcomes. Down-regulating AGAP2-AS1 was able to repress lung cancer cell growth and induce greater Erastin-mediated ferroptosis. Lungcancer cells treated with Erastin exhibited a remarkable decrease inglutathione (GSH) levels. The mechanical findingsindicated that AGAP2-AS1 enhanced the stabilization of SLC7A11 mRNA via the IGF2BP2.

Conclusion We identified a novel effect of AGAP2-AS1 on TNM staging and the prognosis of patientswith lungcancer by modulating SLC7A11 mRNA stability and ferroptosis.

Received: 25 November 2022
Revised: 15 March 2023
Accepted: 18 April 2023

Key words: AGAP2-AS1; ferroptosis; lung cancer; mRNA stability

Lung carcinoma is a malignant neoplasm characterized by mutations in lung cells and their proliferation. Patients with advanced metastatic lung cancer have a low survival rate [1, 2]. Lung cancer is responsible for over 30% of all malignant mortalities [3]. Factors that can induce these conditions include environmental factors (e.g. air pollution) and genetics. Early stage patients with lung cancer have a higher five-year survivability after prolonged resection and lymph node dissection [4]; however, the five-year survival rate for patients with distant metastasis is extremely low, and the prognosis is poor. In metastatic lung cancer patients with advanced chemotherapy and radiotherapy, 15%–20% of treatments succeed, but their survival time is short [5].

Iron toxicity is a relatively new form of controlling cell death (RCD). Ergot inhibits the onset of RCD, particularly in cancer cells with mutations in the RAS signaling pathway [6]. Increasing tumorigenesis by suppressing

✉ Correspondence to: Zuowei Hu. Email: 827823053@qq.com
* Supported by the Wuhan Municipal Health Commission Medical Research Project-Youth Project (No. WZ20Q04).

Table 1 PCR primer Sequence

Gene	F Sequence (5'-3')	R Sequence (5'-3')
AGAP2-AS1	TACCTTGACCTTGCTGCTCTC	TACCTTGACCTTGCTGCTCTC
U6	CTCGCTTCGGCAGCACAT	TTTGCGTGTCATCCTTGCG
GAPDH	GTCTCCTCTGACTTCAACAGCG	ACCACCCTGTTGCTGTAGCCAA
SLC7A11	TCCTGCTTTGGCTCCATGAACG	AGAGGAGTGTGCTTGCGGACAT

ferroptosis, which plays a critical role in the progression of malignancies, enhances the initiation of neoplasms [7]. Ferroptosis is not fully understood as the mechanism underlying lung cancer growth [8, 9].

Long non-coding RNAs (lncRNAs) have been consistently regarded as "noise" in transcription [10]. Studies have shown lncRNAs could regulate genomic expression and affect organism growth and development [11]. It has been found that lncRNAs are involved in several crucial processes and regulate gene expression at various levels [12]. An increasing amount of data has shown that lncRNAs are the most diverse functional ncRNAs [13]. LncRNA malfunction has a significant influence on cytoplasmic integrity. Non-expression of *AGAP2-AS1* contributes to GXP4 mRNA deterioration via m5C-dependent regulation as well as the modification of SLC7A11 mRNA by m5C and its binding to *AGAP2-AS1*.

Materials and methods

TCGA database retrieval

From the TCGA (http://tcga-adtaa. nci. nih. gov/tcga/) database using the Epicalc function package of R 2.15.3 software to download and preprocess the *AGAP2-AS1* data from the lung cancer data set for analysis.

Cell culture

Human lung cancer cells (A549 cells) were cultured in DMEM medium containing 10% fetal bovine serum (FBS). An incubator with 5% CO_2 and 95% humidity at 37°C was used for all of lung-cancer cells. Regular observations of cell morphology were performed using an inverted phase-contrast microscope.

CCK-8 assay

The cells were trypsinized, rinsed and incubated at 5000 cells/well in 96-well plates. Erastin was applied at various concentrations to the cells. After incubation for approximately 24 h, supernatants were collected. Cell viability was assessed using the CCK-8 (Enzo Life Sciences) according to the manufacturer's instructions. The absorbance at 450 nm was measured using a microplate reader. Proliferation assays were performed independently and repeatedly in triplicate. Culture conditions were as follows (1) The 6-well plate was laid according to the steps of instructions, and cells were transfected overnight according to the steps of instructions. (2) After 12 h of transfection, the cells were counted and the transfected cells were inoculated on a 96-well plate with a density of 2×10^3/well, with three wells in each group. (3) The 96-well plates of A549 cells were cultured in a 5% CO_2 incubator at 37°C. Then cell proliferation was measured at 0, 24, 48, 72 and 96 h using the CCK-8 kits (Tokyo Dojindo, Japan). The CCK-8 working solution was added as gently as possible to prevent air bubbles from interfering with the subsequent absorbance measurements. The ratio of CCK-8 to serum-free medium was approximately 1:10. (4) A 96-well plate with the CCK-8 working solution was incubated in a cell incubator for 2 h, and the absorbance at 450 nm was measured using an enzyme-labeling instrument, which was used for the CCK-8 analysis to indirectly reflect the number of living cells (American Bole).

Real-time (RT) quantitative PCR test

After 24 h plasmid transfection, total RNA was extracted from tissues or cells using TRIzol reagent (Invitrogen) and purified using RNase R reagent (Epicenter). Total RNA was reverse-transcribed into cDNA using the Prime Script RT Reagent Kit (Takara, Japan). Total RNA was reverse transcribed from each specimen using an RNAiso Plus Kit (Takara, Japan). Following the completion of the RT-PCR reactions, the data were calculated using the Threshold cycle approach for comparison, and each specimen's expression of β-actin served to standardize the results. The primer sequences used are listed in Table1. The relative expression level of total RNA was analyzed by $2^{-\Delta Ct}$ method.

Flow cytometric analysis

Following a 48-h transfection, flow cytometric measurements were prepared by Click-iT™ Plus TUNEL Assay for In Situ Apoptosis Detection, Alexa Fluor™ 594 dye (Invitrogen) as instructed. Individual stages were classified, and the proportions of dying, presorting, and apoptotic cells were evaluated based on standards. The cells were cultured for 48 h, rinsed with PBS, 500μl binding buffer was added, and then mixed with 10μL

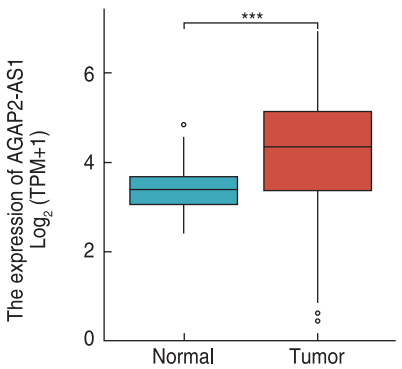

Fig. 1 The levels of *AGAP2-AS1* in normal and lung cancer cases in TCGA. *** $P < 0.001$ for comparison between groups

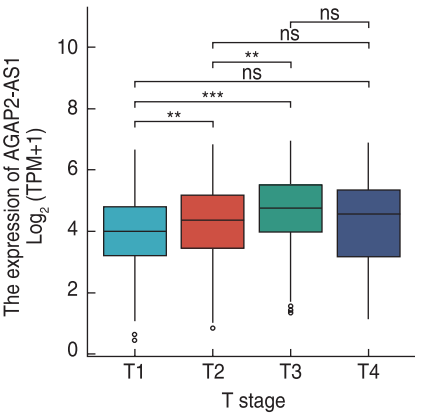

Fig. 2 According to the TCGA database, levels of *AGAP2-AS1* correlations were analyzed relative to lung cancer specimens and the clinical features of the patients. * $P < 0.05$ and ** $P < 0.01$ for comparison between groups

AnnexinV-FITC and 5μL PI solution. The solution was incubated for 10 min out of direct sunlight. The rate of apoptosis was determined using flow cytometry.

Staining of reactive oxygen species assay

To remove serum, the cells were rinsed with PBS at least twice, then resuspended in Hanks' Balanced Salt Solution (HBSS) (containing Mg^{2+} and Ca^{2+}) at a density of 1×10^6 /mL. Afterwards, the cell suspension was mixed and maintained at 37°C in a darkroom for 10 min, before being labeled by adding 5–6 liters of HBSS. After rinsing once with ice-cold complete media, all cells were assessed simultaneously using a FACSCalibur.

RNA immunoprecipitation (RIP) assay

The RIP test was performed using an RIP kit (Bersin Bio) as per the manufacturer's instructions. When cells reached 85% confluency, they were lysed with RIP buffer. Multiwell spectrophotometers (Bio-Rad, USA) were used to calculate RNA concentration, and specific foci (Agilent, USA) were used to determine RNA integrity. Finally, the immunoprecipitated RNA was harvested and analyzed by qRT-PCR.

Statistical analysis

All data collected from several tests are expressed as mean ± SD. In addition to one-way and two-way ANOVA, Student's *t*-tests were used to determine the levels of significance. All statistical analyses were performed using Graphpad Prism 9.0 Software.

Results

Upregulated *AGAP2-AS1* could predict patient prognosis

First, the levels of *AGAP2-AS1* in normal and lung carcinoma specimens were obtained from the TCGA database. There was a dramatic difference in *AGAP2-AS1* levels in normal tissues compared to lung cancer tissues,

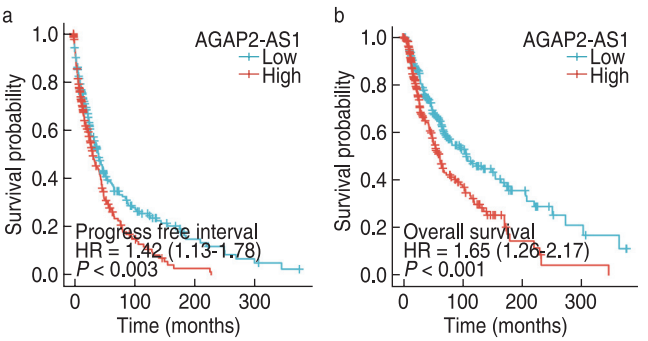

Fig. 3 PFS and OS of lung-cancer patients with various *AGAP2-AS1* levels

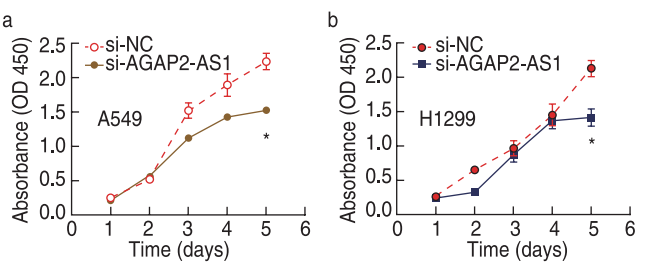

Fig. 4 *AGAP2-AS1* can promote proliferation of lung-cancer cells. * $P < 0.05$ for comparison between groups

where *AGAP2-AS1* levels were lower in cancerous samples (Fig. 1).

According to our findings, *AGAP2-AS1* levels in cancerous tissues were remarkably related to the TNM stage (Fig. 2).

A clear association was observed between higher *AGAP2-AS1* levels and shorter life expectancy. Patients with higher *AGAP2-AS1* levels had not only a significantly shorter progression-free survival (PFS) but

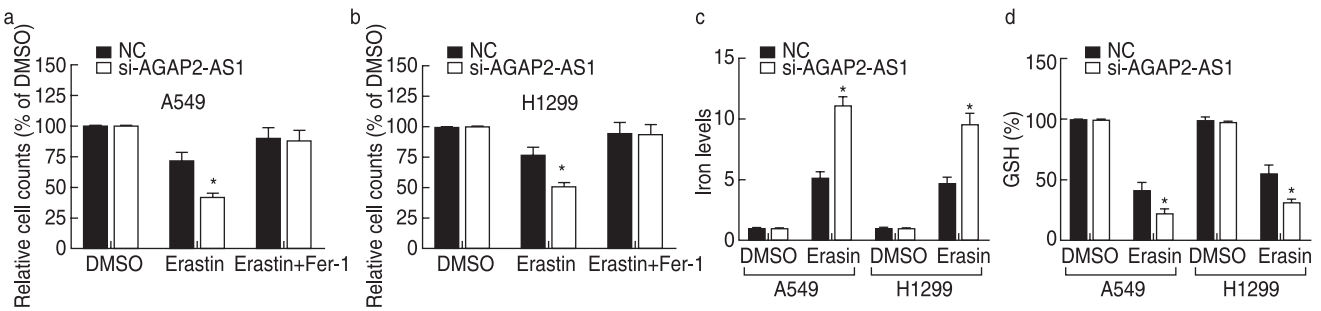

Fig. 5 *AGAP2-AS1* prevents ferroptosis of lung cancer cells. * $P < 0.05$ for comparison between groups

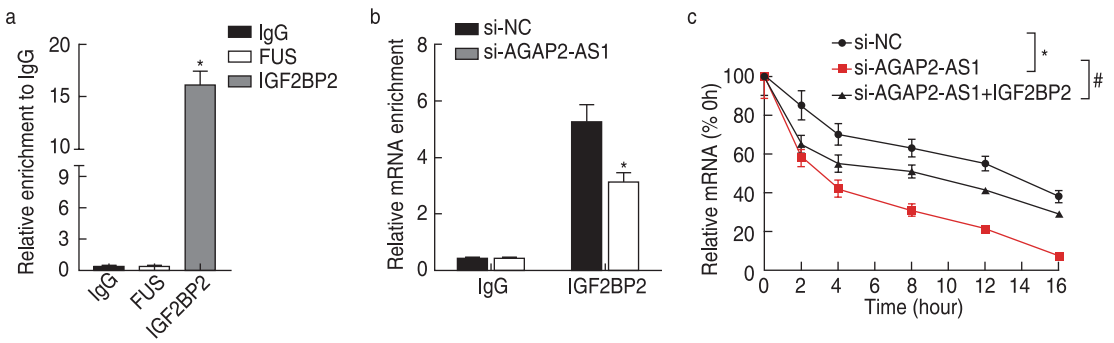

Fig. 6 *AGAP2-AS1* was able to regulate the mRNA stabilization of SLC7A11 via IGF2BP2. * $P < 0.05$ for comparison between IgG and IGF2BP2 groups; # $P < 0.05$ for comparison between si-AGAP2-AS1 and si-AGAP2-AS1+IGF2BP2 groups

also a significantly shorter overall survival (OS; Fig. 3).

AGAP2-AS1 promotes the proliferation of lung-cancer cells

After 48 and 72 h, CCK-8 data showed that the uptake rate of *AGAP2-AS1* was considerably lower than that of the other two groups, with increasing differences over time. These findings suggest that the downregulation of *AGAP2-AS1* inhibits the growth of lung cancer cells (Fig. 4).

AGAP2-AS1 could prevent ferroptosis of lung cancer cells

We tested the effects of the ferroptosis inducer erastin on the activity of tumor cells. After transfection and erastin treatment, the knockdown of *AGAP2-AS1* amended Erastin-mediated ferroptosis (Fig. 5a and 5b). Concomitantly, we found that the ferroptosis inhibitor FERSINT-1 restored this effect, whereas erastin caused lung cancer cell mortality (Fig. 5a and 5b). This indicates that *AGAP2-AS1* downregulation enhances ferroptosis. These results suggest that *AGAP2-AS1* silencing inhibited the proliferation of lung cancer cells and enhanced ferroptosis. Subsequently, the influence of *AGAP2-AS1* accumulation on ferroptosis and GSH levels was assessed. Because Fe^{2+} is an essential contributor to ferroptosis, we initially evaluated the effects of *AGAP2-AS1* on intracellular Fe^{2+} concentrations. The findings showed that intracellular iron and Fe^{2+} levels were upregulated upon *AGAP2-AS1* silencing with erastin (Fig. 5c). Furthermore, *AGAP2-AS1* knockdown led to a remarkable decrease in GSH content in rastin-treated lung cancer cells (Fig. 5d). Blocking *AGAP2-AS1* facilitates ferroptosis in lung cancer cells, implying that *AGAP2-AS1* contributes to anti-ferroptosis effects.

AGAP2-AS1 can enhance SLC7A11 mRNA stabilization via IGF2BP2

Therefore, we investigated the modulatory association between SLC7A11 and *AGAP2-AS1*. Initially, RIP assays were performed to examine the interplay between SLC7A11 and IGF2BP2. SLC7A11 and IGF2BP2 could interact, however *AGAP2-AS1* knockdown reduced this interaction. Moreover, subsequent mRNA degradation revealed that *AGAP2-AS1* knockdown reduced SLC7A11 mRNA stabilization, while over-expression reversed the functionality of *AGAP2-AS1*. These findings revealed that *AGAP2-AS1* enhanced the stabilization of SLC7A11 mRNA via IGF2BP2.

Discussion

While immunosuppressive therapy significantly improved survival rates in some populations with lung

cancer, it does not help about 40–60% of patients [14]. The same group of chemotherapeutic drugs has shown remarkable benefits in the treatment of lung cancer subtypes [10]. LncRNAs are integral to the multiplication, differentiation, and apoptotic processes of various malignancies. LncRNAs have been shown to be involved in the neoplastic cell cycle, cell signaling pathways, and genetic modifications, leading to the emergence of lncRNAs as potential candidates for investigation [15].

An lncRNA is a protein-coding gene that is unable to encode a protein, although it directly performs biofunctions in the form of RNA [16]. With a length of over 200 of nucleotides, it is incomplete in its open read frame [17, 18]. LncRNAs are then transcribed by RNA Polymerase II and subsequently amended by 5' end-capping, splicing, and 3' end-polyadenylation [19]. Primarily, they are believed to serve non-biological roles; however, the findings of numerous assays revealed that lncRNAs mediate genetic regulation in the form of RNA along numerous layers, including transcription, post-transcriptional profiling, and epigenetics [20, 21]. LncRNAs mainly perform their effects in four ways: first, by induction, lncRNAs are able to associate with particular miRNAs and hence regulate targeted genes obliquely; second, lncRNAs can serve as signaling agents working on pathways to modulate associated genes up and downstream of their targeted genes [22, 23]. Furthermore, lncRNAs can regulate specific target genes by guiding associated RNA-binding proteins via cis- or trans-regulation of protein complexity sites [24, 25]. Finally, in scaffolding, lncRNAs may serve as a platform on which a diverse combination of relevant regulatory compounds can act to strengthen messaging and the interplay between molecular complexities [26].

We investigated the functions of *AGAP2-AS1* by examining the clinical characteristics of patients with lung carcinoma and lung carcinoma cell lines. We found that *AGAP2-AS1* was more highly expressed in lung carcinoma than in normal and healthy neighboring tissues, while *AGAP2-AS1* was more strongly expressed in the lung metastasis group than in the non-distant metastasis group. This is in agreement with the results of other investigators who analyzed lncRNA expression levels in other neoplastic specimens, indicating that *AGAP2-AS1* might be involved in the initiation and promotion of lung carcinoma [27]. Additionally, the presence of *AGAP2-AS1* in lung carcinoma samples may influence the OS of patients with lung carcinoma. The greater the expression of *AGAP2-AS1* in lung carcinoma, the worse the prognosis. In vitro experiments demonstrated that elimination of *AGAP2-AS1* expression suppressed cell growth and caused ferrotoxicity in cells. The use of ROCK suppressors has gained attention in contemporary medicine with increasingly efficient targeted approaches [17].

In conclusion, this study identified a novel behavior of *AGAP2-AS1* and the underlying mechanisms of ferroptosis and lung cancer initiation, which may aid in the development of new lung cancer therapies. We identified a novel effect of *AGAP2-AS1* on TNM staging and prognosis of patients with lung cancer by acting on SLC7A11 mRNA stability and ferroptosis.

Acknowledgments

We thank all the people who helped us during the experiment and writing stage. They gave us a lot of useful advice.

Funding

This study was supported by the Wuhan Municipal Health Commission Medical Research Project-Youth Project (No.WZ20Q04).

Conflicts of interest

The authors declare no conflicts of interest.

Author contributions

All authors contributed to data acquisition and interpretation and reviewed and approved the final version of this manuscript.

Data availability statement

The data supporting the findings of this study are available from the first author upon request.

Ethical approval

Not applicable.

References

1. Wu FY, Wang L, Zhou CC. Lung cancer in China: currentand prospect. Curr Opin Oncol. 2021;33(1):40-46.
2. Gérard Zalcman, Valérie Gounant.Does lung cancer patients' survival increase? Rev Prat. 2020;70(8):827-833.
3. Minca EC, Al-Rohil RN, Wang M, et al. Comparison between lung cancer gene expression score and fluorescence in situ hybridization for the classification of melanocytic lesions. Mod Pathol. 2016;29(8):832-843.
4. Schabath MB, Cote ML. Cancer progress and priorities: lung cancer. Cancer Epidemiol Biomarkers Prev. 2019;28(10):1563-1579.
5. Schenk EL, Patil T, Pacheco J, Bunn PA Jr. 2020 Innovation-based optimism for lung cancer outcomes. Oncologist. 2021;26(3):e454-e472.
6. Sun S, Zhang G, Zhang L. A novel ferroptosis-related lncRNA prognostic model and immune infiltration features in skin cutaneous melanoma. Front Cell Dev Biol. 2022;9:790047.
7. Mou YH, Wang J, Wu JC, et al. Ferroptosis, a new form of cell death: opportunities and challenges in cancer. J Hematol Oncol. 2019;12(1):34.
8. Wu XY, Jin SL, Yang YW, et al. Altered expression of ferroptosis markersand iron metabolism reveals a potential role of ferroptosis in

vitiligo. Pigment Cell Melanoma Res. 2022;35(3):328-341.
9. Liu CJ, Liu YH, Yu YF, et al. Comprehensive analysis of ferroptosis-relatedgenes and prognosis of cutaneous melanoma. BMC Med Genomics. 2022;15(1):39.
10. Kunej T, Obsteter J, Pogacar Z, et al. The decalog of long non-codingRNA involvement in cancer diagnosis and monitoring. Crit Rev Clin.Lab Sci. 2014;51(6):344-357.
11. Ghafouri-Fard S, Abak A, Talebi SF, et al. Role of miRNA and lncRNAs in organ fibrosis and aging. Biomed Pharmacother. 2021; 143:112132.
12. Gil N, Ulitsky I. Regulation of gene expression by cis-acting long non-coding RNAs. Nat Rev Genet. 2020;21(2):102-117.
13. Peng WX, Koirala P, Mo YY. LncRNA-mediated regulation of cellsignaling in cancer. Oncogene. 2017;36(41):5661-5667.
14. Spain L, Diem S, Larkin J. Management of toxicities of immunecheckpoint inhibitors. Cancer Treat Rev. 2016;44:51-60.
15. Santoni G, Morelli MB, Amantini C, et al. Urinary markers in bladder cancer: an update. Front Oncol. 2018;8:362.
16. Le M, Muntyanu A, Netchiporouk E. lncRNAs and circRNAsprovide insight into discoid lupus pathogenesis and progression. AnnTransl Med. 2020;8(6):260.
17. Gu CL, Meng YG, Meng QQ, et al. Exploring the Potential Key lncRNAswith Endometriosis by Construction of a ceRNA Network. Int J GenMed. 2021;14:4161-4170.
18. Li L, Zhang YM, Luo HH, et al. Systematic identification and analysis of expression profiles of mRNAs and incrnas in macrophage inflammatory response. Shock. 2019;51(6):770-779.
19. Gandhy SU, Imanirad P, Jin UH, et al. Specificity protein (Sp) transcription factors and metformin regulate expression of the longnon-coding RNA HULC. Oncotarget. 2015;6(28):26359-26372.
20. Sun TC, Zhang Y, Yu K, et al. LncRNAs induce oxidative stress andspermatogenesis by regulating endoplasmic reticulum genes and pathways. Aging (Albany NY). 20216;13(10):13764-13787.
21. Beylerli O, Gareev I, Sufianov A, et al. Long noncoding RNAs aspromising biomarkers in cancer. Noncoding RNA Res. 2022;7(2): 66-70.
22. Abdi E, Latifi-Navid S, Latifi-Navid H. Long noncoding RNA polymorphisms and colorectal cancer risk: Progression and futureperspectives. Environ Mol Mutagen. 2022;63(2):98-112.
23. Huang WX, Li H, Yu QS, et al. LncRNA-mediated DNA methylation: anemerging mechanism in cancer and beyond. J Exp Clin Cancer Res. 2022;41(1):100.
24. Wang W, Hao LP, Song HZ, et al. The potential roles of exosomalnon-coding RNAs in hepatocellular carcinoma. Front Oncol. 2022;12:790916.
25. Nukala SB, Jousma J, Cho Y, et al. Long non-coding RNAs and microRNAs as crucial regulators in cardio-oncology. Cell Biosci. 2022;12(1):24.
26. Yang CB, Chen KS. Long Non-coding RNA in esophageal cancer: Areview of research progress. Pathol Oncol Res. 2022;28:1610140.
27. Pierce JB, Zhou HY, Simion V, et al. Long noncoding RNAs astherapeutic targets. Adv Exp Med Biol. 2022;1363:161-175.

DOI 10.1007/s10330-022-0620-0
Cite this article as: Huang L, Li B, Hu ZW. AGAP2-AS1 affects TNM staging and prognosis of lung cancer patients by acting on SLC7A11 mRNA stability and ferroptosis. Oncol Transl Med. 2023;9(3):115–120.

Oncology and Translational Medicine
DOI 10.1007/s10330-022-0601-1

June 2023, Vol. 9, No. 3, P121–P132

ORIGINAL ARTICLE

MiR-183-5p promotes the progression of non-small cell lung cancer through targeted regulation of FOXO1

Yan Deng, Zhengguang He, Xiaobin Luo, Rong Qiu (✉), Yong Zhao, Wen Luo

Department of Respiratory and Critical Care Medicine, Suining Central Hospital, Suining 629000, China

Abstract

Objective To investigate miR-183-5p targeting to forkhead box protein O1 (FOXO1) and its corresponding effect on the proliferation, migration, invasion, and epithelial-mesenchymal transition (EMT) of non-small cell lung cancer (NSCLC) cells.

Methods NSCLC tissues and adjacent normal tissues from 60 patients with NSCLC adenocarcinoma were obtained via pathological biopsy or intraoperative resection. Several cell lines were cultured *in vitro*, including the human normal lung epithelial cell line BEAS-2B and human NSCLC cell lines A549, SPCA-1, PC-9, and 95-D. miR-183-5p and FOXO1 mRNA expression in tissues and cells were detected by qRT-PCR; the corresponding correlations in NSCLC tissues were analyzed using the Pearson test, and the relationship between miR-183-5p expression and clinicopathological parameters was analyzed. The miR-183-5p-mediated regulation of FOXO1 was verified by bioinformatics prediction alongside double luciferase, RNA-binding protein immunoprecipitation (RIP) assay, and pull-down experiments. A549 cells were divided into control, anti-miR-NC, anti-miR-183-5p, miR-NC, miR-183-5p, miR-183-5p+pcDNA3.1, and miR-183-5p+pcDNA3.1-FOXO1 groups. Cell proliferation, invasion, migration, apoptosis, and cell cycle distribution were detected using an MTT assay, clone formation assay, Transwell assay, scratch test, and flow cytometry, respectively. The expression of EMT-related proteins in the cells was analyzed by western blotting. The effect of miR-185-3p silencing on the development of transplanted tumors was detected by analyzing tumor formation in nude mice.

Results miR-183-5p expression was significantly higher in NSCLC tissues and cells than in adjacent normal tissues, whereas FOXO1 mRNA expression was significantly down-regulated. There was a significant negative correlation between miR-183-5p and FOXO1 mRNA in NSCLC tissues ($P < 0.05$). Additionally, the expression of miR-183-5p was significantly correlated with tumor size, tumor differentiation, and tumor-node-metastasis stage in patients with NSCLC ($P < 0.05$). miR-183-5p targeted and inhibited FOXO1 expression. Compared to the anti-miR-NC group, the cell proliferation, scratch healing rate, N-cadherin and vimentin protein expression, and the proportion of S phase cells were significantly lower in the anti-miR-183-5p group, whereas the protein expression of E-cadherin and α-catenin and the proportion of G0/G1 phase cells were significantly higher; additionally, the frequency of colony formation and invasion were significantly lower in the anti-miR-183-5p group ($P < 0.05$). Compared to the miR-NC group, the cell proliferation, scratch healing rate, N-cadherin and vimentin protein expression, and the proportion of S phase cells in the miR-183-5p group were significantly higher, whereas the E-cadherin and α-catenin protein expression and the proportion of G0/G1 phase cells were significantly lower; furthermore, the frequency of colony formation and invasion were significantly higher in the miR-183-5p group ($P < 0.05$). Compared with the miR-183-5p+pcDNA3.1 group, the OD value, scratch healing rate, N-cadherin and vimentin protein expression, and the proportion of S phase cells were significantly lower in the miR-183-5p+pcDNA3.1-FOXO1 group, whereas E-cadherin and α-catenin protein expression and the proportion of G0/G1 phase cells were significantly higher; additionally, the frequency of colony formation and invasion was significantly lower in the miR-183-5p+pcDNA3.1-FOXO1 group ($P < 0.05$). Overall, silencing miR-185-3p inhibited the growth of transplanted tumors and promoted FOXO1 expression.

Conclusion Overexpression of miR-183-5p can inhibit apoptosis and promote the proliferation, migration, invasion, and EMT, of NSCLC cells by down-regulating FOXO1 expression.

Key words: non-small cell lung cancer; miR-183-5p; forkhead box protein O1; malignant biological behavior; targeted regulation

Received: 12 October 2022
Revised: 23 May 2023
Accepted: 15 June 2023

✉ Correspondence to: Rong Qiu. Email: 443182163@qq.com

Lung cancer is a malignant tumor with the highest morbidity and mortality of all cancers in China [1]. According to histological characteristics, lung cancer is divided into small cell lung cancer and non-small cell lung cancer (NSCLC), with NSCLC accounting for approximately 80% of total lung cancer diagnoses [2]. Approximately 90% lung cancer patient deaths are attributed to distal metastasis [3]; therefore, it is of particular importance to elucidate the mechanism of lung cancer cell metastasis and invasion. MicroRNA (miRNA) is a type of non-coding RNA that plays a key role in post-transcriptional gene regulation and target protein degradation. In recent years, miRNAs have been determined to be closely associated with the biological function of many kinds of tumor cells, including NSCLC cells [4, 5]. miR-144-3p expression is down-regulated in NSCLC tissues and cells; in contrast, its overexpression promotes apoptosis and inhibits the proliferation and migration of NSCLC cells [6]. Additionally, miR-183-5p is closely related to the occurrence and development of various diseases; for example, miR-183-5p is highly expressed in acute myeloid leukemia cells. The up-regulation and silencing of miR-183-5p expression are related to cell proliferation, differentiation, and development of acute myeloid leukemia; therefore, miR-183-5p is a novel prognostic biomarker and therapeutic target [7]. Wang *et al.* [8] established that miR-183-5p acts as a tumor-promoting factor in NSCLC, and down-regulation of its expression can inhibit cell proliferation and promote apoptosis, thereby inhibiting NSCLC progression. However, at present, few studies have evaluated the relationship between miR-183-5p and NSCLC progression, and its mechanism is yet to be elucidated. Forkhead box protein O1 (FOXO1) belongs to the FOXO family; it is abnormally expressed in colon and gastric cancer and is closely associated with the prognosis of patients [9, 10]. Additionally, some studies have confirmed that FOXO1 is associated with the proliferation, migration, invasion, and anti-radiation of NSCLC cells; therefore, this protein may be a potential therapeutic target for the enhancement of NSCLC radiosensitivity [11]. Through bioinformatics prediction, a targeted relationship between miR-183-5p and FOXO1 has been found. Down-regulation of miR-183-5p can promote the expression of FOXO1 and inhibit the proliferation, invasion, and angiogenesis of colorectal cancer cells; therefore, miR-183-5p can inhibit the progression of colorectal cancer [12]. However, the effects of miR-183-5p and FOXO1 on the biological functions of NSCLC cells have not yet been reported. Therefore, this study was conducted to explore the effects of miR-183-5p on the proliferation, migration, invasion, and epithelial-mesenchymal transition (EMT) of NSCLC cells through the targeted regulation of FOXO1 to provide further molecular targets for the treatment of NSCLC.

Materials and methods

Samples and participants

Lung cancer tissue (taken from > 5 cm of tumor foci) and corresponding paracancerous tissue samples were collected from 60 patients with lung cancer adenocarcinoma that were treated in our hospital from September 2020 to September 2022 and then preserved in liquid nitrogen. The clinical data, such as sex, age, and tumor diameter, were collected. No patients were treated with radiotherapy or chemotherapy. All the samples were collected following informed consent from the patients and their families. The research scheme was approved by the Ethics Committee of our hospital (051237L).

Reagents and instruments

Normal human lung epithelial cell line BEAS-2B and human NSCLC cell lines A549, SPCA-1, PC-9, and 95merD were purchased from Shanghai Cell Resource Center (Chinese Academy of Sciences, China). Reagents used include the following: Dulbecco's modified eagle medium (DMEM; Gibco Company, USA); fetal bovine serum (Sijiqing, China); Lipofectamine 2000 kit, Opti-MEM medium, TRIzol reagent, reverse transcriptase kit, trypsin (Thermo Fisher Scientific Company, USA); MTT solution (Sigma-Aldrich Co., Ltd., USA); Matrigel (Millipore Co., Ltd., USA); BCA Kit (Shanghai enzyme Union Biotechnology Co., Ltd., China); horseradish peroxidase labeled rabbit anti-IgG secondary antibody (LI-COR Biosciences Co., Ltd., USA); ECL developer (Shanghai Biyuntian Biotechnology Co., Ltd., China). The pcDNA3.1 vector and FOXO1 overexpression plasmid were purchased from Addgene (Addgene, USA); N-cadherin, vimentin, E-cadherin, and α-catenin primary antibodies were purchased from Abcam (Abcam Co., Ltd., UK). The equipment is listed as follows: NanoDrop 2000 ultramicro spectrophotometer (Thermo Fisher Scientific Co., Ltd., USA), BD FACSAria flow cytometer (BD Biosciences, USA), and IX71 inverted microscope (Olympus, Japan).

Cell culture, grouping, and transfection

The human NSCLC and normal lung epithelial cell lines were cultured in DMEM containing 10% fetal bovine serum and 100 U/mL penicillin and streptomycin at 37 °C and 5% CO_2. When adherent growth of the cells was observed, and confluence reached 85%, 25% trypsin was added for cell digestion. The digested cells were placed in the DMEM culture medium to continue culturing and passage; then, the expression of miR-183-5p and FOXO1 mRNA in each cell line was detected using qRT-PCR.

A549 cells were divided into 7 groups: control (untreated), anti-miR-NC (anti-miR-183-5p negative control), anti-miR-183-5p (anti-miR-183-5p

Table 1 PCR primer sequences

Genes	Upstream primer (5'-3')	Downstream primer (5'-3')
miR-183-5p	ATCTCACCAAACGACCGACT	TCCTGGCATCATTGGAGGAG
FOXO1	GGATGTGCATTCTATGGTGTACC	TTTCGGGATTGCTTATCTCAGAC
U6	GCGCGTCGTGAAGCGTTC	GTGCAGGGTCCGAGG

transfection), miR-NC (miR-183-5p negative control), miR-183-5p (miR-183-5p transfection), MiR-183-5p+pcDNA3.1 (transfected with miR-183-5p and pcDNA3.1-FOXO1 negative control pcDNA3.1), and miR-183-5p+pcDNA3.1-FOXO1 (transfected with miR-183-5p and pcDNA3.1-FOXO1). Transfection was conducted using the Lipofectamine 2000 kit, containing 500 μL Opti-MEM medium (100 nM mimic/inhibitor or its negative control), and 2 μL Lipofectamine 2000; the corresponding reagents were added to a 24-well plate inoculated with the A549 cells. After 48 h of culture, the cells were collected for follow-up experiments.

Target gene prediction and dual luciferase reporter assay

The related target genes of miR-183-5p were predicted using the DIANA-mirPath v.3 tools (http://diana.imis.athena-innovation.gr); consequently, the *FOXO1* gene was determined to be a potential target gene of miR-183-5p. The 3′ untranslated region (UTR) of FOXO1 wild type (FOXO1 3′UTR-WT) and FOXO1 mutant 3′UTR (FOXO1 3′UTR-MUT) luciferase expression vectors were constructed and co-transfected into A549 cells with miR-NC and miR-183-5p, using the Lipofectamine 2000 kit. Luciferase activity was detected according to the manufacturer's instructions, and the experiment was repeated 3 times.

RNA-binding protein immunoprecipitation (RIP) assay

A Magna RIP RNA binding protein immunoprecipitation kit (Merck Millipore, USA) was used for RIP analysis. The specific procedure was as follows: the cultured A549 cells were collected and resuscitated with RIP lysis buffer; the cells were then incubated with magnetic beads conjugated with anti-AGO2 antibody or IgG antibody overnight at 4 °C; the following day, after washing 3 times, the magnetic beads were incubated with protease K. Finally, the total RNA was extracted, and cDNA was synthesized; the relative expression of miR-183-5p and FOXO1 mRNA were determined using qRT-PCR.

RNA pull-down

Approximately 2×10^7 A549 cells were cultured in two 15 cm petri dishes. Then, the biotin-labeled miRNA probe (miR-183-5p-Bio group) and negative control probe (Bio-NC group) were transfected. After 48 hours of culture, the cells were washed twice with precooled phosphate-buffered saline (PBS). An miRNA pull-down kit (Guangzhou Boxin Biotechnology Co., Ltd., China) was used for miRNA pull-down test. According to the manufacturer's instructions, magnetic bead sealing, cell lysis, hybridization incubation, elution, and RNA precipitation were conducted in turn. After completing the pull-down experiment, enrichment was detected by qRT-PCR.

qRT-PCR of miR-183-5p and FOXO1 mRNA in tissues and cells

Total RNA in tissues and cells was extracted using TRIzol reagent; this RNA was then reverse transcribed into cDNA according to manufacturer's instructions. For post-transcriptional amplification, 1 μL of cDNA was used; U6 was used as the internal reference. qRT-PCR reaction conditions were as follows: an initial pre-denaturation at 95 °C for 30 s, followed by 40 cycles of 95 °C for 10 s and 60 °C for 30 s. The relative expression levels of miR-183-5p and FOXO1 mRNA were calculated using the $2^{-\Delta\Delta CT}$ formula. PCR primer sequences are shown in Table 1.

MTT assay

The transfected A549 cells were inoculated into a 96-well plate at a density of 5×10^3 cells per well and incubated with 180 μL of DMEM for 0, 24, 48, and 72 h. Additionally, 20 μL of MTT solution and 150 μL of dimethyl sulfoxide were added to each well after 10 min. The optical density (OD) of each well was measured at 490 nm using an enzyme labeling instrument (Thermo Fisher Scientific, USA).

Clone formation experiment

The transfected A549 cells were inoculated in a 6-well plate at a density of 1×10^3 cells per well and cultured for 2 weeks. When the clone colony was visible to the naked eye, the culture was terminated, fixed with formaldehyde, stained with Giemsa, washed, and dried. The colony formation of cells was observed and counted under light microscope. This experiment was repeated 3 times.

Transwell chamber experiment

A Transwell system (aperture 8 mm; Corning Costar, USA) with Matrigel (Millipore) was used to measure cell migration ability. The transfected A549 cells were

suspended in a serum-free RPMI 1640 medium and inoculated into the upper chamber, which contained RPMI 1640 medium supplemented with 20% fetal bovine serum. After 24 h of culture, methanol was used to fix the samples; cells were then stained with 0.1% crystal violet. An IX71 inverted microscope (Olympus) was used to image the samples to observe the samples and count the number of invading cells.

Scratch test

The transfected A549 cells were inoculated into a 6-well plate. After reaching 80% confluence, the tip of the pipette was used to form scratches in the middle of each hole. PBS was used to wash the cells; serum-free medium was then added. Using a microscope, cells were observed and the scratch width was determined; cells were then cultured for 24 h, followed by further observation and determination of the scratch width. Consequently, the scratch healing rate could be calculated.

Flow cytometry

The transfected A549 cells were collected and fixed overnight at -20 °C. The cells were collected by centrifugation, washed with PBS, then resuscitated with 450 μL PBS and 50 μL of 0.5 mg/mL propidium iodide (PI) in a water bath at 37 °C for 30 min; cells were then centrifuged and resuscitated with PBS. The cell cycle distribution was measured and analyzed using a BD FACSAria flow cytometer.

The transfected A549 cells were collected and washed with PBS. The cells were suspended with precooled 1 × binding buffer (500 mL). Then, 5 μL of Annexin-V-FITC and 2.5 μL of PI were added to the samples. Apoptosis was detected using a BD FACSAriaTM flow cytometer.

Tumorigenesis experiment in nude mice

A549 cells (2×10^6) stably transfected with anti-miR-NC or anti-miR-183-5p were subcutaneously injected into 6-week-old female BALB/c nude mice, which were purchased from Beijing Weitong Lihua Experimental Animal Technology Co., Ltd (China). Animal health was monitored every day, and tumor size was measured every week. After 4 weeks, the mice were euthanized, the tumor tissue was removed, the tumor volume was measured, and the relative expression levels of miR-183-5p and FOXO1 mRNA in the tumor tissue were detected by qRT-PCR.

Western blotting

Total protein was extracted from the transfected A549 cells and corresponding total protein concentration was determined. The total protein was separated using electrophoresis and transferred into 5% skimmed milk. The cells were blocked with 5% skimmed milk for 1 h, and then incubated overnight at 4 °C with N-cadherin (1:2000), vimentin (1:2000), E-cadherin (1:7000), or α-catenin (1:5000). After washing the polyvinylidene difluoride membrane, rabbit anti-IgG secondary antibody labeled with horseradish peroxidase (1:10000) was added and incubated at Billerica for 2 h. ECL chromogenic agent was added to avoid light exposure. The gray level of the strip was analyzed using a Li-Cor Odyssey infrared imaging system (version 3.0 software, LI-COR Biosciences); β-actin was used as internal reference.

Statistical analysis

The data were analyzed using SPSS software (version 22, SPSS Inc., USA). The counting and measurement data were expressed in the form of rate (%) and mean ± standard deviation; the differences between two groups were compared using a χ^2 test and t-test for counting and measurement data, respectively. $P < 0.05$ was defined as statistically significant.

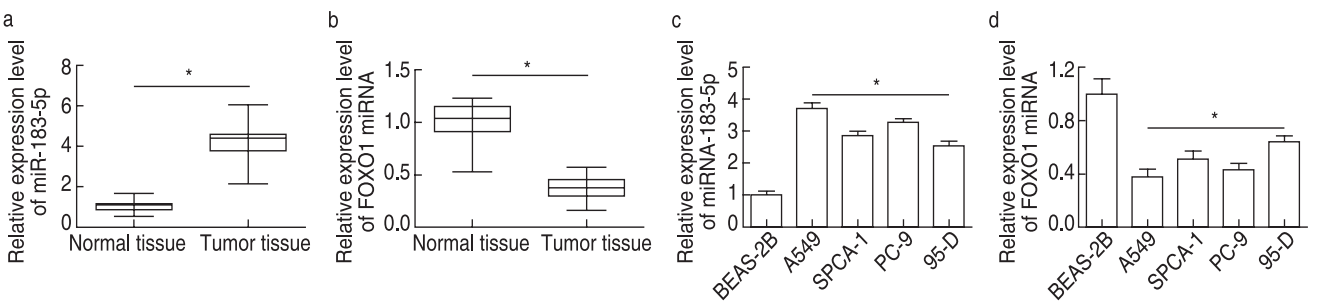

Fig. 1 The expression of miR-183-5p and FOXO1 in NSCLC tissues and cells. (a) miR-183-5p expression in NSCLC and normal tissues detected by qRT-PCR; (b) FOXO1 mRNA expression in NSCLC and normal tissues detected by qRT-PCR; (c) miR-183-5p is higher in NSCLC cell lines and lower in a normal human lung epithelial cell line (BEAS-2B); (d) FOXO1 mRNA expression is lower in NSCLC cell lines and higher in a normal human lung epithelial cell line (BEAS-2B). *$P < 0.05$

Results

Expression of miR-183-5p and FOXO1 in NSCLC tissues and cells

The qRT-PCR results (Fig. 1) demonstrated that the expression level of miR-183-5p in NSCLC tissues was significantly higher than that in normal tissues, whereas the expression level of FOXO1 mRNA was significantly lower than that in normal tissues ($P < 0.05$). Further, compared with the normal human lung epithelial cell line BEAS-2B, the miR-183-5p expression in the NSCLC cell lines A549, SPCA-1, PC-9, and 95-D was significantly higher, whereas the FOXO1 mRNA expression was significantly lower ($P < 0.05$).

Relationship between miR-183-5p expression and clinicopathological parameters in patients with NSCLC

According to the median relative expression of miR-183-5p in NSCLC tissues, 60 NSCLC patients were divided into the miR-183-5p low expression ($n = 30$) and miR-183-5p high expression ($n = 30$) groups. The relationship between miR-183-5p expression and clinicopathological parameters of NSCLC patients was analyzed. As shown in Table 2, miR-183-5p expression was significantly correlated with tumor size, tumor differentiation, and tumor-node-metastasis (TNM) stage in NSCLC patients ($P < 0.05$). Nonetheless, there was no significant correlation between miR-183-5p expression and age, sex, smoking, histological type, or lymph node metastasis ($P > 0.05$).

Table 2 Relationship between miR-183-5p expression and clinicopathological parameters in patients with NSCLC [*n* (%)]

Pathological features	Case	miR-183-5p		χ^2	*P*
		High expression	Low expression		
Age (years)				2.411	0.121
≤ 49	32	13 (40.63)	19 (59.38)		
> 49	28	17 (60.71)	11 (39.29)		
Gender				2.443	0.118
Male	34	14 (41.18)	20 (58.82)		
Female	26	16 (61.54)	10 (38.46)		
Smoking history				2.400	0.121
No	30	12 (40.00)	18 (60.00)		
Yes	30	18 (60.00)	12 (40.00)		
Tumor size (cm)				16.484	< 0.001
≤ 3	21	18 (85.71)	3 (14.29)		
> 3	39	12 (30.77)	27 (69.23)		
Tumor differentiation				11.380	0.001
High-middle grade	33	10 (30.30)	23 (69.70)		
Low grade	27	20 (74.07)	7 (25.93)		
Lymph node metastasis				0.287	0.592
No	22	12 (54.55)	10 (45.45)		
Yes	38	18 (47.37)	20 (52.63)		
TNM stage				10.000	0.002
I-II	24	6 (25.00)	18 (75.00)		
III	36	24 (66.67)	12 (33.33)		

Targeted inhibition of FOXO1 expression by miR-183-5p

The DIANA TOOLS prediction results indicated that there are potential binding sites for miR-183-5p in the FOXO1 3′UTR (Fig. 2a). The double luciferase assay (Fig. 2b) demonstrated that the luciferase activity of wild type FOXO1 in the miR-183-5p group was significantly lower than that in the miR-NC group ($P < 0.05$), indicating that miR-183-5p conferred targeted down-regulation of FOXO1. Additionally, the Pearson test results (Fig. 2c) showed that there was a significant negative correlation between miR-183-5p and FOXO1 mRNA expression in NSCLC ($P < 0.05$). Further, RIP results demonstrated that both miR-183-5p and FOXO1 could bind to AGO2 protein, indicating that miR-183-5p may bind to FOXO1 protein, thereby reducing FOXO1 expression (Fig. 2d). Following RNA pull-down analysis (Fig. 2e), clear bands were observed in the miR-183-5p-Bio pull-down group, but no clear bands were observed in the Bio-NC pull-down group; this indicated that FOXO1 could bind to and be pulled down by the miR-183-5p biotin probe in this assay. Additionally, the corresponding miR-4319 enrichment in the miR-183-5p-Bio group was significantly higher than that in the Bio-NC group ($P < 0.05$).

miR-183-5p overexpression regulates FOXO1 to promote proliferation, migration, invasion, and EMT of NSCLC cells

The results from the MTT assay (Fig. 3a), clone formation (Fig. 3b), Transwell assay (Fig. 3c), scratch test (Fig. 3d), and western blot analysis (Fig. 4) demonstrated that there was no significant difference in OD value, frequency of colony formation, frequency of invasion, scratch healing rate, and N-cadherin, vimentin, E-cadherin and α-catenin protein expression among the control, anti-miR-NC, and miR-NC groups ($P < 0.05$). Compared to the anti-miR-NC group, the OD value, scratch healing rate, N-cadherin and vimentin protein expression, and frequency of colony formation and invasion were significantly lower, whereas the E-cadherin and α-catenin protein expression were significantly higher in the anti-miR-183-5p group ($P < 0.05$). Additionally, the OD value, scratch healing rate, N-cadherin and vimentin protein expression, and frequency of colony formation and invasion were significantly higher, and E-cadherin and α-catenin protein expression were significantly lower in the miR-183-5p group than in the miR-NC group ($P < 0.05$). Further, compared to the miR-183-5p+pcDNA3.1

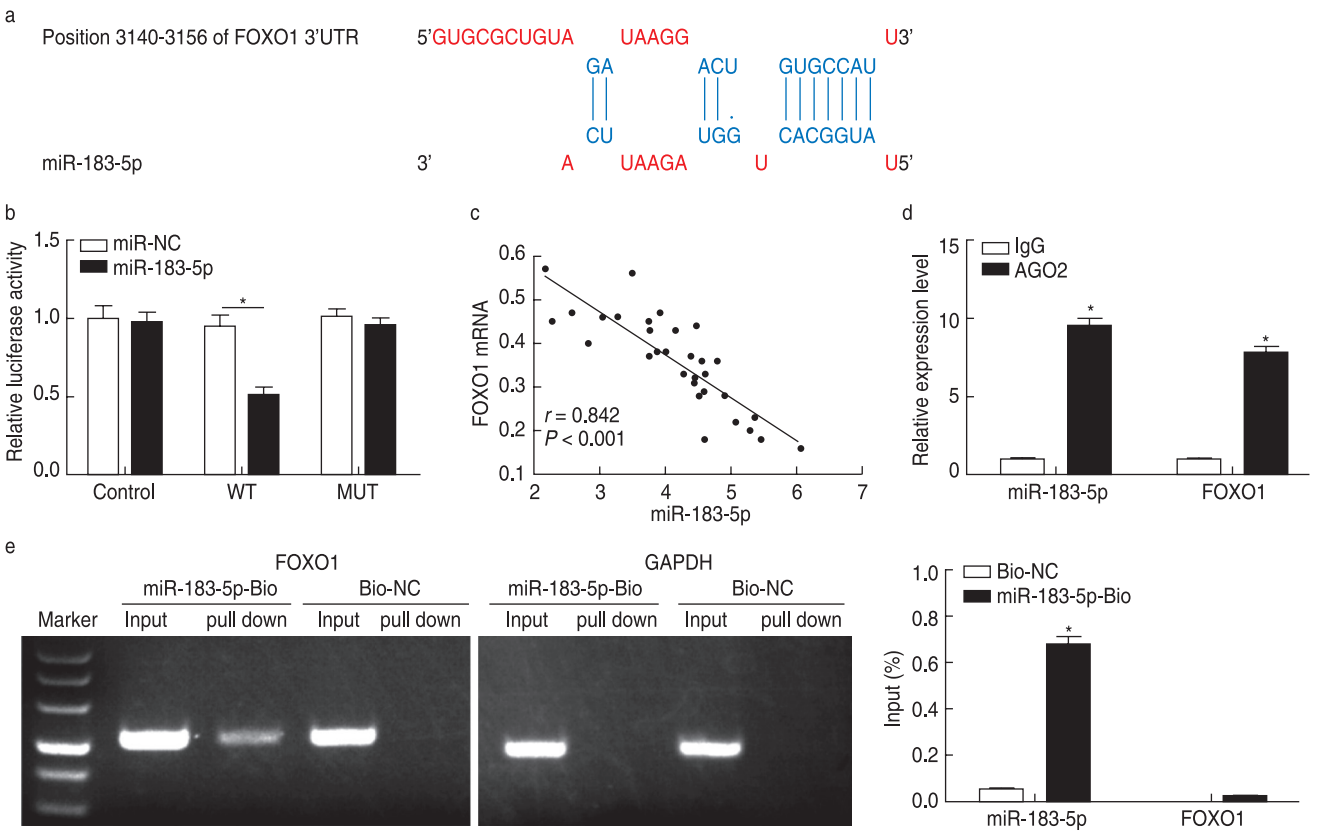

Fig. 2 miR-183-5p targets and inhibits FOXO1 expression. (a) DIANA TOOLS predicts the potential binding sites of miR-183-5p to FOXO1; (b) Verification of the targeting relationship between miR-183-5p and FOXO1 (double luciferase test); (c) Pearson test to analyze the correlation between miR-183-5p and FOXO1 mRNA expression in NSCLC tissues; (d) RIP assay results; (e) Pull-down assay results. *$P < 0.05$

group, the OD value, scratch healing rate, N-cadherin and vimentin protein expression, and frequency of colony formation and invasion were significantly lower, whereas E-cadherin and α-catenin protein expression were significantly higher in the miR-183-5p+pcDNA3.1-FOXO1 group ($P < 0.05$).

miR-183-5p overexpression targets the effects of FOXO1 on the cell cycle and apoptosis of NSCLC cells

Flow cytometry was used to analyze the effects of miR-183-5p overexpression on the cell cycle and apoptosis of NSCLC cells by targeted regulation of FOXO1. The PI single staining results indicated that (Fig. 5a) there was no significant difference in the proportion of cells in G0/G1 phase and S phase among the control, anti-miR-NC, and miR-NC groups ($P > 0.05$). Compared to the anti-miR-NC group, the proportion of G0/G1 phase cells in the anti-miR-183-5p group was significantly higher, whereas the proportion of S phase cells was significantly lower. Additionally, the proportion of G0/G1 phase cells was lower and S phase cells was higher in the miR-183-5p group than in the miR-NC group. Further, compared to the miR-183-5p+pcDNA3.1 group, the proportion of G0/G1 phase cells in the miR-183-5p+pcDNA3.1-FOXO1 group was significantly higher, whereas the proportion of S phase cells was significantly lower. However, there was no significant difference in the proportion of cells in the G2/M phase among the different groups ($P > 0.05$). The Annexin-V-FITC and PI double staining results showed that there was no significant difference in the apoptosis rate among the control, anti-miR-NC, and miR-NC groups ($P > 0.05$; Fig. 5b). Nonetheless, compared to the anti-miR-NC group, the apoptosis rate of the anti-miR-183-5p group was significantly higher. Compared to the miR-NC group, the apoptosis rate of the miR-183-5p group was significantly lower. Additionally, the apoptosis rate of the miR-183-5p+pcDNA3.1-FOXO1 group was significantly higher than that of the miR-183-5p+pcDNA3.1 group ($P < 0.05$).

Silencing miR-183-5p expression inhibits tumor growth *in vivo*

A549 cells stably infected with anti-miR-NC and anti-miR-183-5p were subcutaneously injected into nude mice; the corresponding tumor growth four weeks later

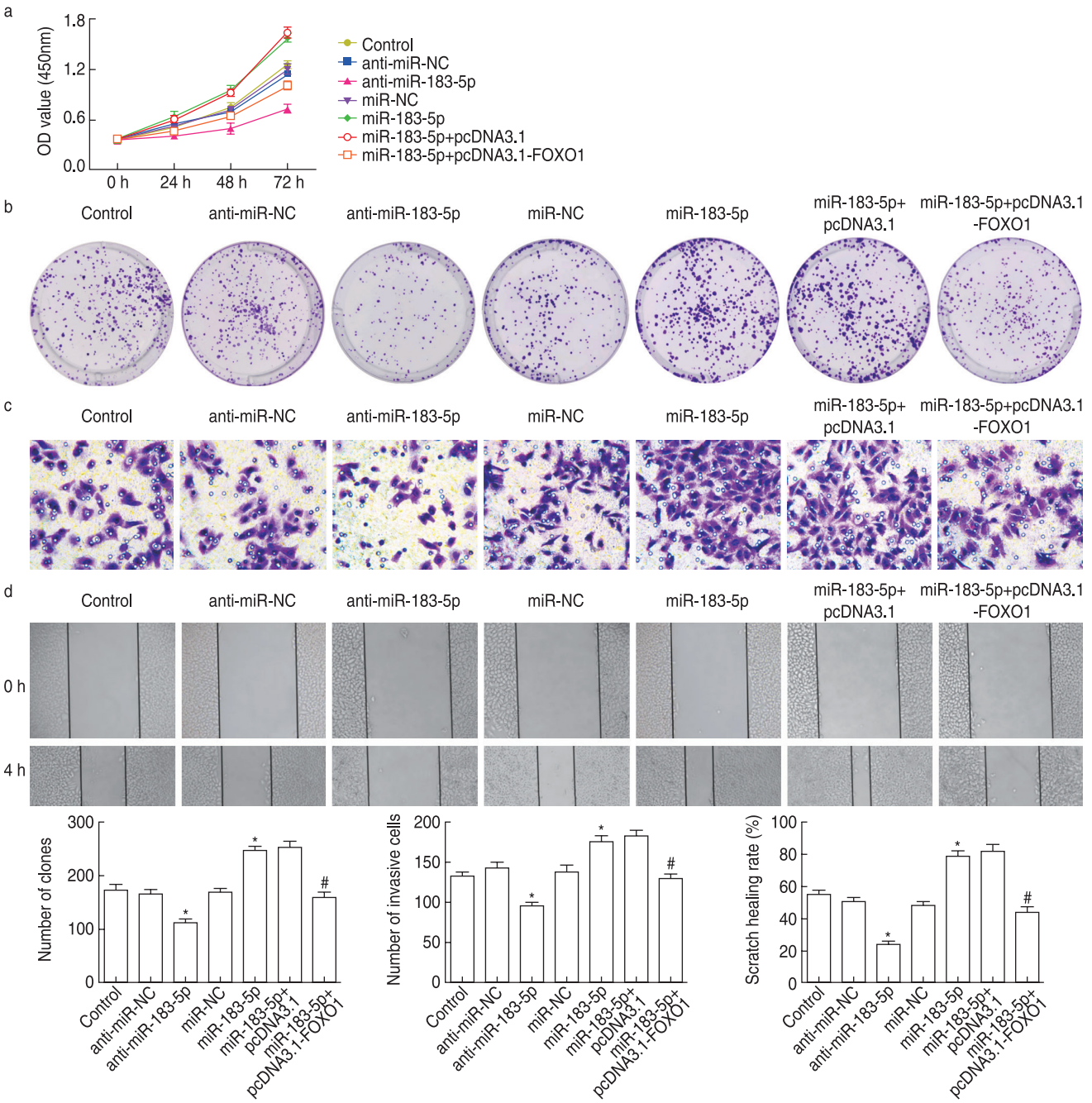

Fig. 3 Overexpression of miR-183-5p regulates FOXO1, thereby promoting the proliferation, migration, invasion, and EMT of NSCLC cells. (a) MTT assay for cell viability; (b) Clone formation test for cell proliferation; (c) Transwell chamber test for cell invasion; (d) Scratch test for cell migration. $^{*}P < 0.05$, compared with the control, anti-miR-NC, and miR-NC groups; $^{\#}P < 0.05$, compared with the miR-183-5p+pcDNA3.1 group

is shown in Fig. 6a. Compared to the anti-miR-NC group, the volume (Fig. 6b) and mass (Fig. 6c) of the transplanted tumor in the anti-miR-183-5p group were significantly lower; additionally, the relative miR-183-5p expression in the transplanted tumor (Fig. 6d) was significantly lower and the relative FOXO1 mRNA expression (Fig. 6e) was significantly higher in the anti-miR-183-5p group than that in the anti-miR-NC group.

Mechanism of miR-183-5p-targeted inhibition of FOXO1 in the proliferation, migration, invasion, and EMT of NSCLC cells

By detecting the expression of miR-183-5p and FOXO1, we found that both were significantly up-

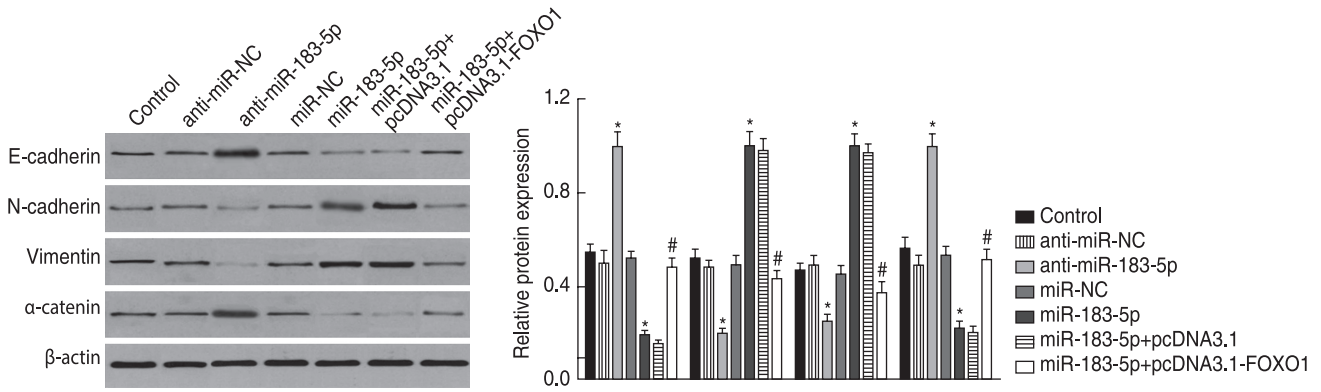

Fig. 4 Western blot analysis for the expression of EMT-related proteins in the cells of each group. **P* < 0.05, compared with the control, anti-miR-NC, and miR-NC groups; #*P* < 0.05, compared with the miR-183-5p+pcDNA3.1 group

regulated in NSCLC tissues and cells. Additionally, miR-183-5p could specifically inhibit the expression of FOXO1. To further observe the effects of miR-183-5p and FOXO1 on the malignant biological behavior of NSCLC cells, we detected the proliferation, invasion, migration, EMT-related protein expression, cell cycle, and apoptosis of NSCLC cells. Overexpression of miR-183-5p was observed to promote cell proliferation, invasion, migration, EMT, and cell cycle progression, whilst inhibiting apoptosis and FOXO1 expression. Nonetheless, up-regulation of FOXO1 expression can ameliorate these malignant effects. Therefore, it was inferred that miR-183-5p overexpression promotes the malignant biological behavior of NSCLC cells by targeting the inhibition of FOXO1 expression (Fig. 7).

Discussion

In recent years, the role of miRNA in cancer progression has been continuously explored. During tumor occurrence and development, miRNA can regulate the biological functions of tumor cells by regulating the expression of tumor suppressor genes or proto-oncogenes. Additionally, several miRNAs play an important role in the occurrence and development of NSCLC [13, 14]. Zhao *et al.* [15] confirmed that miR-641 inhibits NSCLC tumor development; therefore, up-regulation of miR-641 expression inhibits the proliferation, migration, and invasion of NSCLC cells, thus reducing the cisplatin resistance of NSCLC cells. Further, Luo *et al.* [16] established that miR-195-5p expression is down-regulated in NSCLC, and miR-195-5p overexpression can inhibit the proliferation of NSCLC cells, arrest the cell cycle in G0/G1 phase, and promote apoptosis; ultimately, this provides a potential target for the treatment of NSCLC. Alternatively, the miR-183-5p expression is significantly up-regulated in lung cancer tissue; therefore, miR-183-5p has been established as the differentially expressed of miRNA in lung cancer tissue, indicating that this miRNA may play an important role in the occurrence and development of lung cancer [17]. The prognosis of patients with NSCLC largely depends on their corresponding clinical stage and tumor differentiation [18]. In the current study, miR-183-5p was determined to be highly expressed in NSCLC tissues and cells; further, its corresponding expression levels were determined to be related to tumor size, TNM stage, and tumor differentiation in NSCLC patients. Overexpression of miR-183-5p was determined to promote NSCLC cell proliferation, invasion, migration, EMT, and cell cycle progression, whilst also inhibiting apoptosis, which is consistent with the corresponding results obtained by Wang *et al.* [8]; this indicates that miR-183-5p plays a role as a cancer-promoting factor in NSCLC. However, at present, few studies have been conducted on the effects of miR-183-5p on NSCLC; therefore, the specific mechanism of action of this miRNA is yet to be fully elucidated.

Forkhead box proteins are a type of transcription factor that primarily exist in invertebrates and mammals. FOXO is one of the largest subfamilies of the forkhead box family. At present, four FOXO subtypes (FOXO1, FOXO3a, FOXO4, and FOXO6) have been identified in mammals, all of which have homologous genes in nematodes [19]. Specifically, FOXO1 has been widely studied as a hypertranscription factor with complex activity, which can regulate the expression of genes involved in apoptosis, the cell cycle, metabolism, stress responses, and differentiation [20]. The abnormal expression of FOXO1 is also involved in the occurrence and development of various cancers. Ma *et al.* [21] demonstrated that FOXO1 expression is significantly down-regulated in ovarian cancer tissues and cells, and its low expression is significantly correlated with paclitaxel resistance, poor prognosis, short disease-free survival

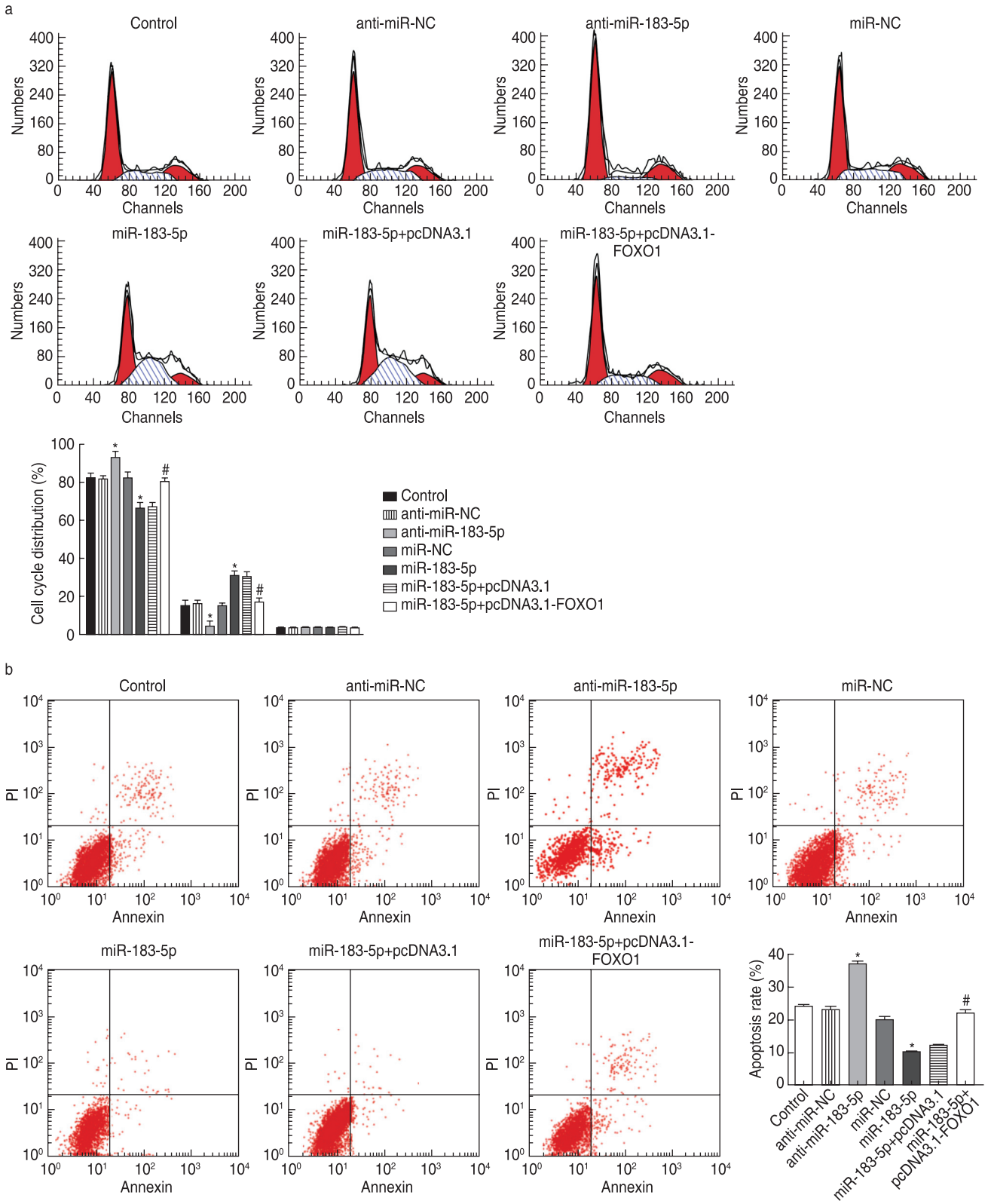

Fig. 5 miR-183-5p overexpression targets the effect of FOXO1 on the cell cycle and apoptosis of NSCLC cells. (a) PI single staining to compare the cell cycle distribution of each group; (b) Annexin-V-FITC and PI double staining to compare the apoptosis rate of cells in each group. **P* < 0.05, compared with the control, anti-miR-NC, and miR-NC groups; #*P* < 0.05, Compared with the miR-183-5p+pcDNA3.1 group

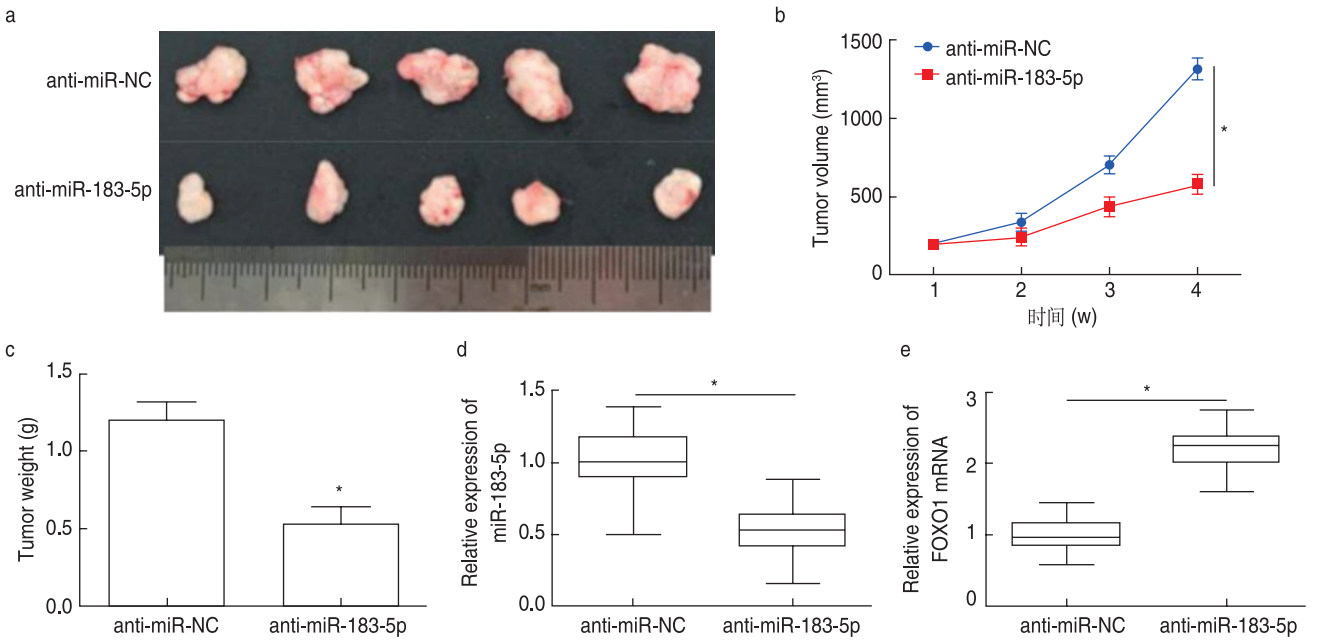

Fig. 6 Silencing miR-183-5p expression inhibits tumor growth in vivo. (a) Images of tumors 4 weeks after inoculation with anti-miR-NC or anti-miR-183-5p; (b) Comparison of the transplanted tumor volumes; (c) Comparison of the transplanted tumor weights; (d) Comparison of the relative miR-183-5p expression in transplanted tumors; (e) Comparison of the relative FOXO1 mRNA expression in transplanted tumors. *P < 0.05, compared with the anti-miR-NC group

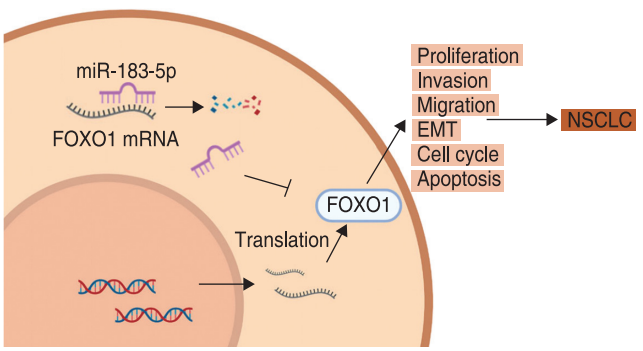

Fig. 7 Mechanism of miR-183-5p-targeted inhibition of FOXO1, resulting in an increase in the proliferation, migration, invasion, and EMT of NSCLC cells

and overall survival in patients with ovarian cancer. Therefore, FOXO1 can be used as a novel therapeutic target and prognostic marker for ovarian cancer. Further, Gheghiani *et al.* [22] have indicated that FOXO1 is a differentially expressed gene in prostate cancer, with its expression being significantly down-regulated in prostate cancer. This low FOXO1 expression is closely associated with the occurrence of prostate cancer and poor prognosis. However, few studies have evaluated the role of FOXO1 in the development of NSCLC; therefore, the function of FOXO1 in NSCLC remains unclear. In the current study, FOXO1 expression is down-regulated in NSCLC tissues and cells; in contrast, FOXO1 up-regulation was observed to inhibit the proliferation, invasion, migration, EMT, and other malignant biological behaviors of NSCLC cells. A variety of miRNAs can participate in the occurrence and development of cancer through targeting the regulation of FOXO1 expression. Bioinformatic prediction indicated that there were complementary binding sites between the 3'UTR of FOXO1 and miR-183-5p. Additionally, Han *et al.* [23] confirmed that down-regulation of miR-183-5p can promote the expression of FOXO1, thereby inhibiting the proliferation, migration, invasion, and glycolysis of thyroid cancer cells, and ultimately inhibiting the progression of thyroid cancer. However, the effects and mechanisms of miR-183-5p and FOXO1 on the biological processes of NSCLC cells are yet to be reported.

The double luciferase, RIP, and RNA pull-down experiments in this study also confirmed that miR-183-5p could specifically inhibit the expression of FOXO1, and that there was a significant negative correlation between miR-183-5p and FOXO1 mRNA expression in NSCLC; this indicated that FOXO1 may be regulated by miR-183-5p. In the present study, we interfered with miR-183-5p and FOXO1 expression in NSCLC cells. Overall, after co-transfection of miR-183-5p and FOXO1, the miR-183-5p-mediated up-regulation of proliferation, invasion, and migration of NSCLC cells was eliminated; this indicated that FOXO1 could reverse the effect of miR-183-5p on NSCLC cells. EMT is a key step in the early stages of cancer metastasis and primarily manifests as the transformation of epithelial cells to stromal

cells. In this study, overexpression of miR-183-5p was determined to promote the expression of N-cadherin and vimentin and inhibit the expression of E-cadherin and α-catenin. Nonetheless, this could be reversed by FOXO1 overexpression; therefore, it was established that miR-183-5p could affect EMT in NSCLC cells by regulating the expression of FOXO1. In addition, this study found that miR-183-5p can affect the cell cycle and apoptosis of NSCLC cells by regulating FOXO1 expression. *In vivo* experiments in this study also confirmed that down-regulating miR-183-5p expression can inhibit the growth of transplanted tumors and promote the FOXO1 expression.

In conclusion, the overexpression of miR-183-5p can promote the proliferation, migration, invasion, EMT, and cell cycle process of NSCLC cells, whilst also inhibiting apoptosis. Additionally, this mechanism was determined to occur via the miR-183-5p-mediated down-regulation of FOXO1 expression. This study provides a novel experimental basis for the progression of NSCLC and indicates that miR-183-5p may be a potential target for the corresponding clinical treatment of NSCLC. Nonetheless, some limitations remain regarding the understanding of miR-183-5p in NSCLC. First, the effects of silent FOXO1 expression on the proliferation, invasion, migration, and other malignant biological behaviors of NSCLC cells have yet to be explored; second, the specific mode of cell death initiated by this process has not been further evaluated. Therefore, these limitations need to be addressed in future research.

Acknowledgments
Not applicable.

Funding
Not applicable.

Conflicts of interest
The authors indicated no potential conflicts of interest.

Author contributions
All authors contributed to data acquisition, data interpretation, and reviewed and approved the final version of this manuscript.

Data availability statement
Not applicable.

Ethical approval
This study was approved by the Ethics Committee of Suining Central Hospital (051237L).

References

1. Zhuang Q, Huang Y, Hong Y, et al. Vinpocetine enhances cisplatin sensitivity of non-small cell lung cancer cells by reducing the nuclear factor erythroid 2-related factor 2 signaling. J Investig Med. 2022; 70(6):1358-1364.
2. Hatami E, Nagesh PKB, Chauhan N, et al. In situ nanoparticle self-assembly for combination delivery of therapeutics to non-small cell lung cancer. ACS Appl Bio Mater. 2022;5(3):1104-1119.
3. Waterhouse D, Lam J, Betts KA, et al. Real-world outcomes of immunotherapy-based regimens in first-line advanced non-small cell lung cancer. Lung Cancer. 2021;156:41-49.
4. Mirtavoos-Mahyari H, Rismani E, Lotfabadi AS, et al. Primary erlotinib resistance in a patient with non-small cell lung cancer carrying simultaneous compound EGFR L718A, Q849H, and L858R mutations. Biomol Concepts. 2021;12(1):164-174.
5. Wang J, Mo J, Xie Y, et al. Ultrasound microbubbles-mediated miR-216b affects MALAT1-miRNA axis in non-small cell lung cancer cells. Tissue Cell. 2022;74:101703.
6. Wang ZY, Li DL, Tian X, et al. A copper-free and enzyme-free click chemistry-mediated single quantum dot nanosensor for accurate detection of microRNAs in cancer cells and tissues. Chem Sci. 2021; 12(31):10426-10435.
7. Li M, Liu Y, Jiang X, et al. Inhibition of miR-144-3p exacerbates non-small cell lung cancer progression by targeting CEP55. Acta Biochim Biophys Sin (Shanghai). 2021;53(10):1398-1407.
8. Wang H, Ma Z, Liu X, Zhang C, et al. MiR-183-5p is required for non-small cell lung cancer progression by repressing PTEN. Biomed Pharmacother. 2019;111:1103-1111.
9. Chae YC, Kim JY, Park JW, et al. FOXO1 degradation via G9a-mediated methylation promotes cell proliferation in colon cancer. Nucleic Acids Res. 2019;47(4):1692-1705.
10. Xie C, Guo Y, Lou S. LncRNA ANCR promotes invasion and migration of gastric cancer by regulating FoxO1 expression to inhibit macrophage M1 polarization. Dig Dis Sci. 2020;65(10):2863-2872.
11. Yin H, Wang X, Zhang X, et al. UBE2T promotes radiation resistance in non-small cell lung cancer via inducing epithelial-mesenchymal transition and the ubiquitination-mediated FOXO1 degradation. Cancer Lett. 2020;494:121-131.
12. Shang A, Wang X, Gu C, et al. Exosomal miR-183-5p promotes angiogenesis in colorectal cancer by regulation of FOXO1. Aging (Albany NY). 2020;12(9):8352-8371.
13. Liang Z, Xu J, Ma Z, et al. MiR-187 suppresses non-small-cell lung cancer cell proliferation by targeting FGF9. Bioengineered. 2020; 11(1):70-80.
14. Gai C, Liu C, Wu X, et al. MT1DP loaded by folate-modified liposomes sensitizes erastin-induced ferroptosis via regulating miR-365a-3p/NRF2 axis in non-small cell lung cancer cells. Cell Death Dis. 2020; 11(9):751.
15. Zhao Y, Zheng R, Chen J, et al. CircRNA CDR1as/miR-641/HOXA9 pathway regulated stemness contributes to cisplatin resistance in non-small cell lung cancer (NSCLC). Cancer Cell Int. 2020;20:289.
16. Luo J, Pan J, Jin Y, et al. MiR-195-5p inhibits proliferation and induces apoptosis of non-small cell lung cancer cells by targeting CEP55. Oncol Targets Ther. 2019;12:11465-11474.
17. Meng F, Zhang L. miR-183-5p functions as a tumor suppressor in lung cancer through PIK3CA inhibition. Exp Cell Res. 2019;374(2):315-322.
18. Zhang T, Li W, Gu M, et al. Clinical significance of miR-183-3p and miR-182-5p in NSCLC and their correlation. Cancer Manag Res.

2021;13:3539-3550.
19. Dai X, Cai D, Wang P, et al. Cold atmospheric plasmas target breast cancer stemness via modulating AQP3-19Y mediated AQP3-5K and FOXO1 K48-ubiquitination. Int J Biol Sci. 2022;18(8):3544-3561.
20. Xie C, Guo Y, Lou S. LncRNA ANCR promotes invasion and migration of gastric cancer by regulating FoxO1 expression to inhibit macrophage M1 polarization. Dig Dis Sci. 2020;65(10):2863-2872.
21. Ma L, Sun Y, Li D, et al. Overexpressed ITGA2 contributes to paclitaxel resistance by ovarian cancer cells through the activation of the AKT/FoxO1 pathway. Aging (Albany NY). 2020;12(6):5336-5351.
22. Gheghiani L, Shang S, Fu Z. Targeting the PLK1-FOXO1 pathway as a novel therapeutic approach for treating advanced prostate cancer. Sci Rep. 2020;10(1):12327.
23. Han C, Mo K, Jiang L, et al. miR-183-5p promotes proliferation, invasion, and glycolysis of thyroid carcinoma cells by targeting FOXO1. Mol Cell Biochem. 2022;477(4):1195-1206.

DOI 10.1007/s10330-022-0601-1
Cite this article as: Deng Y, He ZG, Luo XB, *et al*. MiR-183-5p promotes the progression of non-small cell lung cancer through targeted regulation of FOXO1. Oncol Transl Med. 2023;9(3):121–132.

Oncology and Translational Medicine
DOI 10.1007/s10330-022-0581-1
June 2023, Vol. 9, No. 3, P133–P146

ORIGINAL ARTICLE

Prognostic value of the long noncoding RNA *AFAP1-AS1* in cancers*

Lixiu Zhu[1], Jiawen Yan[1] (Co-first author), Guoqiang Xu[1] (Co-first author), Qiaoli Wang[2] (Co-first author), Tianrui Xu[1], Ruixue Cao[1], Chuanzheng Sun[3] (✉), Yan Xi[3] (✉), Wei Xiong[1] (✉)

[1] Department of Radiotherapy, Yunnan Cancer Hospital, The Third Affiliated Hospital of Kunming Medical University, Kunming 650000, China
[2] Department of Radiotherapy, People's Hospital of Yuxi City, The Sixth Affiliated Hospital of Kunming Medical University, Yuxi 653100, China
[3] Department of Head and Neck Surgery, Yunnan Cancer Hospital, The Third Affiliated Hospital of Kunming Medical University, Kunming 650000, China

Abstract

Objective This meta-analysis explored whether the expression of actin filament-associated protein 1 antisense RNA 1 (*AFAP1-AS1*) is related to the prognosis and clinicopathological features of patients with cancer.

Methods PubMed, EMBASE, and Cochrane Library were systematically searched. Hazard ratios (HRs) with 95% confidence intervals (CIs) were used to assess the prognostic value based on overall survival (OS), disease-free survival (DFS), and progression-free survival (PFS). Odds ratios (ORs) with 95% CIs were used to determine the relationships between *AFAP1-AS1* and clinicopathological features, such as large tumor size (LTS), high tumor stage (HTS), poor histological grade (PHG), lymph node metastasis (LNM), and distant metastasis (DM).

Results Thirty-five eligible articles and 3433 cases were analyzed. High *AFAP1-AS1* expression, compared to low *AFAP1-AS1* expression, correlated with significantly shorter OS (HR = 2.15, 95% CI = 1.97–2.34, $P < 0.001$), DFS (HR = 1.37, 95% CI = 1.19–1.57, $P < 0.001$), and PFS (HR = 1.97, 95% CI = 1.56–2.50, $P < 0.001$) in patients with cancer. In various cancers, elevated *AFAP1-AS1* expression was significantly associated with LTS (OR = 2.76, 95% CI = 2.16–3.53, $P < 0.001$), HTS (OR = 2.23, 95% CI = 1.83–2.71, $P < 0.001$), and PHG (OR = 1.39, 95% CI = 1.08–1.79, $P = 0.01$) but not LNM (OR = 1.59, 95% CI = 0.88–2.85, $P = 0.12$) or DM (OR = 1.81, 95% CI = 0.90–3.66, $P = 0.10$).

Conclusion High *AFAP1-AS1* expression was associated with prognostic and clinicopathological features, suggesting that *AFAP1-AS1* is a prognostic biomarker for human cancers.

Key words: long noncoding RNA (lncRNA); actin filament-associated protein 1 antisense RNA 1 (*AFAP1-AS1*); prognostic; meta-analysis

Received: 14 June 2022
Revised: 29 August 2022
Accepted: 27 March 2023

Cancer is an important factor that affects human health and is a leading cause of death worldwide. According to recent epidemiological statistics, there are an estimated 19.3 million new cancer cases and nearly 10.0 million cancer deaths worldwide each year [1]. Global cancer cases are expected to reach 28.4 million cases in 2040, an increase of 47% compared to that in 2020, which may further increase the economic burden [1]. With advancements in medicine and science, cancer deaths have decreased; however, the five-year survival rate is still inadequate. Although many studies have focused on biomarkers for cancer diagnosis and prognosis, the results have not been optimistic. Therefore, new prognostic biomarkers are needed to drive cancer development.

Long noncoding RNAs (lncRNAs), which are transcriptional regulatory factors that operate in cis or trans, are defined as transcripts that do not encode proteins of more than 200 nucleotides [2]. lncRNAs are associated

✉ Correspondence to: Chuanzheng Sun. Email: scz007@126.com; Yan Xi. Email: xiyan616@126.com; Wei Xiong. Email: panda_wei_wei@163.com
* Supported by a grant from the "Ten Thousand Plan" Youth Talent Project in Yunnan Province (no grant number is applicable).

with a variety of functions, such as the regulation of epigenetic, transcriptional, and post-transcriptional mechanisms [3–4]. Mounting evidence has shown that lncRNAs are dysregulated in various cancers and play important roles in invasion and metastasis, suggesting that lncRNAs may act as regulators of gene expression and affect tumor progression [5]. Several studies have shown that lncRNAs have multiple functions in many cellular processes that may play important roles in carcinogenesis and cancer progression. Evidence supporting the use of abnormally expressed lncRNAs as biomarkers of various human cancers has facilitated the development of lncRNA-based diagnostic tools and treatments.

Actin filament-associated protein 1 antisense RNA 1 (*AFAP1-AS1*), the antisense transcript of the *AFAP1* gene, has a length of 6810 bp and is located in the 4p16.1 region of the human genome [6]. *AFAP1-AS1*, originally identified in 2013, has been shown to be present in esophageal adenocarcinoma [7]. Previous studies have indicated that lncRNAs can be used as molecular markers of location, time, developmental stage, and gene expression regulation [8]. Among lncRNAs with upregulated expression in cancer, *AFAP1-AS1* plays a carcinogenic role in different human cancer cells as well as an important regulatory role. Studies have shown that in hepatocellular carcinoma (HCC), the knockout of *AFAP1-AS1* with an *si-AFAP1-AS1* construct can reduce proliferation and invasion *in vitro* and *in vivo*, induce apoptosis, and block the cell cycle in the S phase [9]. In addition, lncRNAs can be used as guides to recruit chromatin-modifying enzymes to target genes [8]. Furthermore, *AFAP1-AS1* recruited LSD1 to the promoter region of HBP1 and inhibited its transcription by mediating H3K4me2 demethylation [10]. A previous study showed that AFAP1 expression could be regulated by DNA methylation [11]. lncRNAs also function by interacting with various RNA-binding proteins, leading to the inactivation or activation of gene expression through chromosomal reprogramming, DNA methylation, RNA decay, and histone modification [12]. In particular, *AFAP1-AS1*, an oncogene, binds to *EZH2* to inhibit p21 transcription and promote tumor cell formation [12].

Notably, these lncRNAs have more functions than those of the aforementioned lncRNAs. Studies have shown that lncRNAs can interfere with transcriptional mechanisms and maintain the structure of nuclear spots [13]. In addition, lncRNAs may hybridize with DNA and affect chromatin. Furthermore, lncRNAs interact with chromatin proteins to promote or inhibit their binding and activity in target regions [14]. Unfortunately, to date, investigations of *AFAP1-AS1* have been insufficient, and the above functions have not yet been identified for this lncRNA. In addition, the basic mechanisms and related functions of *AFAP1-AS1* remain unclear.

AFAP1-AS1 is a well-known lncRNA that is overexpressed in several malignancies. *AFAP1-AS1* is involved in cell proliferation, angiogenesis, invasion, and metastasis of various cancers [15]. In addition, *AFAP1-AS1* can be used as a diagnostic marker for various cancers. Moreover, high expression of *AFAP1-AS1* is closely related to clinical prognostic indicators, including overall survival (OS) [16], disease-free survival (DFS) [17], and progression-free survival (PFS) [10]. A meta-analysis reported that the *AFAP1-AS1* expression level was associated with clinical outcomes, including survival, tumor size and stage, and histological differentiation [18]. As the literature included in this article has been updated, we performed a meta-analysis to evaluate the prognostic utility of *AFAP1-AS1* in patients with cancer in a clinical setting.

Methods

Literature search

We searched for relevant articles in the PubMed, EMBASE, and Cochrane Library electronic databases. The search terms were as follows: ((“Neoplasia” OR “Neoplasias” OR “Neoplasm” OR “Tumors” OR “Tumor” OR “Cancer” OR “Cancers” OR “Malignancy” OR “Malignancies” OR “Malignant Neoplasms” OR “Malignant Neoplasm” OR “Neoplasm, Malignant” OR “Neoplasms, Malignant” OR “Benign Neoplasms” OR “Neoplasms, Benign” OR “Benign Neoplasm” OR “Neoplasm, Benign” OR “acral tumor” OR “acral tumour” OR “embryonal and mixed neoplasms” OR “germ cell and embryonal neoplasms” OR “glandular and epithelial neoplasms” OR “hormone-dependent neoplasms” OR “neoplasia” OR “neoplasms” OR “neoplasms by histologic type” OR “neoplasms, cystic, mucinous, and serous” OR “neoplasms, embryonal and mixed” OR “neoplasms, germ cell and embryonal” OR “neoplasms, glandular and epithelial” OR “neoplasms, hormone-dependent” OR “neoplasms, post-traumatic” OR “neoplastic disease” OR “neoplastic entity” OR “neoplastic mass” OR “post-traumatic neoplasms” OR “tumor” OR “tumoral entity” OR “tumoral mass” OR “tumorous entity” OR “tumorous mass” OR “tumour” OR “tumoural entity” OR “tumoural mass” OR “tumourous entity” OR “tumourous mass”) OR (“Neoplasms”[Mesh])) AND ((“lncRNA-AFAP1-AS1, human” OR “AFAP1 antisense RNA, human” OR “long non-coding RNA AFAP1-AS1” OR “lncRNA AFAP1-AS1” OR “AFAP1-AS1” OR “AFAP1 antisense RNA 1” OR “actin filament-associated protein 1 antisense RNA1”) OR (“AFAP1-AS1 long noncoding RNA, human” [Supplementary Concept])). The search was conducted on November 21, 2020. To obtain potential eligible papers, we manually reviewed the reference lists to identify additional relevant articles.

Inclusion and exclusion criteria

The following inclusion criteria were used: (1) articles with histopathologically confirmed carcinoma; (2) articles in which the expression levels of *AFAP1-AS1* in tissues of cancer patients were determined; (3) articles in which patients were divided into two distinct groups, including high- and low-expression groups; (4) articles that statistically analyzed patient prognosis or clinicopathological features; and (5) articles written in English.

The following exclusion criteria were applied: (1) articles not related to carcinoma; (2) letters, expert opinions, case reports, editorials, and reviews; (3) studies with duplicate data; and (4) studies without usable data or data from animal experiments.

Data extraction and quality assessment

Two reviewers (Lixiu Zhu and Guoqiang Xu) independently searched the databases for eligible articles based on the inclusion and exclusion criteria. Tianrui Xu and Ruixue Cao evaluated the quality of the included studies. Information was independently extracted from the included studies by two operators (Jiawen Yan and Qiaoli Wang). Upon disagreement, three authors (Lixiu Zhu, Guoqiang Xu, and Jiawen Yan) discussed and resolved the issue. The following information was collected for each qualified article: first author's last name, year of publication, country, tumor type, sample size, detection method, reference gene, cutoff values, number of patients with large tumor size (LTS), high tumor stage (HTS), poor histological grade (PHG), lymph node metastasis (LNM), and distant metastasis (DM) between the high and low expression groups. For studies that did not provide hazard ratios (HRs) and 95% confidence intervals (CIs), widely proven and accepted scientific methods were used, and Engauge Digitizer 10.8 was used to extract data from the survival curve [19–20]. The data were entered into an HR calculation spreadsheet developed by Tierney *et al* [21]. The HRs, standard errors (SE), and corresponding 95% CIs were then estimated according to the curve.

The Newcastle-Ottawa Scale (NOS) was used to appraise the quality of the literature; this method adopts a "star" rating system, with the full credit of 9 stars. It is generally used to judge the quality of a methodology, including the selection (0–4 stars), comparability (0–2 stars), and results (0–3 stars) [22]. Articles with scores > 5 were considered high quality; other articles were considered low quality.

External validation

Transcriptome and clinical data of 33 tumors were downloaded from the UCSC Xena database (http://xena.ucsc.edu/). The data were collated and the expression levels of *AFAP1-AS1* in each neoplastic tissue were extracted. According to the median expression level of *AFAP1-AS1* in each tumor, each cohort was divided into high and low expression groups using R. Cox regression analysis was used to evaluate the relationship between *AFAP1-AS1* expression and OS, DFS, and PFS in patients with tumors. The results were presented as forest maps. Statistical significance was set at $P < 0.05$.

Statistical analysis

Review Manager version 5.4 and R version 4.1.1 were used for all statistical analyses. The combined HRs and 95% CIs were used to estimate the prognostic significance of *AFAP1-AS1* in terms of OS, DFS, and PFS in various cancers. Comprehensive odds ratios (ORs) and 95% CIs were used to estimate the association between *AFAP1-AS1* and clinicopathological features, such as tumor size and stage, histological grade, LNM, and DM. Heterogeneity between articles was detected by the I^2 test, and both $P < 0.1$ and I^2 values > 50% were considered to indicate obvious heterogeneity. Therefore, random- and fixed-effects models were selected to analyze the data according to heterogeneity. The OS, DFS, and PFS of patients with different types of tumors were analyzed using R, and HR values were calculated based on the Cox proportional hazards model. Additionally, publication bias was measured using Begg's funnel plots.

Results

Study selection

After searching the PubMed, Embase, and Cochrane Library databases, a total of 228 studies were found; 94 studies were deleted due to duplication, of which 88 were reclassified as unqualified by automatic tools and six were reclassified as unqualified by manual assessment. Further exclusions were made by reviewing the full texts of the remaining 134 articles. After examining the titles and abstracts, 58 irrelevant studies were excluded. Further, four articles could not be retrieved and were excluded. Next, 37 articles were excluded: six meta-analyses or reviews, 30 articles with incomplete data, and one article written in Chinese. Finally, we included 35 studies that met the criteria [9–10, 12, 16–17, 23-52], with a total of 3433 patients. The flow diagram is shown in Fig. 1.

Characteristics of the included studies

All the included studies were conducted in China between 2015 and 2020. Patient sample sizes in the 35 studies ranged from 30 to 256, with an average sample size of 143. In all but one [25], the expression of the lncRNA *AFAP1-AS1* was measured by real-time quantitative polymerase chain reaction (qRT-PCR) [9–10, 12, 16–17, 23–24, 26-52]. The genes used for the normalization of *AFAP1-AS1* expression were not consistent, and *U6* [27, 36, 45], *GAPDH*

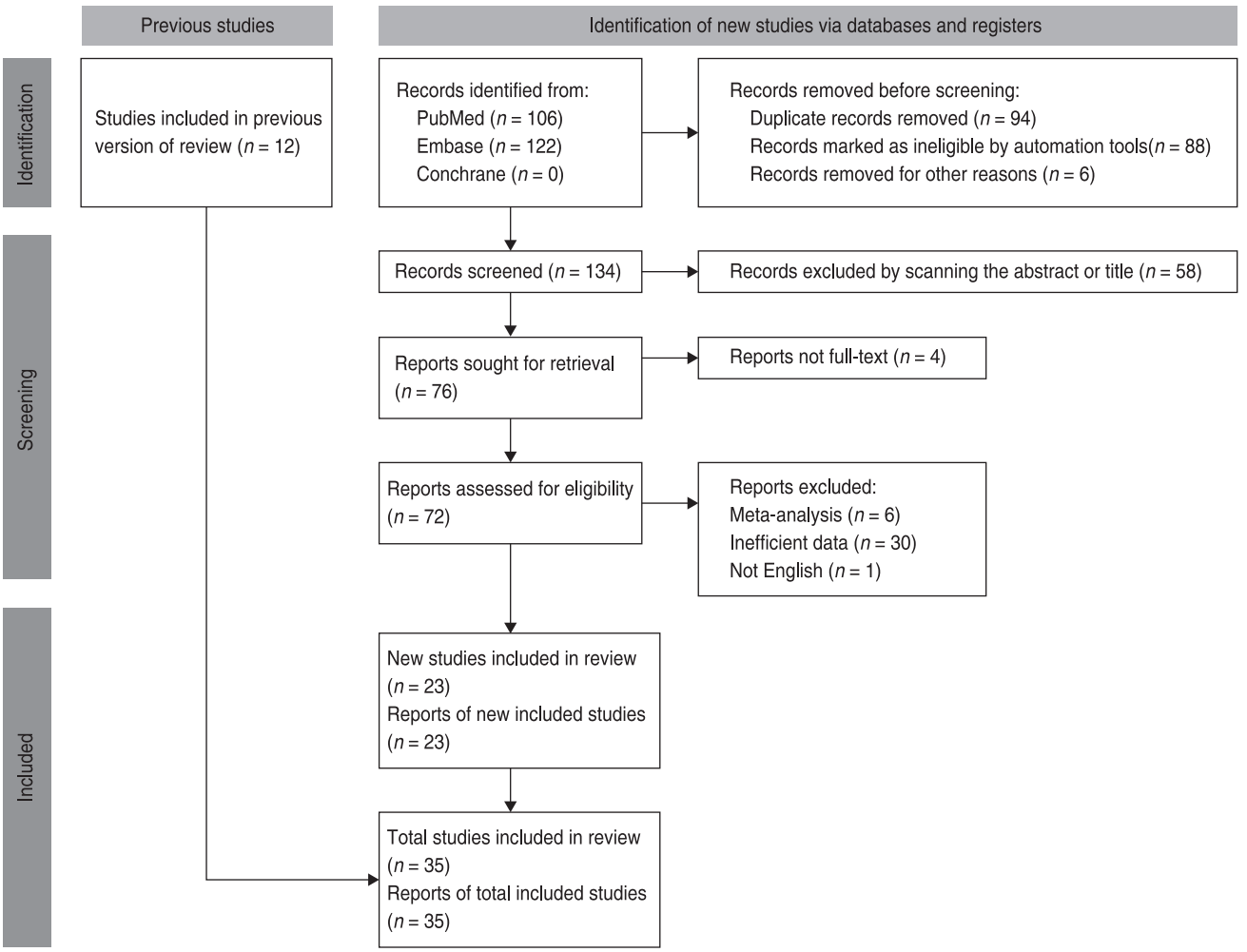

Fig. 1 Flowchart of the study search and screening in this meta-analysis

[9–10, 12, 16, 23–24, 26, 28–29, 33–35, 37–38, 40–41, 43–44, 46–51], *β-actin* [30–32, 39, 42, 52], and *HPRT1* [17] were used. The cutoff value was expressed in various forms; however, 13 studies did not provide a clear cutoff value. With regard to prognostic outcomes, OS was reported in 33 studies [9–10, 12, 16, 23–26, 28–32, 34–38, 40-46, 48, 50–52], DFS in six studies [17, 26, 32–33, 38, 42]; and PFS in four studies [10, 24, 30, 36]. In this meta-analysis, a total of 25 cancers were assessed: non-small cell lung cancer (NSCLC), endometrial carcinoma (EC), triple-negative breast cancer (TNBC), tongue squamous cell carcinoma (TSCC), prostate cancer (PCA), clear cell renal cell carcinoma (ccRCC), retinoblastoma (RB), bladder cancer (BCA), colon cancer (CC), lung adenocarcinoma (LUAD), esophageal squamous cell carcinoma (ESCC), lung cancer (LC), pancreatic ductal adenocarcinoma (PDAC), ovarian cancer (OC), gastric cancer (GC), colorectal cancer (CRC), gallbladder cancer (GBC), cholangiocarcinoma (CCA), nasopharyngeal carcinoma (NPC), breast cancer (BC), glioma, osteosarcoma (OS), HCC, thyroid cancer (TC), and pancreatic cancer (PC). The NOS score for the quality assessment of all studies ranged from 5 to 8, and the quality assessment achieved a good consensus between the two reviewers.

Association between *AFAP1-AS1* and prognosis

Association between AFAP1-AS1 and shorter OS

Of the 35 included studies, 33 reported prognosis in terms of OS according to *AFAP1-AS1* expression levels, with a total of 3141 patients. A fixed-effects model was used because of non-significant heterogeneity (I^2 = 12%, P_Q = 0.27). The pooled results showed that high expression of *AFAP1-AS1*, compared to low *AFAP1-AS1* expression, was associated with shorter OS (HR = 2.15, 95% CI: 1.97–2.34, Fig. 2).

Association between AFAP1-AS1 and shorter DFS and PFS

According to *AFAP1-AS1* expression levels DFS was reported for 978 patients in six articles and PFS was

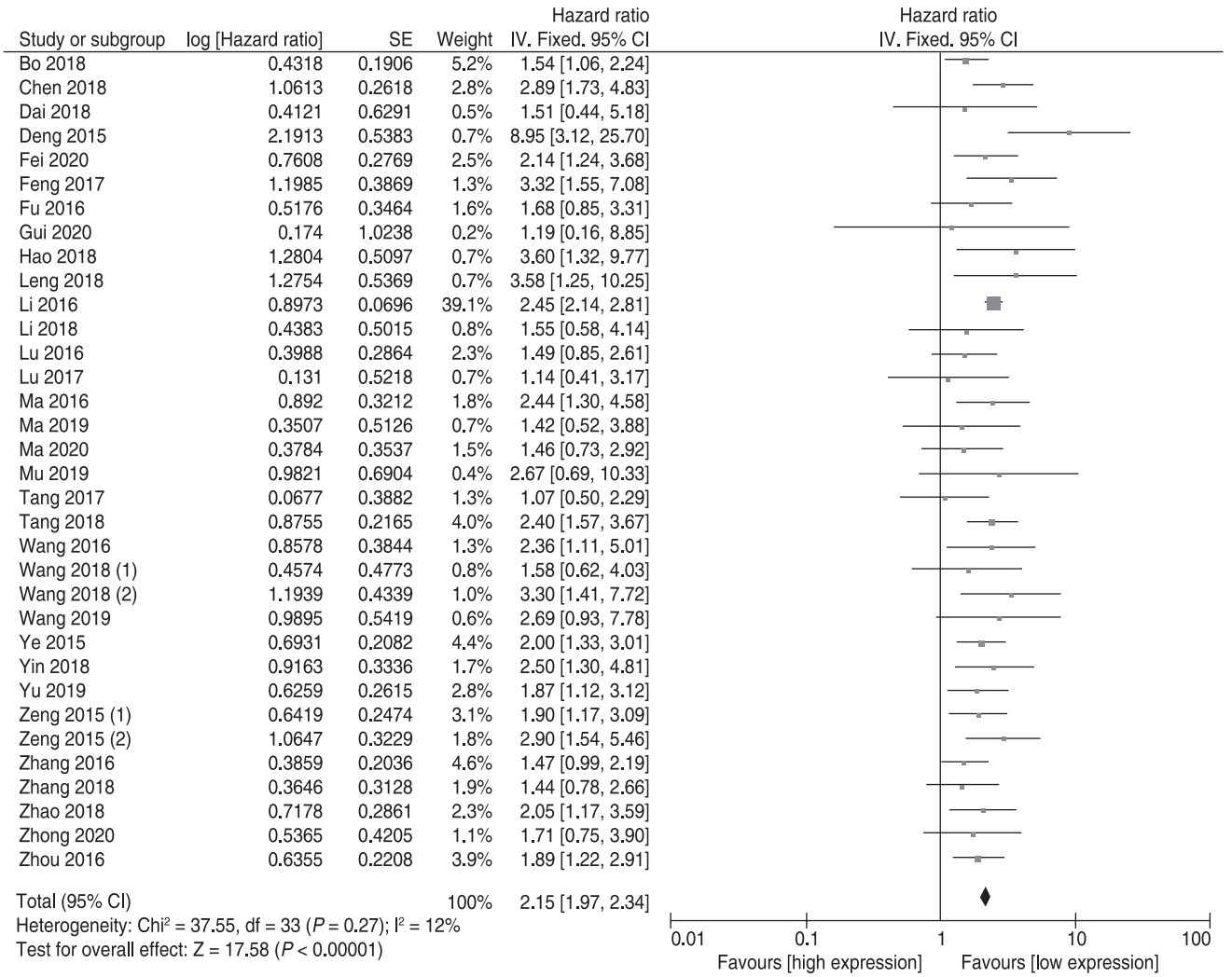

Fig. 2 Forest plot of HRs for the association between high *AFAP1-AS1* expression and OS

reported for 397 patients in four articles. There was no apparent heterogeneity among the studies (DFS: I^2 = 0%, P_Q = 0.51; PFS: I^2 = 0%, P_Q = 0.65); thus, a fixed-effects model was used to estimate the pooled HRs and the corresponding 95% CI values. These data indicated that the *AFAP1-AS1* expression level was associated with DFS (pooled HR = 1.37, 95% CI: 1.19–1.57, Fig. 3) and PFS (pooled HR = 1.97, 95% CI: 1.56–2.50, Fig. 4) in patients with various tumors.

Association between *AFAP1-AS1* and clinicopathological features

In this meta-analysis, 16 eligible studies with 1219 patients reported *AFAP1-AS1* expression levels according to LTS data. A fixed-effects model was adopted to account for the data because there was no apparent heterogeneity (I^2 = 17%, P_Q = 0.26). This analysis showed that there may be a significant positive association between the high expression level of *AFAP1-AS1* and LTS (OR = 2.76, 95% CI: 2.16–3.53, Fig. 5). Secondly, twenty-one eligible studies involving 1987 patients reported *AFAP1-AS1* expression levels according to HTS data. No obvious heterogeneity was detected (I^2 = 42%, P_Q = 0.02); therefore, a fixed-effects model was selected, and a pooled OR of 2.23 was obtained (95% CI: 1.83–2.71, Fig. 6). Fifteen eligible studies with 1339 patients reported *AFAP1-AS1* expression levels according to the histological grade. We selected a fixed-effects model because no significant heterogeneity was observed (I^2 = 45%, P_Q = 0.03). The integrated data suggested that elevated *AFAP1-AS1* expression predicted PHG in various cancers (OR = 1.39, 95% CI: 1.08–1.79, Fig. 7). Thirteen eligible studies with 1202 patients reported *AFAP1-AS1* expression levels in LNM. Because there was significant statistical

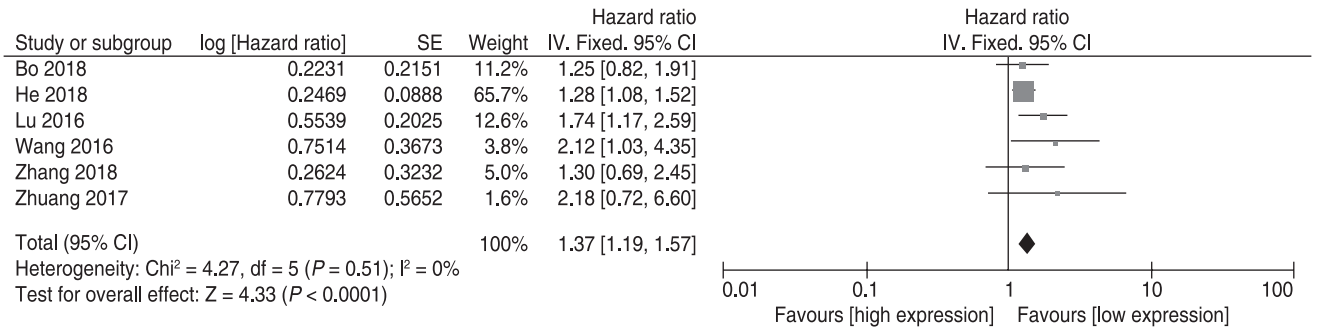

Fig. 3 Forest plot of HRs for the association between high *AFAP1-AS1* expression and DFS

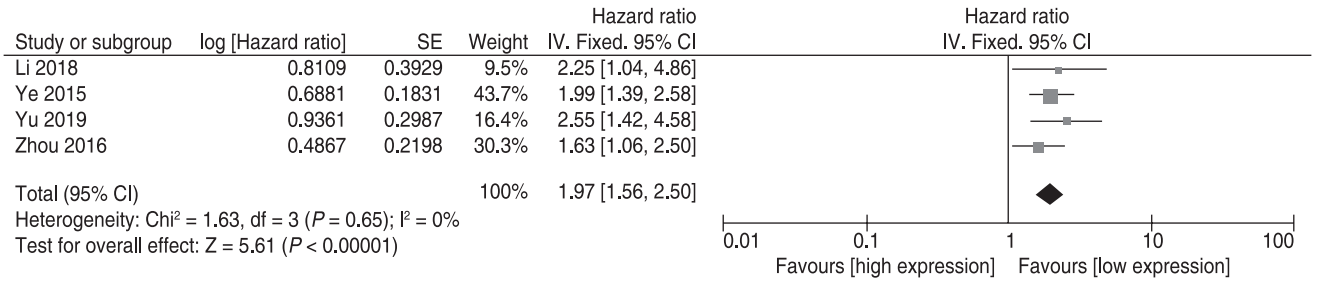

Fig. 4 Forest plot of HRs for the association between high *AFAP1-AS1* expression and PFS

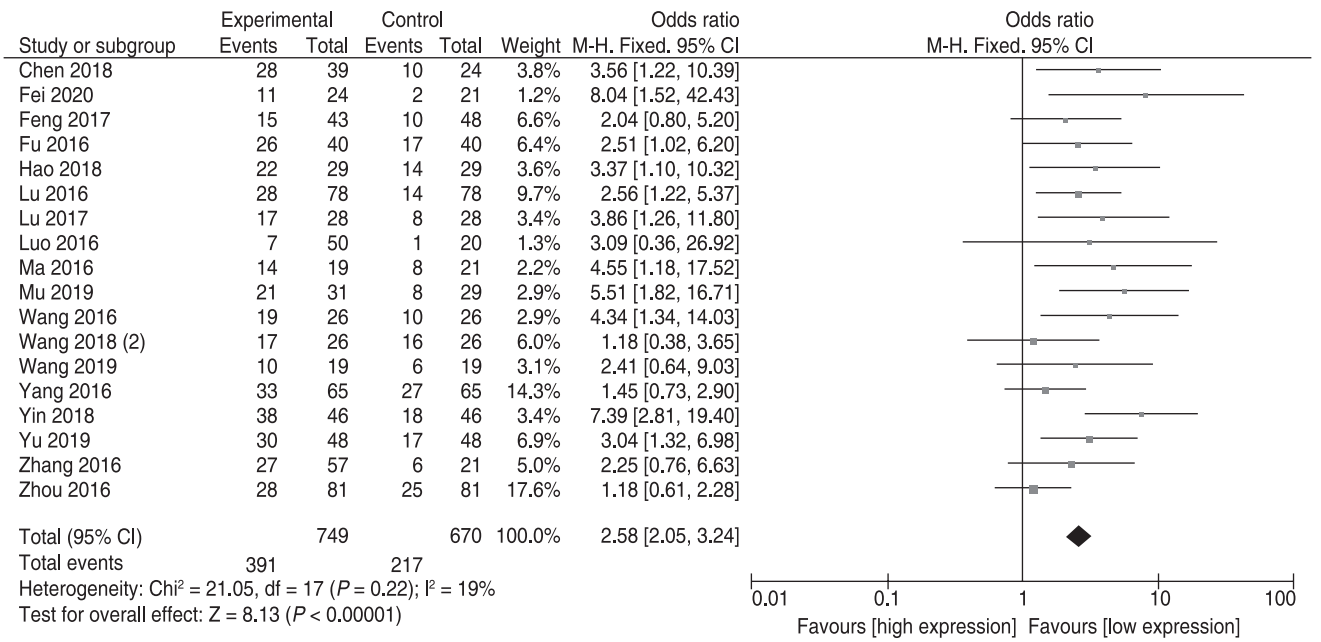

Fig. 5 Forest plot of HRs for the association between high *AFAP1-AS1* expression and LTS

heterogeneity (I^2 = 82%, P_Q < 0.00001), a random-effects model was used. The data showed a synthesized OR of 1.59 (95% CI: 0.88–2.85; high vs. low; Fig. 8). Sensitivity analysis was performed owing to the high heterogeneity. In the sensitivity analysis, the removal of one or two articles did not reduce heterogeneity. Eight eligible studies with 850 patients reported *AFAP1-AS1* expression levels according to DM. Due to severe heterogeneity (I^2 = 65%, P_Q = 0.005), a random-effects model was used. These data showed a pooled OR of 1.81 (95% CI: 0.90–3.66; high *AFAP1-AS1 vs.* low *AFAP1-AS1*; Fig. 9). In the sensitivity analysis, after the study by Wang *et al* [27] was excluded, the heterogeneity decreased (I^2 = 30%, P_Q = 0.20).

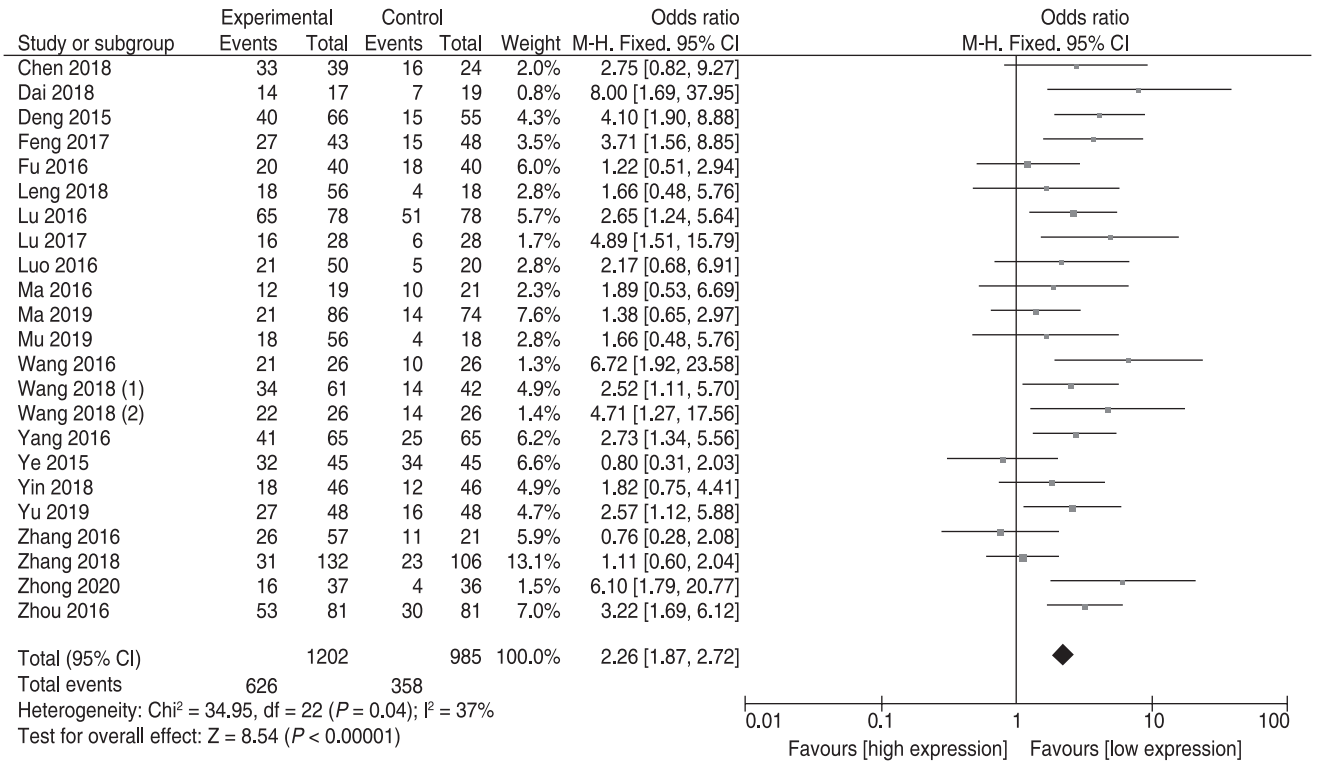

Fig. 6 Forest plot of HRs for the association between high *AFAP1-AS1* expression and HTS

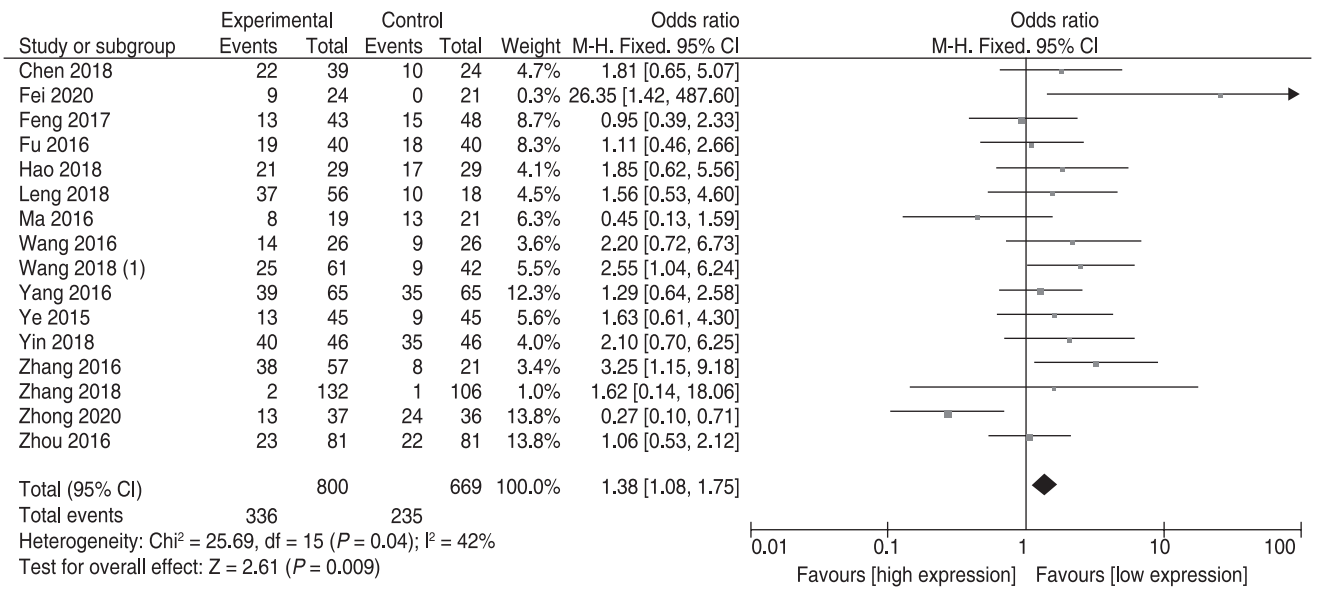

Fig. 7 Forest plot of HRs for the association between high *AFAP1-AS1* expression and PHG

External validation

We used R to analyze the OS, DFS, and PFS of patients with 33 cancer types associated with *AFAP1-AS1* expression. First, for OS, a fixed-effects model was used because of non-significant heterogeneity (I^2 = 41%, P_Q = 0.009). The comprehensive result suggests that high expression of *AFAP1-AS1* was associated with shorter OS (HR = 1.05, 95% CI: 1.02–1.08, Fig. 10). The relationship between *AFAP1-AS1* expression and DFS was studied in 28 of 33 tumors, and the relationship between *AFAP1-AS1* expression and PFS was studied in 32 tumors. There was no significant heterogeneity (DFS: I^2 = 0%, P_Q = 0.58;

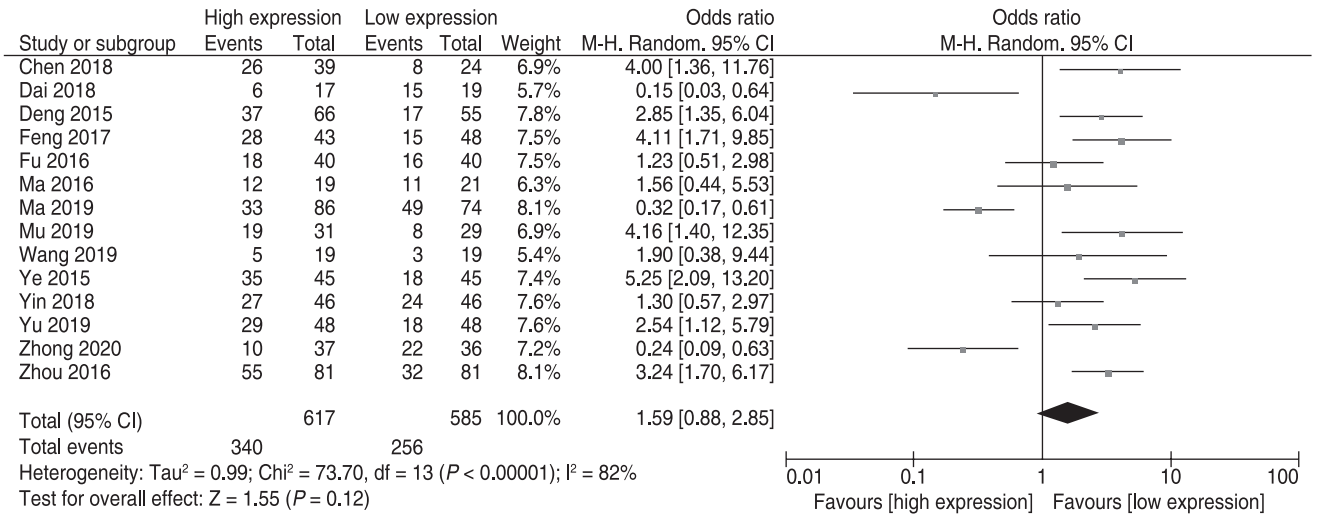

Fig. 8 Forest plot of HRs for the association between high *AFAP1-AS1* expression and LNM

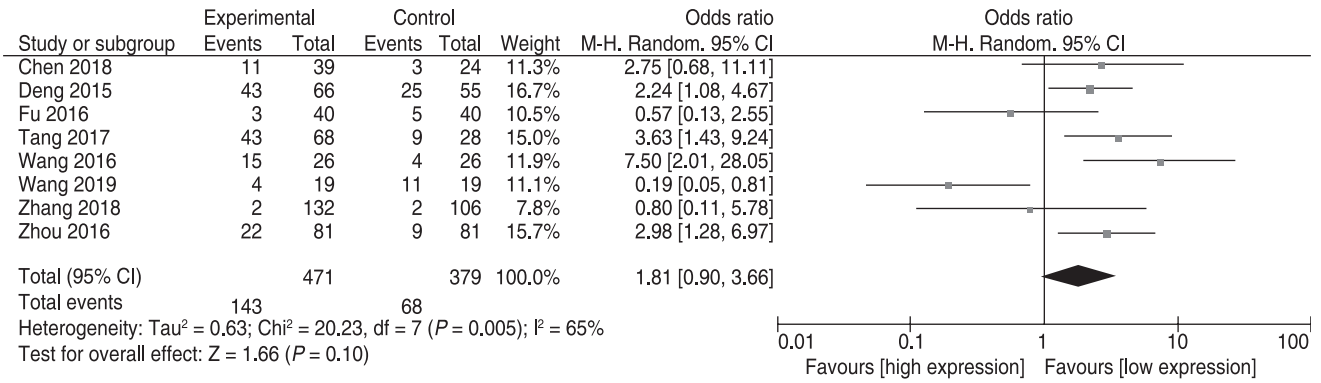

Fig. 9 Forest plot of HRs for the association between high *AFAP1-AS1* expression and DM

PFS: I^2 = 47%, P_Q = 0.002); therefore, we chose the fixed-effects model. The *AFAP1-AS1* expression level was related to DFS (pooled HR = 1.06, 95% CI: 1.00–1.11, Fig. 11) and PFS (pooled HR = 1.04, 95% CI: 1.01–1.07, Fig. 12) in patients with various tumors.

Publication bias

Funnel plots were used to detect publication biases in the included studies. The final results showed no significant asymmetry, suggesting no obvious bias in OS (Fig. 13a), DFS (Fig. 13b), or PFS (Fig. 13c).

Discussion

An increasing number of studies have shown that lncRNAs are abnormally expressed in tumor tissues and are involved in the occurrence and development of tumors. As a molecular blocker, lncRNA can act as a "sponge" to adsorb miRNA and block its inhibitory effect on its downstream target mRNA [53]. *AFAP1-AS1* also acts as a competitive endogenous RNA (ceRNA) that recruits miRNAs to promote tumor progression and metastasis. In endometrial cancer, *AFAP1-AS1* promotes the expression of *VEGFA* by adsorbing *miR-545-3p*, thereby promoting tumor growth and metastasis [16]. Ma *et al* proposed that *AFAP1-AS1* could also regulate the expression of *FGF7* through the sponge absorption of *miR-155-5p*, thereby promoting the GC process [40]. Fei *et al* demonstrated that *AFAP1-AS1* promotes the occurrence and progression of OS through competitive binding of *miR-497* and the regulation of IGF1R expression [46]. In prostate cancer, *AFAP1-AS1* enhances the proliferation, invasion, and metastasis of prostate cancer by regulating *miR-512-3p27*. Zhang *et al* showed that *AFAP1-AS1* promotes TNBC cell proliferation and invasion by targeting *miR-145* to regulate *MTH1* expression [54].

In addition, lncRNAs can be specifically transcribed and participate in specific signaling pathways as signal

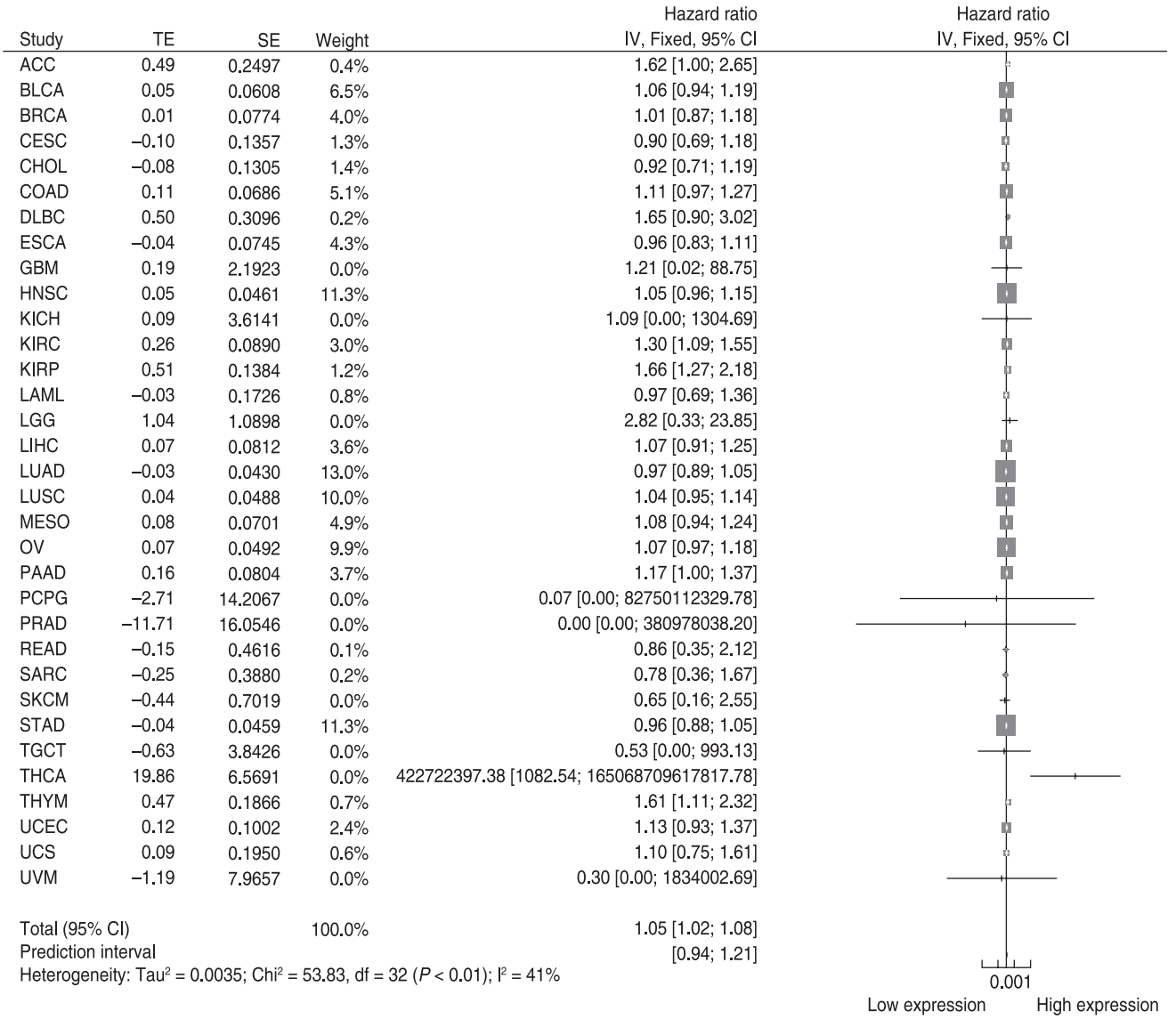

Fig. 10 Forest plot of HRs for the association between high *AFAP1-AS1* expression and OS by external validation

transduction molecules. For example, Shi *et al* confirmed that the lncRNA *AFAP1-AS1* is overexpressed in osteosarcoma and plays a tumorigenic role in osteosarcoma through the RhoC/ROCK1/p38MAPK/Twist1 signaling pathway [55]. *AFAP1-AS1* becomes an oncogene in TSCC by activating the Wnt/β-catenin signaling pathway and inhibiting the expression of EMT-related genes [29]. In pituitary adenomas, *AFAP1-AS1* promotes tumor growth by regulating the PTEN/PI3K/AKT signaling pathway [56].

Resistance to chemoradiotherapy is the main cause of tumor treatment failure; lncRNAs play an important role in this process. lncRNA *AFAP1-AS1* through activation of Wnt/β-catenin signaling pathway, which is induced by promoting cell proliferation, migration and TNBC radiation resistance [57]. Huang *et al* also confirmed that *AFAP1-AS1* promoted chemotherapeutic resistance of NSCLC cells by inhibiting *miR-139-5p* expression and promoting the RRM2/EGFR/AKT signaling pathway [58]. *AFAP1-AS1*, through the PI3K/AKT pathway, induces cisplatin resistance in NSCLC [59].

To investigate the prognostic effect of *AFAP1-AS1* and the relationship between *AFAP1-AS1* expression and the clinicopathological features of different tumors, we performed a meta-analysis of 35 qualified articles and 3433 cases. We found that patients with high *AFAP1-AS1* expression had shorter OS, suggesting that patients with high *AFAP1-AS1* expression may have a worse prognosis. This result was reported in a previous article [13]. In addition, there was no obvious heterogeneity in the included articles, which may have been due

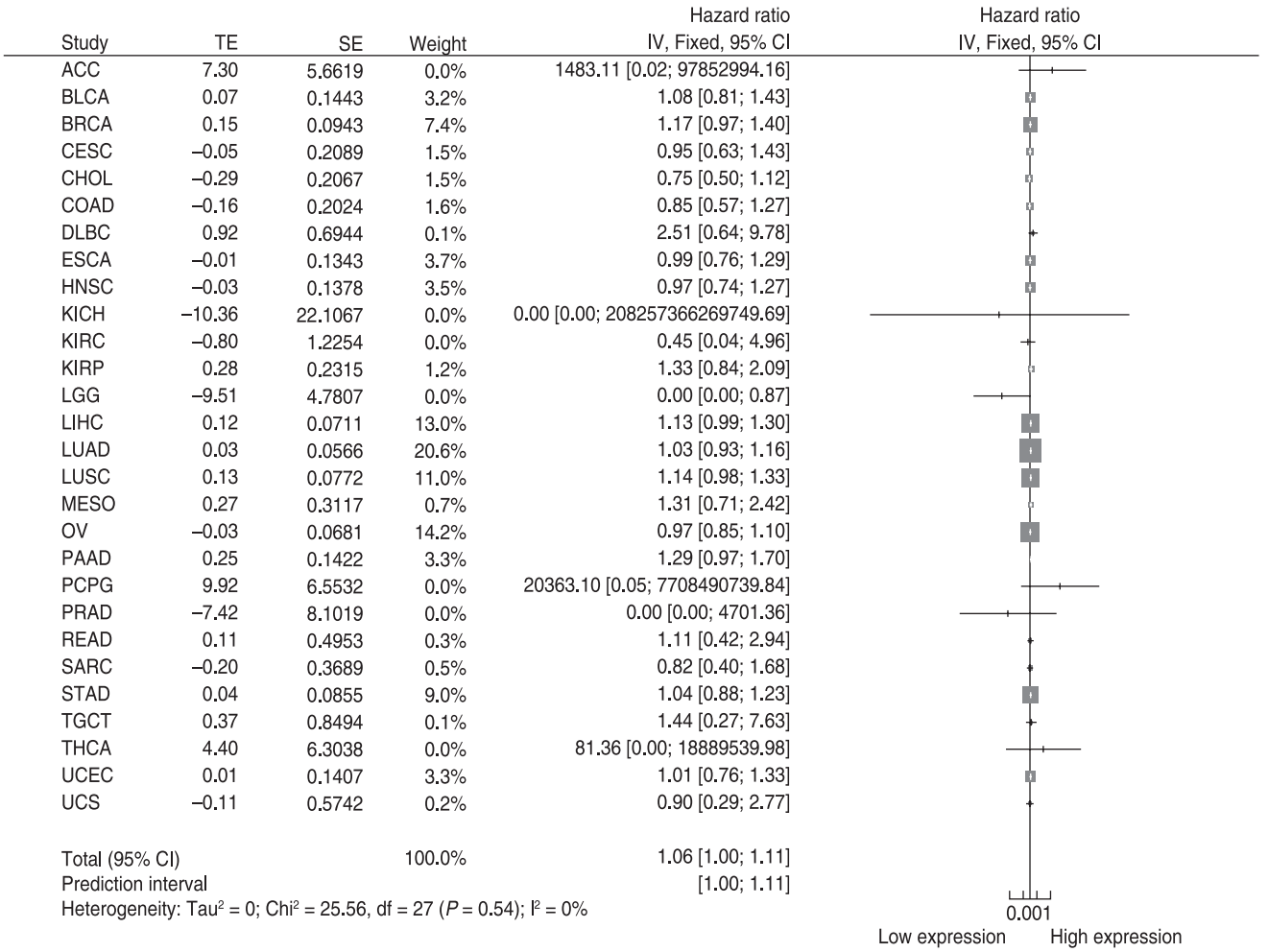

Fig. 11 Forest plot of HRs for the association between high *AFAP1-AS1* expression and DFS by external validation

to experimental errors, small sample sizes, too many cancer types, or different cutoff values. To eliminate heterogeneity, more experiments and sophisticated methods are required. We also observed a relationship between *AFAP1-AS1* expression and DFS and PFS; high *AFAP1-AS1* expression was associated with shorter DFS and PFS. To validate our results, we conducted external verification using R, and the results were found to be consistent with the conclusions of our meta-analysis. Therefore, we speculated that *AFAP1-AS1* could be used as a prognostic molecular marker for different types of cancer.

To examine the relationship between *AFAP1-AS1* and survival, we assessed the association between *AFAP1-AS1* and five clinicopathological features: LTS, HTS, PHG, LNM, and DM. The pooled data showed that high *AFAP1-AS1* expression was associated with LTS, HTS, and PHG, but not with LNM or DM. These results differ from those of previous studies [14, 18]. After accounting for data extraction errors, we analyzed the possible reasons for the differences in this meta-analysis. The included studies and carcinoma types were recently updated, and the inclusion of new cancer types or an increased number of cancer patients may have affected the final results of this study. In this study, considering the relationship between *AFAP1-AS1* and LNM, five new cancer types were identified: TC, GC, CCRCC, PCA, and EC. Additionally, the number of NSCLC cases has increased. Two new articles have been published to study the relationship between *AFAP1-AS1* and DM, and two new cancers, PCA and TNBC, have been added. Unfortunately, the exact reason for these discrepancies remains unknown. Therefore, a larger study with an improved design is required to verify our results.

It is worth noting that the gold standard for tumor diagnosis is pathological results, but tissue-based slices cause harm to patients; therefore, most scholars focus on serological markers. At present, whether lncRNAs can be used in the early stages of tumors or whether the expression of lncRNAs differs at different tumor stages is

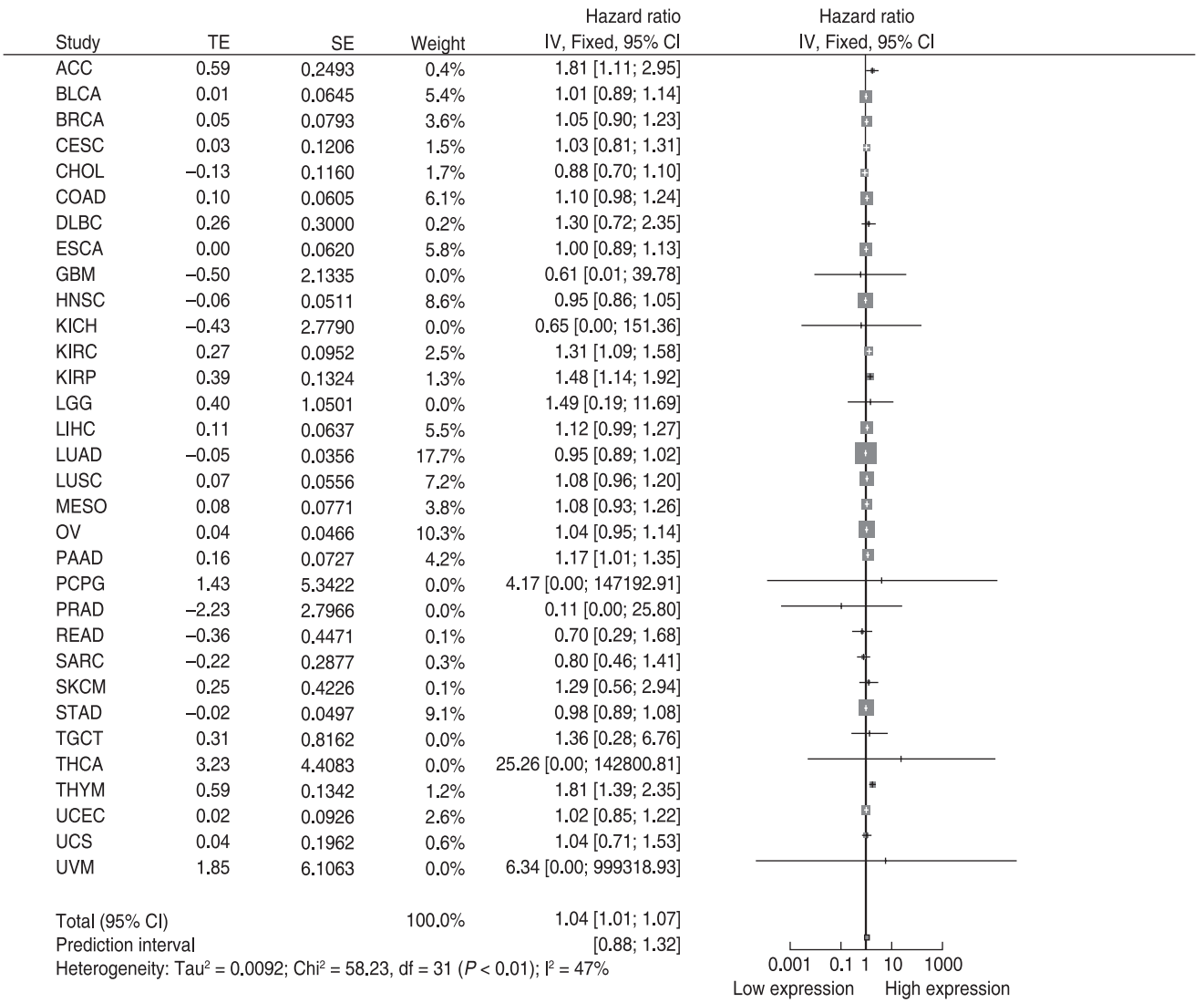

Fig. 12 Forest plot of HRs for the association between high *AFAP1-AS1* expression and PFS by external validation

a challenge that needs to be solved urgently. In addition, attention should be paid to specificity. For example, *AFAP1-AS1* is abnormally expressed in various tumors and is involved in tumorigenesis and development. Finally, the technology's immaturity and high price prevent its clinical use. Therefore, an increasing number of clinical trials must be conducted.

Some limitations of this meta-analysis should be considered. First, all included studies were conducted in China; therefore, our data and research results cannot be applied globally. Second, the data collection may have been inadequate, as non-English articles were excluded, and the number of patients and types of cancer were not sufficient. Third, 13 articles did not mention a cutoff value for high expression, and not all articles had the same cutoff value. Fourth, different types of cancers have different degrees of heterogeneity. Fifth, although the article quality evaluation was completed by two researchers, bias may still exist. Sixth, some HRs were calculated by reconstructing survival curves instead of being extracted directly from the original study; therefore, calculation errors may exist.

Conclusion

We comprehensively searched three databases for relevant studies and according to the inclusion and exclusion criteria, 35 studies with 3433 patients were included in this meta-analysis. It was concluded that an elevated level of lncRNA *AFAP1-AS1* in cancer patients was associated with shorter OS, DFS, and PFS, and that *AFAP1-AS1* was associated with LTS, HTS, and PHG in cancer patients but not with LNM or DM. Further studies

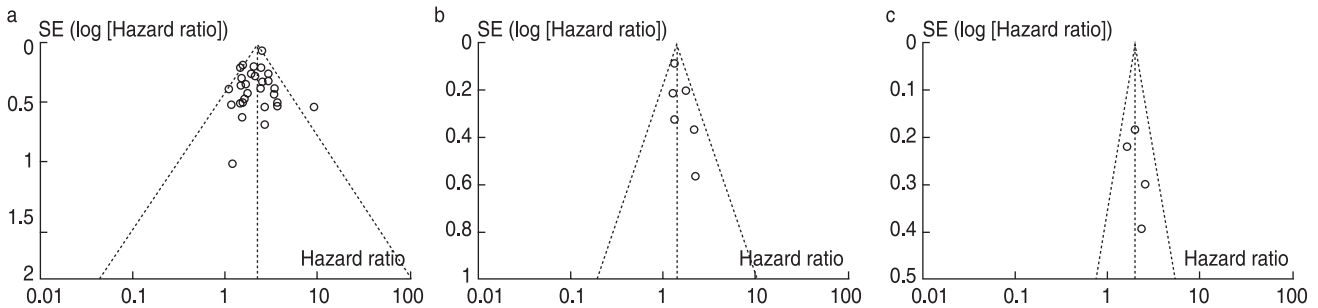

Fig. 13 Funnel plot analysis of potential publication bias in the survival and clinicopathological parameters group. (a) OS, (b) DFS, (c) PFS

are needed to validate the association between *AFAP1-AS1* expression, prognosis, and pathological features in patients with cancer.

Acknowledgments

Not applicable.

Funding

Supported by grant from the "Ten Thousand Plan" Youth Talent Project in Yunnan Province (no grant number is applicable).

Conflicts of interest

The authors indicated no potential conflicts of interest.

Authors' contributions

All authors contributed to data acquisition and interpretation and reviewed and approved the final version of this manuscript.

Data availability statement

Data supporting the findings of this study are available from the corresponding author upon reasonable request.

Ethical approval

Not applicable.

References

1. Sung H, Ferlay J, Siegel RL, et al. Global cancer statistics 2020: GLOBOCAN estimates of incidence and mortality worldwide for 36 cancers in 185 countries. CA Cancer J Clin. 2021;71(3):209-249.
2. Sanchez Calle A, Kawamura Y, Yamamoto Y, et al. Emerging roles of long non-coding RNA in cancer. Cancer Sci. 2018;109(7):2093-2100.
3. Statello L, Guo CJ, Chen LL, et al. Gene regulation by long non-coding RNAs and its biological functions. Nat Rev Mol Cell Biol. 2021;22(2):96-118.
4. Santosh B, Varshney A, Yadava PK. Non-coding RNAs: biological functions and applications. Cell Biochem Funct. 2015;33(1):14-22.
5. Zhang Y, Wang LJ, Li WF, et al. The prognostic value of HOTAIR for predicting long-term prognosis of patients with gastrointestinal cancers. Medicine (Baltimore). 2018;97(26):e11139.
6. Zhang F, Li J, Xiao H, et al. AFAP1-AS1: A novel oncogenic long non-coding RNA in human cancers. Cell Prolif. 2018;51(1):e12397.
7. Wu W, Bhagat TD, Yang X, et al. Hypomethylation of noncoding DNA regions and overexpression of the long noncoding RNA, AFAP1-AS1, in Barrett's esophagus and esophageal adenocarcinoma. Gastroenterology. 2013;144(5):956-966.e4.
8. Wang KC, Chang HY. Molecular mechanisms of long noncoding RNAs. Mol Cell. 2011;43(6):904-914.
9. Zhang JY, Weng MZ, Song FB, et al. Long noncoding RNA AFAP1-AS1 indicates a poor prognosis of hepatocellular carcinoma and promotes cell proliferation and invasion via upregulation of the RhoA/Rac2 signaling. Int J Oncol. 2016;48(4):1590-1598.
10. Yu S, Yang D, Ye Y, et al. Long noncoding RNA actin filament-associated protein 1 antisense RNA 1 promotes malignant phenotype through binding with lysine-specific demethylase 1 and repressing HMG box-containing protein 1 in non-small-cell lung cancer. Cancer Sci. 2019;110(7):2211-2225.
11. He J, Wu K, Guo C, et al. Long non-coding RNA AFAP1-AS1 plays an oncogenic role in promoting cell migration in non-small cell lung cancer. Cell Mol Life Sci. 2018;75(24):4667-4681.
12. Yin D, Lu X, Su J, et al. Long noncoding RNA AFAP1-AS1 predicts a poor prognosis and regulates non-small cell lung cancer cell proliferation by epigenetically repressing p21 expression. Mol Cancer. 2018;17(1):92.
13. Zhou Y, Chen S, Cheng S, et al. The prognostic value of high LncRNA AFAP1-AS1 expression in various cancers: A systematic review and meta-analysis containing 21 studies. Clin Chim Acta. 2018;481:147-153.
14. Liu FT, Xue QZ, Zhu PQ, et al. Long noncoding RNA AFAP1-AS1, a potential novel biomarker to predict the clinical outcome of cancer patients: a meta-analysis. Onco Targets Ther. 2016;9:4247-4254.
15. Yang SL, Lin RX, Si LH, et al. Expression and functional role of long non-coding RNA AFAP1-AS1 in ovarian cancer. Eur Rev Med Pharmacol Sci. 2016;20(24):5107-5112.
16. Zhong Y, Wang Y, Dang H, et al. LncRNA AFAP1-AS1 contributes to the progression of endometrial carcinoma by regulating miR-545-3p/VEGFA pathway. Mol Cell Probes. 2020;53:101606.
17. Zhuang Y, Jiang H, Li H, et al. Down-regulation of long non-coding RNA AFAP1-AS1 inhibits tumor cell growth and invasion in lung adenocarcinoma. Am J Transl Res. 2017;9(6):2997-3005.
18. Liu RH, Wang MY, Chen LY, et al. Meta-analysis of the prognostic value of long non-coding RNA AFAP1-AS1 for cancer patients in China. Oncotarget. 2017;9(8):8100-8110.
19. Parmar MK, Torri V, Stewart L. Extracting summary statistics to

perform meta-analyses of the published literature for survival endpoints. Stat Med. 1998;17(24):2815-2834.
20. Wang W, Yuan F, Xu J. The prognostic role of long noncoding RNA CRNDE in cancer patients: a systematic review and meta-analysis. Neoplasma. 2019;66(1):73-82.
21. Tierney JF, Stewart LA, Ghersi D, et al. Practical methods for incorporating summary time-to-event data into meta-analysis. Trials. 2007;8:16.
22. Oremus M, Oremus C, Hall GB, et al. Inter-rater and test-retest reliability of quality assessments by novice student raters using the Jadad and Newcastle-Ottawa Scales. BMJ Open. 2012;2(4):e001368.
23. Zhao H, Zhang K, Wang T, et al. Long non-coding RNA AFAP1-antisense RNA 1 promotes the proliferation, migration and invasion of gastric cancer cells and is associated with poor patient survival. Oncol Lett. 2018;15(6):8620-8626.
24. Zhou XL, Wang WW, Zhu WG, et al. High expression of long non-coding RNA AFAP1-AS1 predicts chemoradioresistance and poor prognosis in patients with esophageal squamous cell carcinoma treated with definitive chemoradiotherapy. Mol Carcinog. 2016;55(12):2095-2105.
25. Tang Y, He Y, Shi L, et al. Co-expression of AFAP1-AS1 and PD-1 predicts poor prognosis in nasopharyngeal carcinoma. Oncotarget. 2017;8(24):39001-39011.
26. Wang F, Ni H, Sun F, et al. Overexpression of lncRNA AFAP1-AS1 correlates with poor prognosis and promotes tumorigenesis in colorectal cancer. Biomed Pharmacother. 2016;81:152-159.
27. Wang K, Sun H, Sun T, et al. Long non-coding RNA AFAP1-AS1 promotes proliferation and invasion in prostate cancer via targeting miR-512-3p. Gene. 2020;726:144169.
28. Wang Y, Lan Q. Long non-coding RNA AFAP1-AS1 accelerates invasion and predicts poor prognosis of glioma. Eur Rev Med Pharmacol Sci. 2018;22(16):5223-5229.
29. Wang ZY, Hu M, Dai MH, et al. Upregulation of the long non-coding RNA AFAP1-AS1 affects the proliferation, invasion and survival of tongue squamous cell carcinoma via the Wnt/β-catenin signaling pathway. Mol Cancer. 2018;17(1):3.
30. Ye Y, Chen J, Zhou Y, et al. High expression of AFAP1-AS1 is associated with poor survival and short-term recurrence in pancreatic ductal adenocarcinoma. J Transl Med. 2015;13:137.
31. Zeng Z, Bo H, Gong Z, et al. AFAP1-AS1, a long noncoding RNA upregulated in lung cancer and promotes invasion and metastasis. Tumour Biol. 2016;37(1):729-737.
32. Zhang K, Liu P, Tang H, et al. AFAP1-AS1 promotes epithelial-mesenchymal transition and tumorigenesis through Wnt/β-catenin signaling pathway in triple-negative breast cancer. Front Pharmacol. 2018;9:1248.
33. He J, Wu K, Guo C, et al. Long non-coding RNA AFAP1-AS1 plays an oncogenic role in promoting cell migration in non-small cell lung cancer. Cell Mol Life Sci. 2018;75(24):4667-4681.
34. Leng X, Ding X, Wang S, et al. Long noncoding RNA AFAP1-AS1 is upregulated in NSCLC and associated with lymph node metastasis and poor prognosis. Oncol Lett. 2018;16(1):727-732.
35. Li Q, Dai Y, Wang F, et al. Differentially expressed long non-coding RNAs and the prognostic potential in colorectal cancer. Neoplasma. 2016;63(6):977-983.
36. Li R, Liu S, Li Y, et al. Long noncoding RNA AFAP1-AS1 enhances cell proliferation and invasion in osteosarcoma through regulating miR-4695-5p/TCF4-β-catenin signaling. Mol Med Rep. 2018;18(2):1616-1622.
37. Lu X, Zhou C, Li R, et al. Long noncoding RNA AFAP1-AS1 promoted tumor growth and invasion in cholangiocarcinoma. Cell Physiol Biochem. 2017;42(1):222-230.
38. Lu X, Zhou C, Li R, et al. Critical role for the long non-coding RNA AFAP1-AS1 in the proliferation and metastasis of hepatocellular carcinoma. Tumour Biol. 2016;37(7):9699-9707.
39. Ma D, Chen C, Wu J, et al. Up-regulated lncRNA AFAP1-AS1 indicates a poor prognosis and promotes carcinogenesis of breast cancer. Breast Cancer. 2019;26(1):74-83.
40. Ma HW, Xi DY, Ma JZ, et al. Long noncoding RNA AFAP1-AS1 promotes cell proliferation and metastasis via the miR-155-5p/FGF7 axis and predicts poor prognosis in gastric cancer. Dis Markers. 2020;2020:8140989.
41. Mu Z, Dong D, Wei N, et al. Silencing of lncRNA AFAP1-AS1 inhibits cell growth and metastasis in clear cell renal cell carcinoma. Oncol Res. 2019;27(6):653-661.
42. Bo H, Fan L, Li J, et al. High expression of lncRNA AFAP1-AS1 promotes the progression of colon cancer and predicts poor prognosis. J Cancer. 2018;9(24):4677-4683.
43. Chen B, Li Q, Zhou Y, et al. The long coding RNA AFAP1-AS1 promotes tumor cell growth and invasion in pancreatic cancer through upregulating the IGF1R oncogene via sequestration of miR-133a. Cell Cycle. 2018;17(16):1949-1966.
44. Dai W, Tian Y, Jiang B, et al. Down-regulation of long non-coding RNA AFAP1-AS1 inhibits tumor growth, promotes apoptosis and decreases metastasis in thyroid cancer. Biomed Pharmacother. 2018;99:191-197.
45. Deng J, Liang Y, Liu C, et al. The up-regulation of long non-coding RNA AFAP1-AS1 is associated with the poor prognosis of NSCLC patients. Biomed Pharmacother. 2015;75:8-11.
46. Fei D, Zhang X, Lu Y, et al. Long noncoding RNA AFAP1-AS1 promotes osteosarcoma progression by regulating miR-497/IGF1R axis. Am J Transl Res. 2020;12(5):2155-2168.
47. Feng Y, Zhang Q, Wang J, et al. Increased lncRNA AFAP1-AS1 expression predicts poor prognosis and promotes malignant phenotypes in gastric cancer. Eur Rev Med Pharmacol Sci. 2017;21(17):3842-3849.
48. Fu XL, Liu DJ, Yan TT, et al. Analysis of long non-coding RNA expression profiles in pancreatic ductal adenocarcinoma. Sci Rep. 2016;6:33535.
49. Gui JQ, Zhang C, Yang HB, et al. LncRNA AFAP1-AS1 promotes proliferation ability and invasiveness of bladder cancer cells. Eur Rev Med Pharmacol Sci. 2020;24(17):8747-8755.
50. Hao F, Mou Y, Zhang L, et al. LncRNA AFAP1-AS1 is a prognostic biomarker and serves as oncogenic role in retinoblastoma. Biosci Rep. 2018;38(3):BSR20180384.
51. Ma F, Wang SH, Cai Q, et al. Overexpression of LncRNA AFAP1-AS1 predicts poor prognosis and promotes cells proliferation and invasion in gallbladder cancer. Biomed Pharmacother. 2016;84:1249-1255.
52. Tang J, Zhong G, Wu J, et al. Long noncoding RNA AFAP1-AS1 facilitates tumor growth through enhancer of zeste homolog 2 in colorectal cancer. Am J Cancer Res. 2018;8(5):892-902.
53. Zhang MW, Zhu ZH, Xia ZK, et al. Comprehensive circRNA-microRNA-mRNA network analysis revealed the novel regulatory mechanism of Trichosporon asahii infection. Mil Med Res. 2021;8(1):19.
54. Zhang X, Zhou Y, Mao F, et al. lncRNA AFAP1-AS1 promotes triple negative breast cancer cell proliferation and invasion via targeting miR-145 to regulate MTH1 expression. Sci Rep. 2020;10(1):7662.
55. Shi D, Wu F, Mu S, et al. LncRNA AFAP1-AS1 promotes tumorigenesis and epithelial-mesenchymal transition of osteosarcoma through RhoC/ROCK1/p38MAPK/Twist1 signaling pathway. J Exp Clin

Cancer Res. 2019;38(1):375.
56. Tang H, Hou B, Ye Z, et al. Knockdown of long non-coding RNA AFAP1-AS1 inhibits growth and promotes apoptosis in pituitary adenomas. Int J Clin Exp Pathol. 2018;11(3):1238-1246.
57. Bi Z, Li Q, Dinglin X, et al. Nanoparticles (NPs)-meditated lncRNA AFAP1-AS1 silencing to block Wnt/β-catenin signaling pathway for synergistic reversal of radioresistance and effective cancer radiotherapy. Adv Sci (Weinh). 2020;7(18):2000915.
58. Huang N, Guo W, Ren K, et al. LncRNA AFAP1-AS1 supresses miR-139-5p and promotes cell proliferation and chemotherapy resistance of non-small cell lung cancer by competitively upregulating RRM2. Front Oncol. 2019;9:1103.
59. Liu Y, Hu Q, Wang X. AFAP1-AS1 induces cisplatin resistance in non-small cell lung cancer through PI3K/AKT pathway. Oncol Lett. 2020;19(1):1024-1030.

DOI 10.1007/s10330-022-0581-1
Cite this article as: Zhu LX, Yan JW, Xu GQ, et al. Prognostic value of the long noncoding RNA *AFAP1-AS1* in cancers. Oncol Transl Med. 2023;9(3):133–146.

Oncology and Translational Medicine

Volume 9 • Number 3 • June 2023

Aims & Scope

Oncology and Translational Medicine (OTM) is an international, open-access, peer-reviewed academic journal that aims to promote research in oncology and translational medicine as well as levels of service in clinical practice. It publishes the results of novel research investigations which bridge the laboratory and clinical settings including risk assessment, cellular and molecular characterization, prevention, detection, diagnosis and treatment of human cancers with the overall goal of improving the clinical care of oncology patients. OTM covers the types of Original research, Review articles, Consensus and Guideline, Perspectives, Letters to the Editor, Editorials, Commentary, Personage Column, Case Report, etc.

Copyright

Supervised by

Ministry of Education of the People's Republic of China.

Administered by

Tongji Medical College, Huazhong University of Science and Technology.

Submission Information

Manuscripts should be submitted to:
http://otm.tjh.com.cn
otm.office@tjh.tjmu.edu.cn

Subscription Information

ISSN edition: 2095-9621
CN: 42-1865/R

■ Subscription rates

Subscription may begin at any time. Remittances made by check, draft or express money order should be made payable to this journal. The price for 2023 is as follows: US $ 30 per issue; RMB ¥28.00 per issue.

Database

Oncology and Translational Medicine is abstracted and indexed in EMBASE, Index Copernicus, Chinese Science and Technology Paper Citation Database (CSTPCD), Chinese Core Journals Database, Chinese Journal Full-text Database (CJFD), Wanfang Data; Weipu Data; Chinese Academic Journal Comprehensive Evaluation Database.

Business Correspondence

All matters relating to orders, subscriptions, back issues, offprints, advertisement booking and general enquiries should be addressed to the editorial office.

Mailing address
Editorial office of
Oncology and Translational Medicine
Tongji Hospital
Tongji Medical College
Huazhong University of Science and Technology
Jie Fang Da Dao 1095
430030 Wuhan, China
Tel.: +86-27-83662395
Email: otm.office@tjh.tjmu.edu.cn

Printer
Changjiang Spatial Information Technology Engineering Co., Ltd. (Wuhan) Hangce Information Cartorgraphy Printing Filial, Wuhan, China
Printed in People's Republic of China

Editors-in-Chief

Managing Director

Executive Editors